Functional Nucleic Acid Sensors

Juewen Liu, Zehui Cao, and Yi Lu*

Department of Chemistry, University of Illinois at Urbana–Champaign, 600 South Mathews Avenue, Urbana, Illinois 61801

Contents

* To whom correspondence should be addressed: Telephone: 217-333-2619. E-mail: yi-lu@illinois.edu.

1. Introduction

Sensors are devices that respond to physical or chemical stimuli and produce detectable signals.[1−4] They are a critical extension of human perception of the world in many aspects of the modern society. This is largely because we are much less sensitive to the chemical or biological environment than to the physical environment (e.g., light, pressure, temperature, or humidity). However, appropriate chemical or biological compositions are tightly linked to the quality of life. For

Juewen Liu was born in Changsha, China, in 1978. He received his B.S. degree from the University of Science and Technology in Hefei, China, in 2000 and his Ph.D. degree from the University of Illinois at Urbana−Champaign in 2005 under the direction of Professor Yi Lu. Presently, he is working as a postdoctoral fellow at the University of New Mexico with Professor C. Jeffrey Brinker. He is interested in nucleic acid bioinorganic chemistry, functional DNA-based materials and sensors, and the use of mesoporous silica nanomaterials and phospholipids for drug delivery applications.
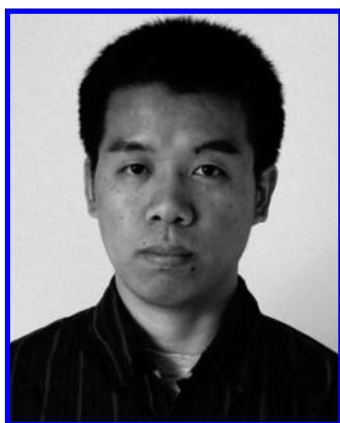
Zehui Cao received his B.S. degree from Nanjing University (P. R. China) in 1998 and his Ph.D. degree in Analytical Chemistry from the University of Florida in 2004. After two years of postdoctoral research following graduation at the University of Florida, he moved to the Department of Chemistry at the University of Illinois at Urbana−Champaign for two more years of postdoctoral research. His research interests include (a) development of assays and sensors for biological targets and interactions using nucleic acid probes and (b) development and application of cell-specific nucleic acid ligands for disease diagnosis, biomarker discovery, and targeted drug delivery.

example, the presence of certain molecules and ion and their concentrations inside a human body (i.e., metabolites, metal ions, hormones, and proteins) reflect the person's health, while chemicals in the environment (i.e., heavy metals, explosives, and toxins) can affect human health. Therefore, the development of highly sensitive and selective sensors to recognize important analytes has long been a focus of research for many areas, including environmental monitoring, industrial quality control, and medical diagnostics.

A sensor contains at least two components: target recognition and signal transduction. The target recognition element can be any chemical or biological entity such as small organic molecules, peptides, proteins, nucleic acids, carbohydrates, or even whole cells. Ideally, this element should have high affinity (low detection limit), high specificity (low interference), wide dynamic range, fast response time, long shelf life, and good generality for detecting a broad range of analytes with the same class of recognition element. Anti-

Yi Lu received his B.S. degree from Peking University (P. R. China) in 1986 and his Ph.D. degree from the University of California at Los Angeles in 1992. After two years of postdoctoral research at the California Institute of Technology, he began his own independent career in the Department of Chemistry at the University of Illinois at Urbana−Champaign. He is now an HHMI Professor and Alumni Research Scholar in the Departments of Chemistry, Biochemistry, Materials Science and Engineering, and Bioengineering at the University of Illinois at Urbana−Champaign. His research interests include (a) design and engineering of artificial metalloproteins as environmentally benign biocatalysts for asymmetric transformations and for bioremediation of aromatic pollutants; (b) design of sensitive and selective sensors and their applications to environmental monitoring, developmental biology, clinical toxicology, and industrial process monitoring; and (c) genetic control of directed assembly of inorganic nanomaterials using functional DNA.

bodies are protein-based binding molecules that have long been used for target recognition because they meet most of the above criteria. Signal transduction elements are responsible for converting molecular recognition events into physically detectable signals such as fluorescence, color, electrochemical signals, or magnetic resonance image changes.

Single-stranded DNAs or RNAs can bind to their complementary strands with high specificity and are useful for nucleic acid detection. With a combinatorial method called in vitro selection or **s**ystematic **e**volution of **l**igands by **ex**ponential enrichment (SELEX), it is possible to evolve nucleic acids in test tubes to bind to a diverse range of analytes beyond DNA or RNA with high affinity and specificity, and these binding nucleic acids are known as aptamers.[5−9] In many aspects, the binding performance of aptamers can rival that of antibodies.[10,11] Interestingly, Nature also utilizes aptamers to bind metabolites in RNA-based gene expression control elements called riboswitches.[12−15]

As the nucleic acid equivalent of antibodies, aptamers possess a number of competitive advantages over antibodies for sensing applications.[10,11] First, because aptamers are isolated in vitro, they can be selected to bind essentially any target of choice. Antibodies, on the other hand, cannot be obtained for molecules too small to have enough binding repertoires (e.g., Mg^{2+} or Pb^{2+} that is not associated with any chelators) or molecules with poor immunogenicity or high toxicity. It is difficult to review all existing aptamers here, given that over one hundred aptamers were isolated for protein targets by NeXstar Pharmaceuticals Inc. and the University of Colorado alone by 1999.[16] The number of aptamers isolated by scientists throughout the world is much greater than that. Ellington and co-workers have created a searchable online aptamer database where more detailed information can be found.[17] Table 1 shows a list of literature reported DNA aptamer targets, which demonstrate that aptamers can bind any analytes of choice. There are even

Table 1. Literature Reported DNA Aptamer Targets

analyte type	examples and refs
metal ions	K(I),[18] Hg(II),[19] Pb(II),[20,21] UO$_2$(II),[22] Cu(II),[23] Zn(II)[24,25]
organic dyes	reactive green 19,[26] sulforhodamine B[27]
amino acids	arginine,[28] L-tyrosinamide[29]
nucleotides	ATP (or adenosine, AMP)[30]
RNA	TAR-RNA[31]
biological cofactors	N-methylmesoporphyrin IX (NMM) or hemin[32]
other small organic molecules	cocaine,[33] cholic acid,[34] aspartame,[35] (R)-thalidomide,[36] 17β-estradiol[37]
oligosaccharides	cellobiose,[38] sialyllactose[39]
peptidesv	Vasopressin,[40] RGD,[41] neuropeptide Y[42]
toxins	ricin,[43] abrin toxin[44]
enzymes	human thrombin,[45] neutrophil elastase,[46] *Taq* DNA polymerase,[47] HIV-1 RNase H,[48] protein kinase C-δ,[49] HIV-1 reverse transcriptase[50]
growth factors	platelet-derived growth factor B-chain,[51] human basic fibroblast growth factor[52]
transcription factors	NF-κB[53]
antibodies	human IgE[54]
viral proteins or components	influenza virus surface glycoproteins,[55] HIV MN envelope glycoprotein[56]
cells and bacteria	anthrax spores,[57] YPEN-1 endothelial,[58] PC12 cells,[59] Jurkat T leukemia cells,[60] CCRF-CEM leukemia cells,[61] small-cell lung cancer (SCLC) cells,[62] B-cell tumor cells[63]

more RNA aptamers reported in the literature, and they generally have comparable binding performance to DNA aptamers.

Even though nucleic acids hold much less chemical functionalities compared to proteins, the target binding property of aptamers can also rival that of antibodies. In terms of binding affinity, for example, among the first one hundred protein aptamers selected by NeXstar Pharmaceuticals Inc. and the University of Colorado, more than 75% have a dissociation constant (K_d) less than 1 nM, while the K_d's for most antibodies are between 1 and 10 nM.[16] A K_d of 49 pM was achieved with a 2′-fluoropyrimidine modified RNA aptamer targeting the 165-amino acid form of the vascular endothelial growth factor,[64] and a K_d of 0.3 pM was reported for an RNA aptamer against the human keratinocyte growth factor.[65] Aptamers also possess very high target specificity. For example, the DNA aptamer against the B-chain of the platelet-derived growth factor (PDGF) has a selectivity of ~370-fold higher for the PDGF-BB homodimer than that for PDGF-AA. Although theophylline and caffeine differ by only one methyl group, the antitheophylline aptamer binds theophylline >10,000 times tighter.[66] The aptamer against L-arginine binds D-arginine with 12,000-fold reduced affinity.[67] Many studies covered in this review have compared aptamers and antibodies for the detection of the same target side by side, and in most cases aptamers worked similarly or even better.[68−71]

Because aptamers are isolated in test tubes and can be chemically synthesized in large quantities, whereas antibody production often requires animals or cell cultures, aptamers are relatively more cost-effective for most applications. Sizewise, most aptamers are less than 100 nucleotides and much smaller than antibodies. For example, a thrombin aptamer contains only 15 nucleotides.[45] Therefore, aptamers can be incorporated into devices with higher surface density. Stability is an important factor for sensing applications. Aptamers, especially DNA aptamers, are more stable compared to antibodies. Aptamers can be thermal denatured and renatured for many cycles without losing binding ability, while denatured antibodies usually cannot be renatured. As a result, aptamer binding is reversible and aptamer-based sensors can be reused, while in most cases antibody-based

sensors are intended only for single use. To improve aptamer stability in biological samples, chemically modified nucleotides or linkages can be used. Moreover, aptamers often adapt a binding tertiary structure in the presence of their targets and thus are sometimes protected from nuclease attack.[72]

Aptamers are also superior to antibodies in terms of signal transduction. As will be presented in this review, most methods developed for antibody-based detection have been successfully adapted to aptamers. In addition, aptamers are suited for many unique signaling methods because of nucleic acids' predictable and tailorable structures. It is possible to design sensors based largely on aptamer secondary structures with minimal knowledge of their tertiary structures. Because aptamers are chemically synthesized, chemical modifications can be introduced essentially at any position of choice. Therefore, aptamers can be a useful alternative to antibodies in sensing and diagnostics.

Due to the lack of a good immobilization method, metal ions have posed a challenge for aptamer selection.[24,73−75] Nucleic acid−based enzymes, on the other hand, show strong metal-dependent activities. Ribozymes (catalytic RNA) have been found in nature,[76−78] while deoxyribozymes (also known as catalytic DNA, DNA enzymes, or DNAzymes) have only been isolated in test tubes.[79−86] Most nucleic acid enzymes (NAEs) require metal ions for their activities, and some even show metal specificity. Therefore, NAEs can be used for metal sensing.[82,85,87−89] A combination of aptamers and NAEs results in allosteric NAEs or aptazymes.[90−92] Aptamers, NAEs, and aptazymes are collectively called functional nucleic acids (FNAs), whose functions are beyond the conventional genetic roles of nucleic acids.

The possibilites provided by FNAs are enormous, and some emerging applications include therapeutics,[93−97] imaging,[98] screening and drug development,[91,99−101] separation,[102−104] materials science,[105,106] nanotechnology,[89,106−109] organic synthesis,[85,86,110] and sensing.[82,87,111−119] This review mainly covers the various signaling methods developed to construct FNA sensors, and most of the research efforts in this area have been made in the last 10 years. NAE-based sensors are covered first, followed by aptamer and aptazyme sensors. This review covers both functional DNA and RNA sensors.

Because of lower costs and higher stability, functional DNA molecules have been used for sensing applications much more than those of functional RNA molecules. Therefore, more work on functional DNA sensors is summarized.

2. Nucleic Acid Enzyme (NAE) Based Sensors

It has long been thought that all enzymes are proteins, and this view has been revolutionized with the discovery of ribozymes by Cech and Altman.[120,121] Thus far, natural ribozymes have been found to catalyze only a few reactions, including RNA cleavage,[122] splicing,[123] and peptide bond formation in ribosomes.[124] On the other hand, in vitro selection allows the identification of many more artificial ribozymes that can catalyze a wide variety of reactions, such as RNA cleavage,[125,126] ligation,[127−129] phosphorylation,[130] capping,[131] polymerization,[132] peptide bond formation,[133,134] aldehyde reduction,[135] alcohol dehydrogenation,[136] Diels−Alder reaction,[137−139] aldol reaction,[140] Michael reaction,[141] porphyrin metalation,[142] acyl transfer,[143−146] aminoacylation,[147,148] and the synthesis of amide,[149] urea,[150] and other small molecules.[151,152] Despite the lack of the 2′-hydroxyl group and their discovery more than a decade later than ribozymes, many DNAzymes have also been isolated to catalyze a diverse range of reactions, including RNA cleavage,[20,22,25,153−161] DNA cleavage,[23,162] RNA ligation,[163−165] DNA ligation,[166,167] RNA branching and lariat RNA formation,[168−170] DNA phosphorylation,[171] capping,[172] deglycosylation,[173] cleavage of the phosphoramidate bond,[174] photocleavage of thymine dimers,[175] porphyrin metalation,[176] and other enzymatic activities as peroxidases.[177] For NAEs, the rate enhancement can be as high as 10^{10} over uncatalyzed reactions, and the catalytic efficiency (k_{cat}/K_m) can reach 10^9 M^{-1} min^{-1},[20] rivaling that of protein enzymes. Their detailed descriptions can be found in more specific reviews for ribozymes[78,178−181] and DNAzymes.[8,79−83,88,182−185] Because NAEs are amenable to in vitro selection, have good stability, and can be prepared and modified with cost-effective chemical synthesis, they have been used as components for many novel biotechnological applications, such as in making antiviral agents,[20] biosensors for metal ions[22,186−195] and organic molecules,[196,197] components for DNA-based logic gates,[198−200] components for nanomotors,[201,202] and proofreading units during nanomaterial assembly.[203]

For NAE-based sensors, the target molecule is usually a cofactor that can accelerate the catalytic reaction or an inhibitor of the reaction. With this in mind, selection pressures can be applied in the selection process so that the desired reaction happens only in the presence of a target analyte. To improve target specificity, negative selections can be performed to remove sequences that are also active with competing analytes.[82,204] Because of the chemical nature of NAE-catalyzed reactions, metal ions are usually required as cofactors, and therefore, NAE sensors are most successful for metal detection.[22,186−195]

Heavy metal contaminations have posed significant health concerns to the general public, and one way to minimize the chance of metal poisoning is to develop analytical tools for metal detection. Analytical techniques, such as atomic absorption spectrometry, inductively coupled plasma mass spectrometry, anodic stripping voltammetry, capillary electrophoresis, X-ray fluorescence spectrometry, and microprobes, have been routinely used for metal ion analysis with high sensitivity (often ≤ ppb level).[205] Many of them can quantify multiple metal ions simultaneously. However, it is

generally believed that most of the above techniques require sophisticated equipments, sample pretreatment, or skilled operators, making it difficult for on-site, real-time monitoring of metal ions.[1,2,206] While important progress has been made to miniaturize many of the above analytical instruments,[207−209] design of sensitive and selective metal sensors using either cost-effective and portable equipment or no equipment at all provides an effective alternative. While rational design of metal sensors has been challenging, the search for metal sensors using combinatorial methods offers new opportunities. As will be clear in the next section, combinatorial selection of DNAzymes may provide a general solution for metal detection. Among the many NAEs, RNA-cleaving DNAzymes are most widely used because they are relatively easy to isolate, generally small in size, have fast reaction rates, and can use versatile signaling methods. As a general consideration, the reaction rate should be greater than 1 min^{-1} to finish the detection in several minutes or less. For metal sensing applications, DNAzymes are preferred over ribozymes because of the relatively high stability, low cost, and ease of synthesis.

2.1. In Vitro Selection of DNAzymes

So far, all known DNAzymes are isolated through in vitro selection.[8,79−83,88,153,182−185] Depending on the nature of each NAE-catalyzed reaction, many methods have been developed to perform such selections; and even for the same reaction, there are many different protocols. Therefore, it is difficult to review all the selection strategies. On the other hand, the selections share the same basic principle of reaction, separation, and amplification (mutation), and it is even possible to perform automated NAE selections with robots.[210] We wish to use the selection of a UO_2^{2+}-specific RNA-cleaving DNAzyme recently reported in our laboratory as an example to illustrate the principle of selection.[22] The DNA pool contained a 50 nucleotide random region (N50 in Figure 1A) flanked by two constant regions (in blue and black). In the middle of this DNA strand, a ribo-adenosine (rA) was introduced as the putative cleavage site, since a ribonucleotide is ∼100,000 fold more susceptible to hydrolytic cleavage than a deoxyribonucleotide. The selection scheme is presented in Figure 1B, and a total of four primers were used in two polymerase chain reactions (PCRs). In the first PCR, P2 and P1 were used to generate a full-length pool, and in the second PCR, rA was introduced by P3. P4 contained a polyethylene glycol (PEG) spacer (denoted as a red dot) that was incorporated into the negative strand without rA to stop the PCR extension.[211] As a result, two strands of unequal lengths were produced, and the positive strand was purified by denaturing polyacrylamide gel electrophoresis (PAGE). UO_2^{2+} was added to search for sequences that could perform the self-cleavage reaction, and the cleaved products were separated by PAGE to seed the next round of selection. To obtain enzymes with high metal affinity, the metal concentration can be decreased after each round of selection.[154] To increase metal specificity, negative selection steps can be introduced to eliminate sequences that are also active with competing metal ions.[204] After the activity of the DNA pool reached a plateau, the DNAs were cloned and sequenced. One of the sequences (clone 39) obtained right after sequencing is shown in Figure 1C.[212] After truncation and rational design of substrate binding sequences, a trans-cleavage DNAzyme was constructed (Figure 1D). The strand containing rA is the substrate (39S),
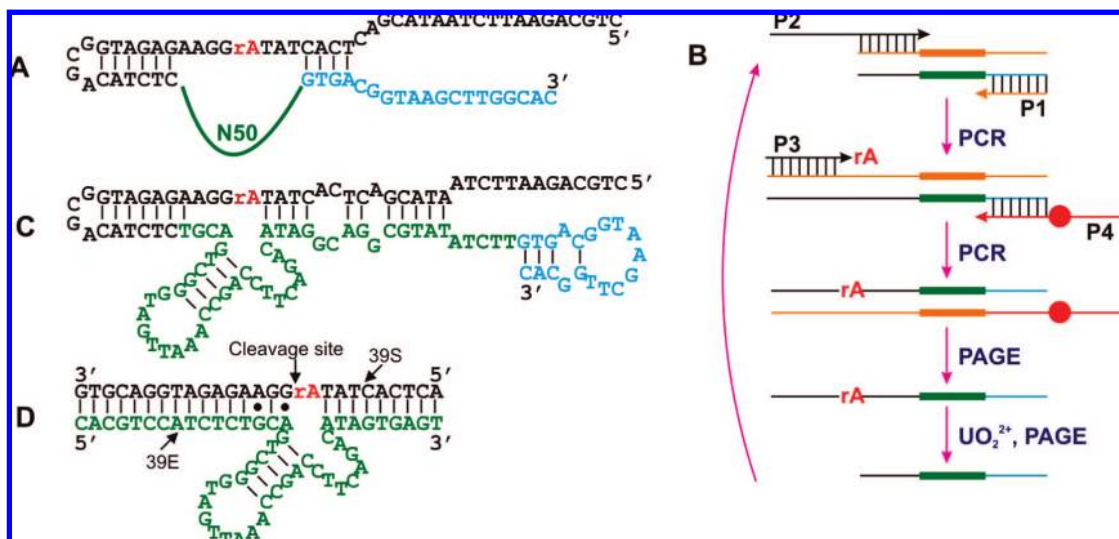
Figure 1. In vitro selection of a UO_2^{2+}-specific DNAzyme. (A) The sequence of the DNA pool for the selection, which contained a 50 nucleotide random region (N50) and a cleavage site (rA). (B) Scheme of the selection procedures. (C) Secondary structure of clone 39 in the cis-cleaving form obtained right after selection. (D) Secondary structure of clone 39 after truncation and rational optimization in the trans-cleaving form. Reprinted with permission from ref 22. Copyright 2007 The National Academy of Sciences.
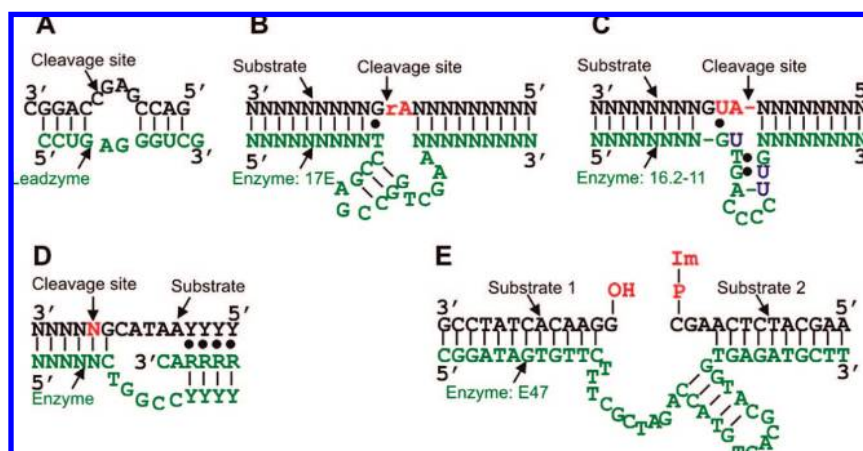
Figure 2. Examples of metal-specific NAEs. In each figure, "N" represents any nucleotide, provided they abide by Watson−Crick base pairing. All the NAEs contain an enzyme strand (in green) and one or two substrate strands (in black). Cleavage and ligation sites are marked in red. (A) The leadzyme: a Pb^{2+}-dependent RNA-cleaving ribozyme. (B) The Pb^{2+}-specific 8−17 DNAzyme. (C) The Zn^{2+}-specific DNAzyme. U in blue denotes C5-imidazole-functionalized deoxyuridine. (D) The Cu^{2+}-specific DNA-cleaving DNAzyme. Y denotes pyrimidine, and R denotes purine. (E) The Cu^{2+}-specific DNA ligation DNAzyme. Im denotes an imidazole group.

and the other strand is the enzyme (39E). In the presence of UO_2^{2+}, 39S is cleaved by 39E and breaks into two fragments. This selection protocol can be adapted to select for NAEs with different properties.[79,81−83,88,184,213] For example, by replacing UO_2^{2+} with another metal ion, DNAzymes with altered metal specificity can be obtained. In addition to gel-based separation of positive and negative strands after PCR, the immobilization of a DNA pool on a column for separation has also been successfully carried out.[153]

2.2. Examples of Metal-Specific NAEs

Most naturally occurring ribozymes employ Mg^{2+} as a metal cofactor, while a number of in vitro selected NAEs showed high specificity for transition metal ions. In addition to the uranium DNAzyme discussed above, some other examples of metal-specific NAEs are presented in Figure 2. The enzyme strands are shown in green, substrate strands in black, and cleavage sites in red. A Pb^{2+}-specific ribozyme known as the Leadzyme selected by Pan and Uhlenbeck is presented in Figure 2A.[125,126] This is one of the smallest

catalytic RNA motifs and requires Pb^{2+} for activity. A Pb^{2+}-dependent DNAzyme, called the 8−17 DNAzyme, is presented in Figure 2B. Interestingly, the same DNAzyme motif has been independently selected under a variety of conditions by several research groups, indicating this sequence has the tendency to dominate the selection pool.[20,21,185,214−217] In a comprehensive study performed by Li and co-workers, the reason for the recurrence of this particular DNAzyme was attributed to its high catalytic rate, its ability to cleave many dinucleotide junctions, its small catalytic core, and its high tolerance to nucleotide mutations.[217] The substrate can be all RNA, or DNA with only a single RNA linkage at the cleavage site (i.e., rA) as shown in the figure. The DNAzyme showed very high activity in the presence of Pb^{2+}.[21] At low metal concentration (nanomolar to low micromolar range), only Pb^{2+} can activate the enzyme. Because of its unique and appealing properties, this DNAzyme has been characterized in detail by many biochemical[21,185,217] and biophysical studies.[218−220] In another example, by introducing imidazole-modified deoxyuridine to extend the chemical functionality

Figure 3. Methods for designing NAE-based fluorescent sensors. (A) The general reaction scheme of a substrate cleaving NAE. (B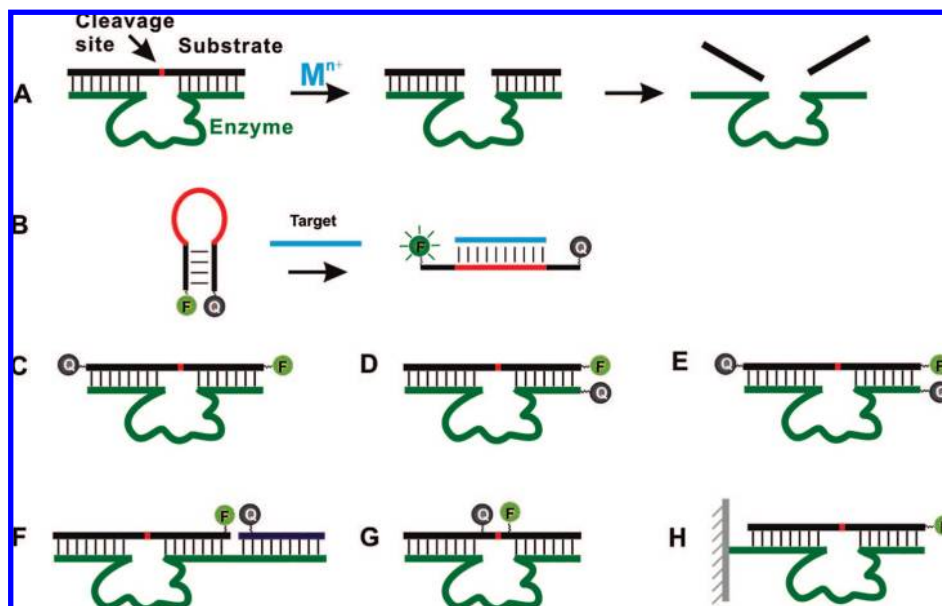) The operation principle of a molecular beacon for DNA detection. (C−G) Various methods in the literature for developing fluorescent NAE sensors (catalytic beacons). (H) Sensing with immobilized NAEs. In each scheme, the substrate, enzyme, and cleavage site are colored with black, green, and red, respectively.

of DNA, and by using Zn^{2+} as a metal cofactor, Joyce and co-workers isolated a Zn^{2+}-specific DNAzyme (Figure 2C). The closest competing metal ion, Cd^{2+}, showed ∼100-fold lower activity compared to Zn^{2+}.[25] Besides RNA-cleaving enzymes, Breaker and co-workers isolated DNA-cleaving DNAzymes using Cu^{2+} as a cofactor (Figure 2D). This DNAzyme catalyzes oxidative cleavage and is highly specific for Cu^{2+}.[23,162,221,222] Metal-dependent ligation enzymes have also been obtained. The DNA ligase in Figure 2E is specific for Cu^{2+}, and with some Zn^{2+} activity at higher metal concentrations.[166] Other metal-specific DNAzymes include DNA phosphorylation[171] and signaling RNA-cleaving DNAzymes,[195,223] isolated by Li and co-workers. Besides metal specificity, NAEs sensitive to other environmental factors such as pH[159] and temperature[224] have also been demonstrated.

2.3. Fluorescent NAE Sensors

Fluorescence detection has high sensitivity.[98,225−227] Many fluorophores can be detected at concentrations lower than 1 nM with common benchtop fluorometers. With more advanced instrumentation, it is possible to detect even single molecule fluorescence. Therefore, the consumption of materials in fluorescent sensors is minimal. In addition, a number of portable fluorometers are commercially available, allowing the use of fluorescent sensors in the field. Fluorescence methods give an immediate response and can often be designed for real time detection without any separation steps. Natural nucleic acids are nonfluorescent, and all fluorescent DNAzyme sensors employ external fluorophores.

2.3.1. Structural Aspects of RNA-Cleaving NAEs

The RNA-cleaving NAEs isolated so far, interestingly, share many similarities in their secondary structures. As can be observed from Figures 1D and 2, all RNA/DNA cleaving NAEs can be separated into substrate and enzyme strands. The cleavage sites on the substrates are flanked by two arms that bind the enzyme strands. Normally, as long as the base pairing interactions are maintained, the content of the

nucleotides can be changed.[228] It is the catalytic core that offers NAE metal specificity. The structure similarity allows the transfer of sensor design knowledge from one NAE to another with high rates of success.

In a typical NAE-catalyzed cleavage reaction (Figure 3A), the substrate and enzyme are first hybridized. In the presence of target metal ions, the annealed substrate is cleaved into two pieces, which subsequently leave the enzyme. As a result, the distance between the two substrate fragments and the distance between the substrate fragments and the enzyme increase during this process, which provides opportunities to use fluorescence energy transfer for signal generation, similar to molecular beacons. A molecular beacon is a single-stranded DNA hairpin with its two ends labeled by a fluorophore and a fluorescence quencher, respectively (Figure 3B).[229−234] The hairpin loop part was designed to be complementary to the target DNA, which forces the hairpin to open when bound to the target and triggers fluorescence increase. Molecular beacons have been successfully applied to nucleic acid detection in many fields of research.[227,229−233] In NAEs, the distance change among nucleic acid strands upon reaction can be even larger compared to the case of molecular beacons. Indeed, the molecular beacon type of signaling method has been successfully adapted to develop NAE sensors. Because catalytic reactions are involved, these signaling NAEs are termed catalytic beacons.[22,186] The term catalytic *molecular* beacon was employed specifically to describe catalytic beacons for oligonucleotide detection.[235]

Unlike molecular beacons, in which limited choices are available for positioning the fluorophore and quencher, there are many different ways to place labeling groups in catalytic beacons. For example, the fluorophore and quencher can be placed at the two ends of the substrate strand (Figure 3C). This strategy represents some of the early works to use fluorophores to replace radioisotopes for monitoring ribozyme kinetics.[236−243] The purpose of these research efforts, however, was not for sensing but rather for kinetics assays or screening. In most of these reports, the quencher was another fluorophore (TAMRA). With a few exceptions,[244,245]
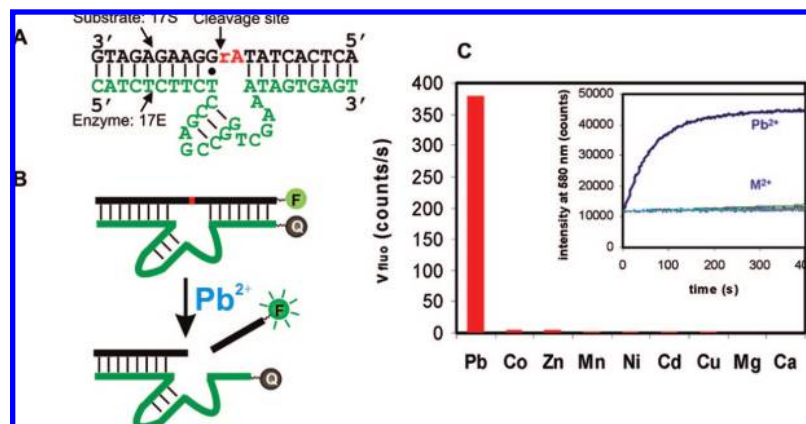
Figure 4. A catalytic beacon Pb^{2+} sensor. (A) The secondary structure of the Pb^{2+}-specific DNAzyme. (B) Schematics of beacon signal generation. (C) Selectivity of the sensor. Inset: Kinetics of fluorescence increase with Pb^{2+} and other divalent metal ions. Reprinted with permission from ref 186. Copyright 2006 American Chemical Society.

the two ends in most nucleic acid enzymes do not approach each other in the uncleaved state. Therefore, the efficiency of quenching may not be very high, resulting in high background fluorescence or low signal increase. Another option is shown in Figure 3D, in which the labels are on the same side but different strands, and in this case, the fluorophore was on the substrate.[186,236,246] Lower background was achieved due to the proximity between the fluorophore and the quencher. However, if the two strands were not 100% hybridized, high background fluorescence would be observed. To overcome this, a second quencher was placed on the other end of the substrate (Figure 3E).[22,188] Therefore, even if the two strands dissociated, the fluorescence was still partially quenched. The modification shown in Figure 3F is similar to that shown in Figure 3D, with the only difference being that the quencher is on another piece of DNA with the extended enzyme part acting as a template to place the quencher close to the fluorophore. This design has not been used in NAEs but in aptazyme signaling that will be described in section 4 later.[247,248] To achieve a high quenching efficiency, the fluorophore and the quencher can be placed right next to the cleavage site on the substrate (Figure 3G).[158−160,195,223,249] Direct modification close to the reaction site, however, may disrupt the catalytic activity of the enzyme because fluorophores and quenchers are relatively bulky. Therefore, systematic tests are needed for optimization.[249] This limitation can be overcome by incorporating both fluorophore and quencher in the process of in vitro selection,[158,159] although once selected, the labels cannot be changed or removed. For immobilized NAEs, since the cleaved and uncleaved substrates are physically separated, quenchers may not be needed for detection.[250,251] As shown in Figure 3H, for example, increased fluorescence in solution will be observed upon cleavage, and only a fluorophore-labeled substrate is needed. In the following sections, applications of catalytic beacons for metal sensing are presented.

2.3.2. Catalytic Beacons with Terminus Labels

2.3.2.1. Catalytic Beacons with a Single Quencher. The 8−17 DNAzyme is highly specific for Pb^{2+}.[21] We first employed the catalytic beacon design shown in Figure 3D to construct a fluorescent Pb^{2+} sensor.[186] The DNA sequence used in this study is shown in Figure 4A. A fluorophore (TAMRA) was labeled on the 5′-end of the substrate, and a quencher (Dabcyl) was labeled on the 3′-end of the enzyme

(Figure 4B). In the presence of Pb^{2+}, the fluorophore-labeled substrate was cleaved and released from the quencher with a ~300% increase in fluorescence observed at 4 °C (inset of Figure 4C). The detection limit was 10 nM, which is lower than the US EPA defined maximum contamination level for lead in drinking water (72 nM). The selectivity over Zn^{2+} and Co^{2+} (the most competitive metal ions) was higher than 80-fold, while the selectivity over other metal ions (i.e., Mg^{2+} and Ca^{2+}) was higher than 1000-fold.

Because chemical transformations take place in enzymatic reactions, such detection processes are usually irreversible and regeneration of the sensor by adding new substrates is needed after each detection application. On the other hand, NAE sensors also possess a number of advantages. For example, since only the kinetics of fluorescence enhancement is monitored, the detection is less affected by background fluorescence in environmental samples. Additionally, because catalytic reactions are responsible for signal generation, each Pb^{2+} ion can turnover multiple catalytic beacons to improve sensitivity.

2.3.2.2. Catalytic Beacons with Dual Quenchers. In the above Pb^{2+} sensor, the data were collected at 4 °C.[186] At room temperature, partial dissociation of the substrate from the enzyme strand occurred, resulting in a relatively high background fluorescence and only ~60% fluorescence increase upon cleavage. To reduce background, a new design with two quenchers (Figure 3E) was employed, and an over 6-fold fluorescence increase was observed at room temperature, which represents a 10-fold increase in performance compared to the old design.[188] Further background suppression was achieved by elongating the substrate binding arm lacking the fluorophore while keeping the other arm the same length, thus generating asymmetric substrate binding arms; an over 10-fold fluorescence enhancement can be routinely achieved with this design (Liu and Lu, unpublished results).

While most sensors used for on-site and real-time detection are not expected to compete with instrumental analysis, we recently reported another catalytic beacon for UO_2^{2+} whose performance exceeded that of many analytical instruments (Figure 5A).[22] This beacon incorporated asymmetric substrate binding arms and dual quenchers (Figure 5B). A 15-fold increase in fluorescence was observed at room temperature. A detection limit of 45 pM for UO_2^{2+} was achieved (insets of Figure 5C), which is much lower than those of most analytical instruments (e.g., ICP-MS for uranium has a detection limit of 420 pM).[252] The toxic level of uranium in
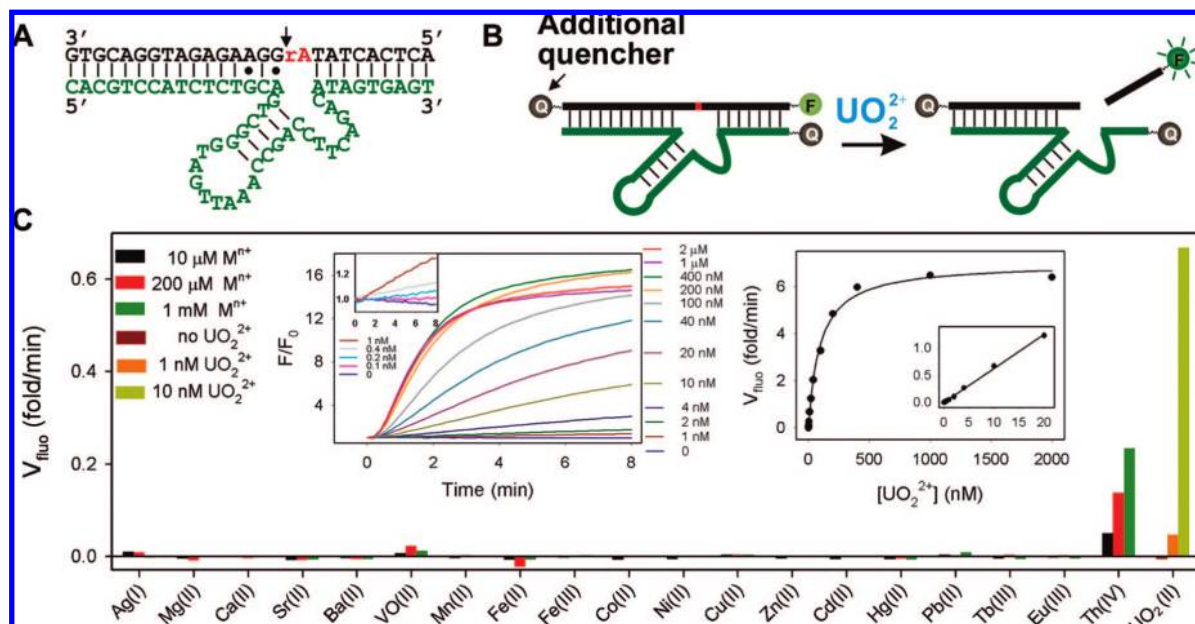
Figure 5. A catalytic beacon UO_2^{2+} sensor. (A) The secondary structure of the UO_2^{2+}-specific DNAzyme. (B) Schematics of beacon signal generation. (C) Selectivity of the sensor. Inset: Kinetics of fluorescence increase with varying concentrations of UO_2^{2+} and UO_2^{2+} quantification. Reprinted with permission from ref 22. Copyright 2007 the National Academy of Sciences.
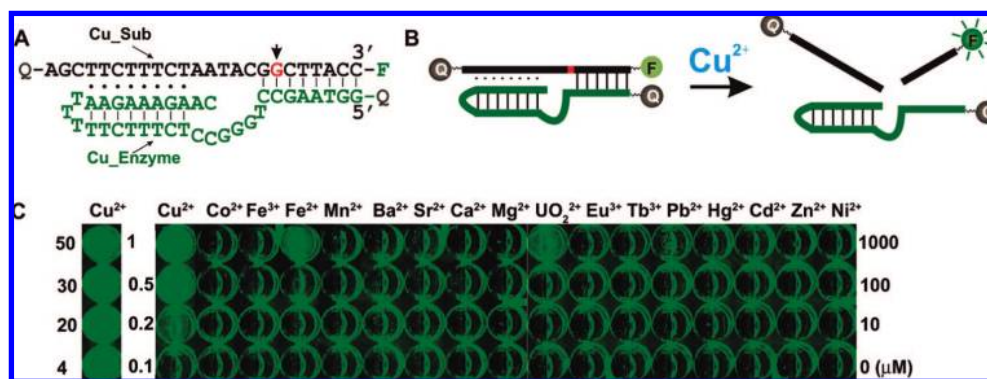
Figure 6. A catalytic beacon Cu^{2+} sensor. (A) The secondary structure of the Cu^{2+}-specific DNAzyme labeled with fluorophore and quenchers. (B) Schematics of beacon signal generation. (C) Selectivity of the sensor. The numbers represent metal concentrations in μM. Reprinted with permission from ref 222. Copyright 2007 American Chemical Society.

water was defined by the U.S. Environmental Protection Agency (EPA) to be 130 nM, which is covered by the dynamic range of the sensor. This sensor also has a selectivity of more than one-million-fold over any other metal ions (Figure 5C).

One of the biggest challenges in fluorescent metal sensor design is sensing paramagnetic metal ions (i.e., those metal ions with unpaired electrons) such as Cu^{2+}, due to their intrinsic fluorescence quenching properties. One way to circumvent this quenching problem is to spatially separate the metal recognition part from the fluorophore so that they are independent of each other. A significant challenge then is to transduce metal binding to signal enhancement when the two parts are well separated. The catalytic beacon approach is ideally suited for such a system. Breaker and co-workers have isolated and characterized a series of Cu^{2+}-dependent DNA-cleaving DNAzymes, and their common structures are shown in Figure 2D.[23,162,221] Based on previous experience in catalytic beacon design, we have constructed a highly sensitive and selective Cu^{2+} sensor. The DNAzyme sequence is shown in Figure 6A, and the cleavage site is the guanine marked in red. The catalytic beacon design presented in Figure 6B showed ~13-fold fluorescence enhancement

in the presence of Cu^{2+} and a detection limit of 35 nM Cu^{2+}, which is much lower than the 20 μM toxic level defined by the US EPA. Only Fe^{2+} and UO_2^{2+} showed a signal at 1 mM concentration (Figure 6C), and over 2,000-fold selectivity for Cu^{2+} was achieved.

2.3.3. Catalytic Beacons with Internal Labels

2.3.3.1. Rational Design Method. The ideal positions to place a fluorophore and quencher would be next to the cleavage site as shown in Figure 3G, so that the initial fluorescence is greatly suppressed. The background problem from incomplete hybridization can also be eliminated. To test the effect of such a labeling method, Chiuman and Li systematically attached different fluorophore-quencher pairs at various locations on the substrate of the 8−17 DNAzyme as shown in Figure 7.[249] Two different quenchers (QSY9 and QSY21) and three different fluorophores (AF488, AF546, and AF647) were tested at different positions, where AF denotes Alexa Fluorophores. Interestingly, the DNAzyme can still perform the cleavage reaction in most of the constructs tested. The highest fluorescence enhancement reached 85-fold with a maximum cleavage of 75%. Gener-

Figure 7. Signaling performance of the 8−17 DNAzyme (boxed) modified with Alexa Fluorophores (AF) and QSY quenchers at various locations. (A−D) For each AF-QSY pair, 12 different substrates were prepared. Each design was tested on three parameters: max F/F_o (maximum fluorescence enhancement), Y_{max} (maximum percentage of cleavage), and $t_{1/2}$ (the time required to reach half of the signaling maximum). Reprinted with permission from ref 249. Copyright 2007 Oxford University Press.

Figure 8. (A) Schematic of in vitro selection of signaling DNAzymes. See text for descriptions. (B) Secondary structure of the DET22−18 DNAzyme. F and Q are fluorescein and Dabcyl, respectively. Reprinted with permission from ref 158. Copyright 2003 American Chemical Society.

ally, placing the labels closer resulted in higher signal gain but slower cleavage rate, while the final yield of the reaction was less affected. This work demonstrated that it is possible to modify NAEs with fluorophore/quencher pairs flanking the cleavage site on the substrate. To achieve the optimal design, however, a number of combinations need to be tested.

2.3.3.2. Combinatorial Selection Method. During selection for RNA-cleaving DNAzymes, if a fluorophore and a quencher are incorporated immediately adjacent to the cleavage site as shown in Figure 3G in the random pool, the resulting NAEs can be used as sensors right after selection, and no further labeling or optimization steps are needed. Li and co-workers first demonstrated this strategy experimentally, and a representative scheme of performing such a selection is shown in Figure 8A.[158,159] A random sequence pool of single-stranded DNA was first phosphorylated at the 5′-end (I), followed by ligation to a piece of oligonucleotide

containing three functionalities (II): a cleavage site as indicated by an arrow (rA), a fluorescein-labeled deoxyribothymidine on the 5′-side (F), and a Dabcyl-labeled deoxyribothymidine on the 3′-side (Q). The ligated molecules were purified by denaturing PAGE (III). At this step, divalent metal ions were added to select for sequences that could perform self-cleavage reactions (IV). The cleaved DNAs were then isolated by PAGE (V) and amplified by PCR (VI). Another PCR step was carried out in step (VII) with a ribo-terminated primer P3 that introduced a ribonucleotide into the double-stranded PCR product. The PCR products were treated with NaOH (VIII) to cleave at the ribonucleotide position, and two strands of different lengths were generated, which were separated by PAGE (IX). The positive strand was phosphorylated at the 5′-end (X) and subject to the next round of selection. After achieving satisfactory pool activity, the downstream procedures were similar to classical selec-

tions described previously. Li and co-workers have performed two systematic selections with such a protocol. In the first selection, a single class of DNAzyme was found in the round 22 selection pool, and the trans-cleaving form of clone 18 DNAzyme (DET22−18) is shown in Figure 8B. This DNAzyme showed ∼13-fold fluorescence enhancement and a k_{cat} value of ∼7 min^{-1},[158] which represents one of the fastest DNAzymes.[20,21] A number of other DNAzymes were also obtained along the selection pathway.[160,223]

In the second experiment, eight rounds of selection were first carried out at pH 4.0 and the pool was subsequently divided into five parallel selections with different pH's ranging from 3.0 to 7.0.[159] Interestingly, the dominant species under each selection condition had the highest activity at the pH they were selected, except for the ones obtained at pH 7.0, whose activity increased as the pH was increased. Detailed biochemical characterizations were performed on these DNAzymes to elucidate their sequence requirements, secondary structures, and activities.[253−257]

2.3.4. Immobilized DNAzymes

In all the NAE sensors reviewed above, the reactions were carried out in the solution phase, and signal generation was made possible by fluorescence quenching and dequenching. Surface immobilization of NAEs provides an alternative means for sensor design (Figure 3H), and it has a number of advantages. For example, immobilization is an important step toward making sensor devices. If the enzyme strand is attached to the surface as shown in Figure 3H, the unhybridized substrate strands can be washed away to eliminate background. Immobilization also allows sensor regeneration and long-term storage, and the signal can be observed either in solution or on the surface. The Pb^{2+}-specific 8−17 DNAzyme was covalently attached to a gold surface. In the presence of Pb^{2+}, a fluorophore-labeled substrate fragment was released into solution for the detection. Due to a very low background, a detection limit of 1 nM was achieved, which is 1 order of magnitude better than that of a solution-based sensor.[250] Gold-coated nanocapillary membranes were also used for DNAzyme immobilization, and enzyme activity was retained even after storing in a dried state for 30 days at room temperature;[251] detailed characterizations on this system were reported.[258] In a collaborative work between the Lu, Kane, and Dordick groups, the DNAzyme was immobilized onto carbon nanotubes, which formed a highly stable hybrid and maintained high activity.[259] Over 400 turnovers were observed for each DNAzyme. Such high activity may allow many applications ranging from the directed assembly of nanotubes to nanoscale cellular therapeutics. In addition to covalent immobilization, Shen et al. entrapped fluorescent signaling DNAzymes in silica gel and metal detection was demonstrated.[195]

Micro- and nanofluidic devices are also promising platforms for a number of applications including sensing. The Pb^{2+}-specific DNAzyme was placed in a microfluidic mother board,[260] and <1 nL of DNA was needed to monitor the cleavage reaction for Pb^{2+} sensing. The same DNAzyme was also assayed in a nanofluidic device containing two perpendicular channels interfaced by a nanocapillary array interconnect. This voltage controlled device was capable of detecting 11 nM of Pb^{2+}.[261]

2.3.5. A DNAzyme with Peroxidase Activity for Signal Amplification

In previously introduced DNAzymes, all the substrates are oligonucleotides. Similar to protein enzymes, some DNAs are capable of recruiting hemin as a cofactor with peroxidase activity and thus can turnover nonoligonucleotide substrates. Sen and co-workers performed an aptamer selection against *N*-methylmesoporphyrin IX (NMM) and isolated a number of guanine rich aptamers.[32] Later, it was found that these aptamers could act as DNAzymes to catalyze porphyrin metalation.[176] The best characterized sequence (PS5.M) contained 24 nucleotides, and rational design led to an 18-nucleotide sequence (PS2.M), which was found to be even more superior in catalyzing porphyrin metalation. Further characterization found that the PS2.M/hemin complex has peroxidase activity.[262] Compared to free hemin, the DNAzyme had 250-fold enhanced peroxidase activity. The proposed secondary structure of PS2.M with hemin is shown in Figure 9A.[177,262−264] As a result, common substrates for monitoring peroxidase activities can also be applied here to monitor DNAzyme activity. For example, this enzyme can catalyze the conversion of luminol in the presence of hydrogen peroxide with the emission of chemiluminescence (Figure 9A). It can also oxidize ABTS (2,2′-azino-bis(3-ethylbenzthiazoline-6-sulfonic acid)) into its radical form (ABTS$^{•+}$), which displays a green color. Given that one DNAzyme can turnover a large number of substrates, signal amplification can be achieved.

The Willner group pioneered the application of this peroxidase DNAzyme for signal amplification in analytical applications.[265,266] For example, as schematically shown in Figure 9B, the DNAzyme was split into two halves with each half containing an extension, and the extended parts were designed as probes to hybridize with target DNA.[267] In the presence of the target DNA, the three DNAs formed two double stranded regions with the DNAzyme halves as overhangs, which were sterically confined and could not form the active DNAzyme complex. Only when the target DNA was absent, could the DNAzyme complex form to produce a chemiluminescence signal in the presence of luminol and hydrogen peroxide. This system showed a decreased signal in the presence of the target, which was undesirable analytically. It also had a poor detection limit of 600 nM. The researchers then made a number of improvements to this system. As shown in Figure 9C, a hairpin was constructed in such a way that a fraction of the DNAzyme sequence was hybridized in the stem region and the DNAzyme could not fold into its active conformation. In the presence of target DNA, the hairpin was opened and the active DNAzyme was allowed to form. This design has a detection limit of 200 nM and is a "turn on" sensor.[268] Further improvement came from using the target DNA as a linker to bridge a surface immobilized DNA with the DNAzyme (Figure 9D), and a detection limit of 1 nM was achieved.[269] By immobilizing the DNAzyme onto AuNPs (Figure 9D), the signal could be further enhanced because many DNAzymes were attached to one nanoparticle. A detection limit of 0.1 nM was reported for this method.[270]

Even larger signal amplification can be achieved by coupling the DNAzyme peroxidase reaction with other catalytic reactions, such as DNA polymerization. A scheme of using such a concept to detect the M13 phage DNA is shown in Figure 9E.[271,272] The M13 phage has a single-
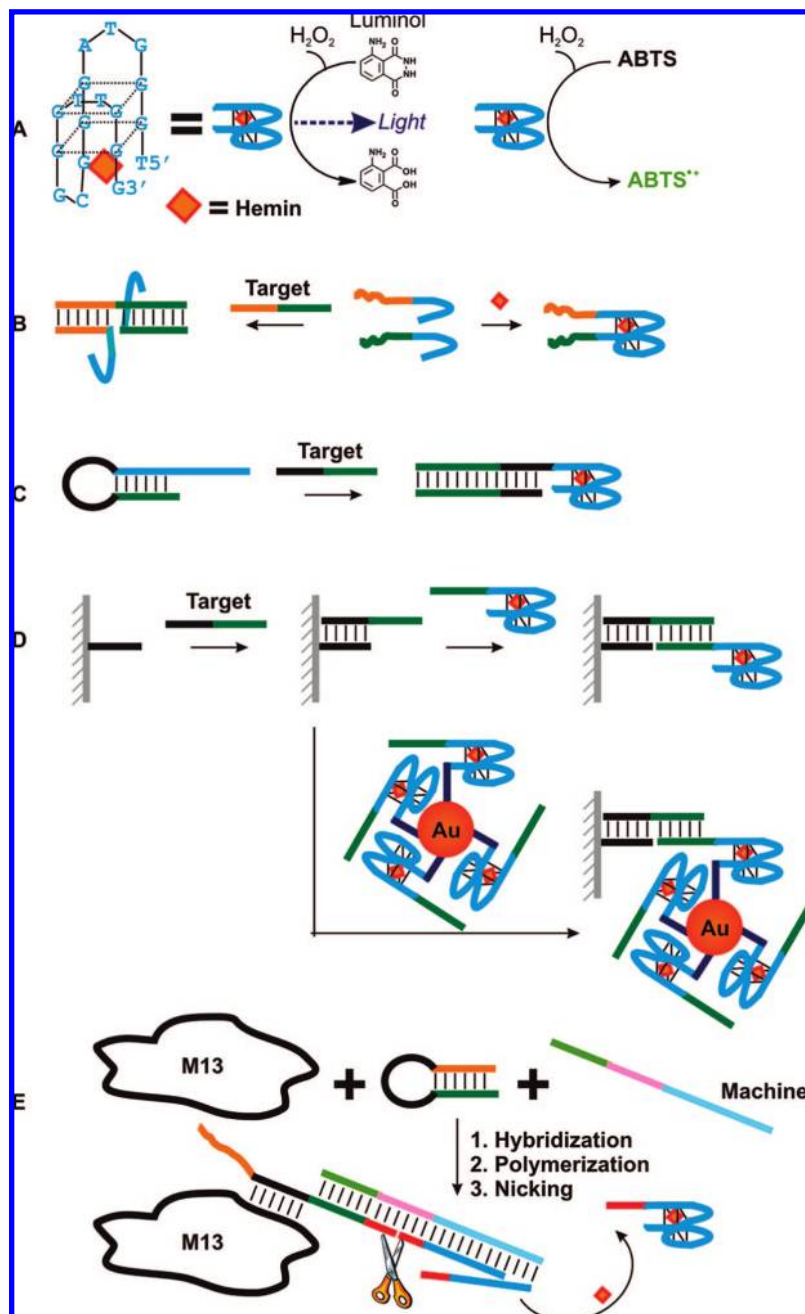
Figure 9. Sensing with a peroxidase DNAzyme for signal amplification. (A) Proposed secondary structure of the 18-nucleotide peroxidase DNAzyme (left); the DNAzyme can catalyze the conversion of luminol with chemiluminescence generation (middle) and the conversion of ABTS with color generation (right). DNA detection based on inhibited DNAzyme activity (B), opening a hairpin to free the DNAzyme domain (C), or with target DNA mediated DNAzyme immobilization and AuNPs for signal amplification (D). (E) Detection of M13 DNA by coupling PCR with the DNAzyme peroxidase reaction for signal amplification.

stranded circular DNA genome. A DNA hairpin was designed in such a way that its loop region acted as a probe to hybridize with a fraction of the M13 DNA. Upon opening the hairpin, one of the stem regions (in green) served as a primer to hybridize to another piece of DNA called the "machine" to initiate polymerase chain reactions in the presence of a DNA polymerase. A nick site was engineered into the machine DNA (in red) so that the polymerized strand was cut by the N.BbvC IA enzyme and displaced by newly polymerized ones. The displaced fragment contained the DNAzyme sequence and thus could generate either a luminescence or colorimetric signal. This system therefore contained two coupled catalytic reactions and could detect the M13 DNA down to the 0.01 pM level. In another work

by the same group, the displaced fragment was used to open molecular beacons for cocaine detection.[273] Similarly, rolling circle amplification was used for signal amplification, which has been demonstrated by both the Willner and the Mao groups.[274,275] Coupling the peroxidase DNAzyme to protein enzymes has also been demonstrated.[276] Tolemerase produces telomere repeats at the 3′-end of the linear chromosomes. Its activity in cancer cells is unusually high and therefore can be a useful cancer marker. The DNA strand generated by telomerase can be probed by the DNAzyme in a similar manner. Detection limits down to 5000 HeLa cells (cervical cancer cells) were achieved with the peroxidase DNAzyme as the signaling group.[267−270]
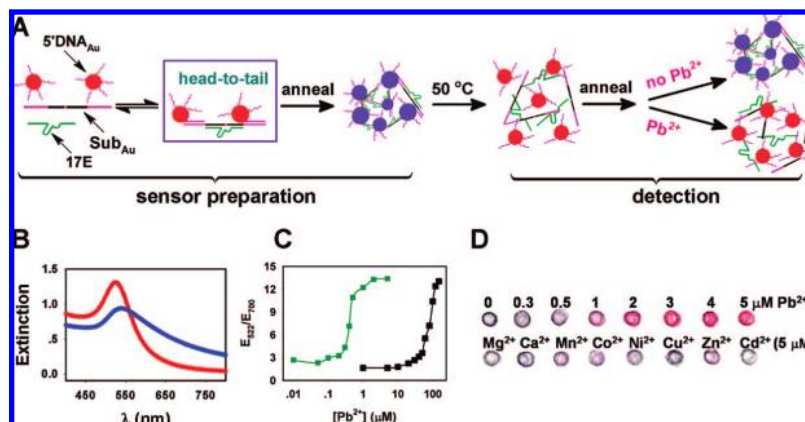
Figure 10. DNAzyme and AuNP-based colorimetric Pb^{2+} detection. (A) Pb^{2+}-directed assembly of DNAzyme-linked AuNPs aligned in a head-to-tail manner. (B) UV−vis spectra of disassembled (red) and assembled (blue) AuNPs. (C) The assembly state or color of AuNPs in response to Pb^{2+} concentration. (D) Color of the AuNPs in the presence of different divalent metal ions. Reprinted with permission from ref 187. Copyright 2003 American Chemical Society.

2.4. Colorimetric NAE Sensors

In a colorimetric sensor, a color change is observed in the presence of target analytes. Compared to other detection methods, colorimetric sensors may minimize or even eliminate the need for analytical instruments, which can make on-site detection more manageable.[277] Native nucleic acids do not show absorption in the visible region, and the construction of a colorimetric aptamer sensor requires the introduction of color reporting groups. The most frequently used color reporting groups include small organic dyes, conjugated polymers, and metallic nanoparticles.

2.4.1. First-Generation Colorimetric Pb^{2+} Sensor

Metallic nanoparticles display strong distance-dependent optical properties and very high extinction coefficients, and therefore, they are useful for developing colorimetric sensors. We employed DNA-functionalized AuNPs for DNAzyme-based Pb^{2+} detection.[187] The substrate strand (see Figure 4A for the original DNAzyme) was extended on both ends (pink fragments on Sub_{Au}, Figure 10A) so that it could bind onto the DNA-coated AuNPs. Only one kind of DNA-functionalized AuNPs were used, and the nanoparticles were aligned in a head-to-tail manner. A heating-and-cooling process (called annealing) was needed to form such aggregates. The aggregates should have the right ratio between the DNAzyme and AuNPs, such that any further cleavage of the DNAzyme would be reflected by the changes in the optical properties of the nanoparticles. Upon heating to 50 °C, the AuNPs and DNAzyme disassembled. The subsequent cooling process was controlled by Pb^{2+}. If Pb^{2+} was present, the substrate would be cleaved and reassembly was inhibited, giving a red color. Otherwise, AuNPs were reassembled to form blue aggregates. The color change could be conveniently monitored by UV−vis spectroscopy (Figure 10B). Upon assembly, the extinction at the 522 nm plasmon peak decreased while extinction at the 700 nm region increased. To quantify the color of AuNPs, the extinction ratio at 522 nm over 700 nm was used. A high ratio is associated with dispersed particles of red color, and a lower ratio is associated with aggregated particles of blue color. With increasing Pb^{2+} concentration, the extinction ratio increased, consistent with a blue-to-red color change (Figure 10C, green squares). A detection limit of ~100 nM was achieved, and the sensor was able to detect lead extracted from paint.[187] The color change could also be

conveniently observed by spotting the sensor solution onto a TLC plate (Figure 10D). Only Pb^{2+} produced a red color, but not other metal ions, suggesting high metal specificity.

2.4.2. Tunable Detection Range

Every sensor has a dynamic range, which by design, is rarely tunable to match the needs of different applications. A sensor allowing simple tuning of dynamic range is highly desirable if the sensor is to be used in practical applications. For example, the US EPA defined toxic threshold for lead in paint is ~2 μM, while the threshold for lead in drinking water is 72 nM. Practitioners such as house inspectors and home owners prefer sensors that change color right at the threshold. A sensor with a tunable dynamic range is required to match the threshold of different applications without having to reselect and redesign new sensors. Such dynamic range tuning is also quite valuable when federal agencies change the threshold levels. Taking advantage of the multiple turnover property of DNAzymes, we have demonstrated a general scheme for tuning the dynamic range of the colorimetric Pb^{2+} sensor system. By changing the G•T wobble pair to a G-C Watson−Crick pair (Figure 4A, highlighted by a dot), DNAzyme activity is abolished.[21] Nonetheless, the mutated DNAzyme could still assemble AuNPs with an efficiency similar to that of the native DNAzyme. When only a small fraction of the active enzyme was used (i.e., 5%), with the rest being the inactive enzyme, the Pb^{2+}-sensitive range shifted to ~1 order of magnitude higher Pb^{2+} concentrations (Figure 10C, black curve). And the dynamic range can be readily tuned to a desirable level through combining different fraction of active and inactive DNAzymes. This tuning property is unique and useful for DNAzyme and nanoparticle based sensors, because it allows detection of Pb^{2+} in a wide concentration range without worrying about signal saturation.[187]

2.4.3. Improved Colorimetric Sensor Designs

The reason that an annealing step was needed to form AuNP aggregates in the above system was attributed to the AuNP alignment.[190,191] Despite that only one kind of AuNP was required, the head-to-tail system suffered from high steric effects. Indeed, by changing the alignment to tail-to-tail, aggregation at a constant temperature was observed.[191] However, with 13 nm diameter AuNPs, the rate of color
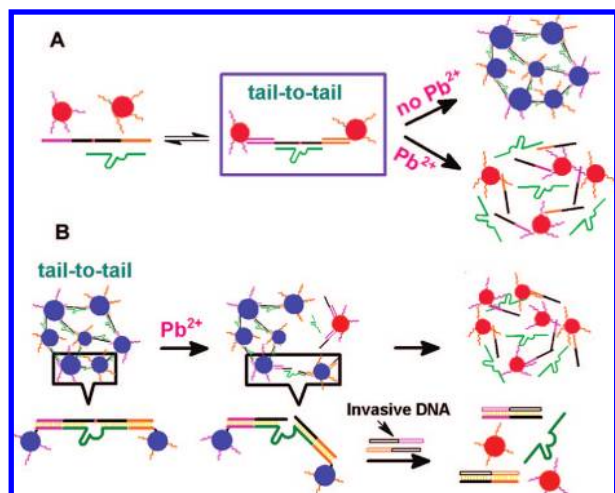
Figure 11. (A) Pb^{2+}-directed assembly of DNAzyme-linked AuNPs aligned in a tail-to-tail manner. (B) Pb^{2+} detection based on Pb^{2+}-induced disassembly of DNAzyme-linked AuNPs. Invasive DNA was used to accelerate the rate of color change. Reprinted with permission from ref 192. Copyright 2005 American Chemical Society.

change was relatively slow. In contrast, when 42 nm AuNPs were used, a distinct color change could be observed in 5 min. Similarly, Pb^{2+} was used to control the assembly state of AuNPs (Figure 11A). In the presence of a high concentration of Pb^{2+}, no color change was observed due to cleavage of the substrate, while in the absence of Pb^{2+}, a red-to-blue color transition was observed. Therefore, this system is useful for fast colorimetric sensing of Pb^{2+}.[191] One disadvantage is that no color change was observed in the presence of Pb^{2+}, while color change to blue was observed only in the absence of Pb^{2+}. From the sensing point of view, this is not a "light-up" sensor. To address this problem, Pb^{2+}-induced disassembly of AuNP aggregates was investigated (Figure 11B).[192,194] Interestingly, it was found that the DNAzyme was inactive in head-to-tail aligned aggregates, while the activity was maintained in tail-to-tail aligned ones, which showed Pb^{2+}-dependent color change.

To accelerate Pb^{2+}-induced color change, small pieces of DNA (called invasive DNA) complementary to the cleaved substrate strands were employed to facilitate AuNP release. Under optimized conditions, a blue-to-red color change was observed in 5 min at room temperature in the presence of Pb^{2+}.[192] Recently, we further optimized the disassembly conditions by designing asymmetric substrate binding arms so that disassembly can occur right after cleavage and no invasive DNA was needed.[194,203] Similar nanoparticle-based colorimetric sensors for uranium detection were also prepared based on the uranyl-specific DNAzyme.[278]

Taking advantage of the fact that the DNAzyme cleavage reaction can produce short DNA pieces, and such short DNA can protect bare AuNPs from salt-induced precipitation, we have designed label-free colorimetric sensors for Pb^{2+} and UO_2^{2+}. Detection limits of 3 nM for Pb^{2+} and 1 nM for UO_2^{2+} were obtained.[278,279] Similar DNAzyme-based Pb^{2+} sensors were also reported by the Dong and Wang groups.[280] The salt stability based on the length of DNA attached to AuNP surface was also utilized for sensing applications. After enzymatic cleaving of a DNA or RNA substrate, the nanoparticles had lower stability and formed aggregates. A Pb^{2+} sensor based on the 8−17 DNAzyme was demonstrated.[281] Detailed descriptions on such lable-free systems are presented in section 3.4.5.

While the above cleavage-based DNAzyme sensors are useful for metal detection, such sensors are vulnerable to interferences in samples that can cause nonspecific nucleic acid cleavage. In addition, because AuNP aggregates contain many DNAs cross-linked with each other, it requires many cleavage events before the aggregates are fully dispersed, making fast detection difficult. In order to address these issues, we also tested a Cu^{2+}-dependent ligation DNAzyme for Cu^{2+} detection, because much fewer interfering species can catalyze ligation reactions, and ligation generates new species against almost zero background to give high sensitivity.[282]

2.5. Electrochemical NAE Sensors

In addition to optical sensors, electrochemical-based detection methods have also been employed to design NAE sensors. Several factors make such sensors attractive in terms of practical applications. Electronic devices can be routinely miniaturized in terms of size and power consumption. Unlike fluorescence-based detection, the instrumentation cost associated with electrochemical detection is much lower. Electronic devices can usually offer ultrahigh sensitivity, good reproducibility, and fast response. Recently, Plaxco and co-workers immobilized the Pb^{2+}-specific 8−17 DNAzyme onto a gold electrode through the 5′-end of the enzyme strand and a methylene-blue (MB) group was attached to the 3′-end (Figure 12A).[283] Hybridization with the substrate strand made the DNAzyme rigid and the MB group was held away from the surface, resulting in a low rate of electron transfer. In the presence of Pb^{2+}, the substrate was cleaved and released, making the immobilized enzyme more flexible with enhanced electron transfer observed. Similar to the optical sensors based on the same DNAzyme, this electrochemical sensor was also highly selective for Pb^{2+} (Figure 12B). A detection limit of 300 nM was reported and the sensor was capable of detecting Pb^{2+} in soil samples (Figure 12C).

3. Aptamer-Based Sensors

3.1. Combinatorial Selection of Aptamers

As described above, NAE-based metal sensors are highly sensitive and selective. The fluorescent sensor for uranyl (UO_2^{2+}), for example, has a detection limit of 45 pM or 11 parts-per-trillion, rivaling that of most analytical instruments. These NAE sensors, however, are used mainly for metal ion detection because NAE catalyzed reactions usually only employ metal ions as cofactors. Although metal independent[155] and histidine dependent[284] NAEs are known, the rates of these enzymes are several orders of magnitude slower compared to those of most metal-dependent enzymes, and they are therefore not yet practically useful for sensing applications. Aptamers, on the other hand, can effectively bind essentially any molecule of choice. This part reviews the research efforts on using aptamers for sensing applications.

Most aptamers are obtained by SELEX.[6,7] Excellent reviews on SELEX are available in the literature;[8,285] thus, only a brief introduction is presented here. In a typical DNA aptamer selection (Figure 13), for example, a large single-stranded DNA library (up to 10^{15} random sequences) is incubated with a target molecule to allow the binding reaction to occur (step I). The bound and unbound DNAs are subsequently separated (II). For small molecule targets, the separation is usually achieved using affinity columns by
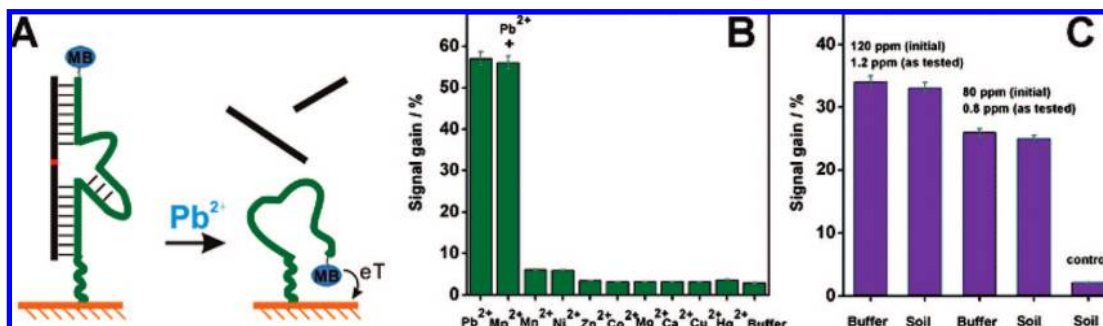
Figure 12. Electrochemical Pb^{2+} detection. (A) Schematics of the sensor design. (B) Metal-dependent sensor response. (C) Detection of Pb^{2+} in soil samples. Reprinted with permission from ref 283. Copyright 2007 American Chemical Society.
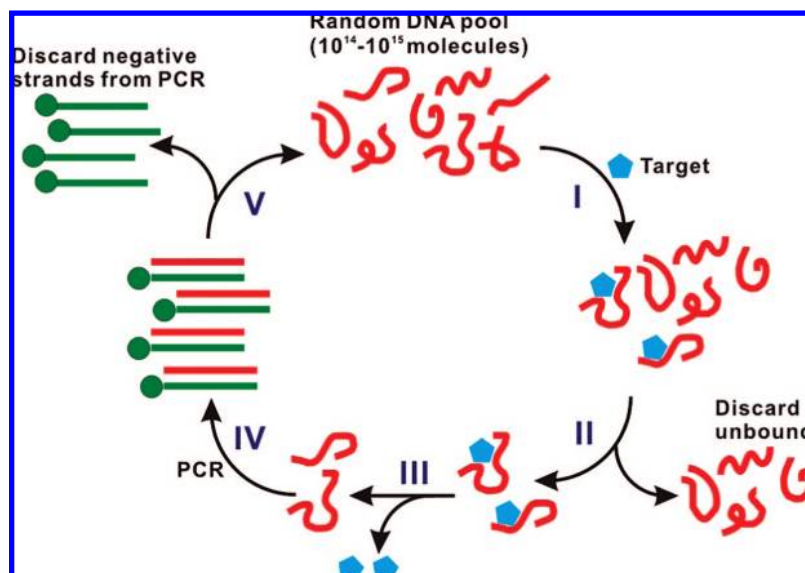

Figure 13. Schematic presentation of a DNA aptamer selection process.

covalently attaching the target molecule onto the column and washing away unbound DNA. For protein targets, the separation can be realized by filtration where protein and bound DNAs are retained. Next, the bound DNAs are dissociated from target molecules (III) and amplified by a polymerase chain reaction (PCR) to generate double-stranded DNA (IV), while only one of the two strands contained the binding sequence (in red). During this PCR process, one of the primers is usually modified either with biotin, a ribonucleotide, or an organic spacer to facilitate the separation of the two strands (V). Finally, the amplified binding strands form the starting point of the new pool for the next round of selection. After achieving the desired performance, the pool is cloned and sequenced, and individual clones are analyzed to identify the conserved binding sequence. To select RNA aptamers, additional steps of in vitro transcription and reverse transcription are needed to interconvert between DNA and RNA, since PCR is only possible for DNA. Mutations can be introduced by error prone PCR to further increase sequence diversity.

Since its conception, aptamer SELEX has experienced many innovations, most of which focused on the separation of bound and unbound DNA. For example, affinity columns, filters, magnetic beads,[286,287] gel electrophoresis, capillary electrophoresis,[42,43,49,288–294] surface plasmon resonance,[295] and atomic force and fluorescence microscopy[296] have all been tested. Automated parallel selections with robots[297–300] and microfluidic devices have also been demonstrated.[301] One of the latest developments is to immobilize a short DNA to

a column and then hybridize a long random DNA pool to the short DNA. DNAs that bind the target molecule strongly through structural switching will fall off the column and be collected. This method eliminates the need to immobilize target molecules, which is often difficult or expensive to carry out.[302] Overall, selection of aptamers is now a relatively common practice that has been conducted successfully in many laboratories around the world.

3.2. Two Model Targets and Their Aptamers

Because many aptamer sensor designs are tested as proof-of-concept studies, and two target molecules, thrombin and ATP (or adenosine), have been mostly used to build such model systems, aptamers for these two molecules are introduced first.

3.2.1. DNA Aptamers for Thrombin

Thrombin is an important serine protease in the blood coagulation cascade. It has a fibrinogen-recognition exosite and a heparin-binding exosite (Figure 14A).[303] In 1992, the first DNA thrombin aptamer was isolated by Bock and coworkers,[45] and the most active strand was a 15-mer oligonucleotide with a K_d around 100 nM (Figure 14B). The structure of the aptamer was determined to be an intramolecular G-quadruplex,[304–306] which interacts with the fibrinogen-recognition exosite. Crystallographic data also suggested that the same aptamer could interact with the herapin binding
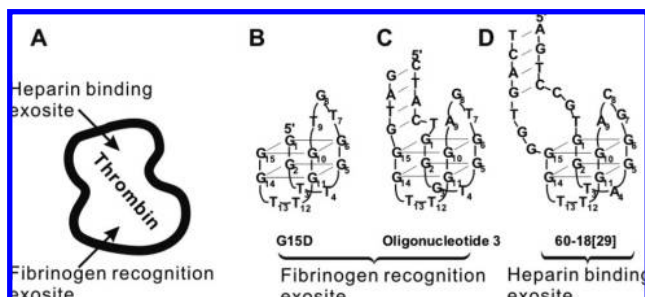
Figure 14. DNA aptamers against thrombin. (A) Schematic representation of the two sites on thrombin that interact with aptamers. (B) The 15-mer aptamer with a G-quadruplex structure targeting the fibrinogen-recognition exosite.[45] (C) Aptamer with an additional duplex region targeting the fibrinogen-recognition exosite.[308] (D) Aptamer targeting the heparin-binding exosite.[310]
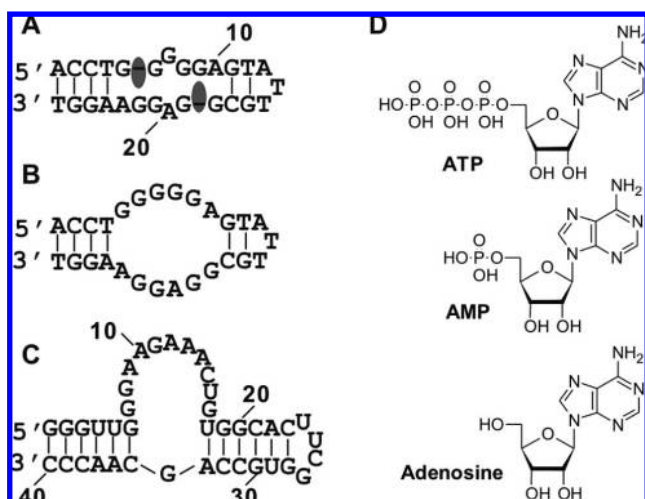

Figure 15. (A) The ATP-binding DNA aptamer with bound ATP.[30] (B) An alternative way of drawing the aptamer in part A. (C) The ATP binding RNA aptamer.[313] (D) Structures of ATP, AMP, and adenosine.

exosite.[307] The same selection was also independently carried out by Macaya and co-workers, and new aptamer structures were obtained with higher affinities ($K_d = 10-25$ nM) that consist of a duplex region in addition to the quadruplex (Figure 14C).[308] Similar selection results were also obtained by Tsiang and co-workers.[309] All these three selections employed the same selection strategy by attaching thrombin to concanavalin A-agarose. Later, a different partition method was used by Tasset and co-workers where a nitrocellulose filter was employed to separate thrombin bound DNA and free DNA. Interestingly, very high affinity aptamers ($K_d = 0.5$ nM) that bound to the herapin binding exosite were isolated (Figure 14D).[310] RNA aptamers for thrombin have also been obtained.[311]

3.2.2. DNA Aptamers for ATP (AMP or Adenosine)

The DNA aptamer for ATP was first selected by Huizenga and Szostak with a K_d of 6 μM (Figure 15A).[30] Structural characterizations indicated that two ATP molecules were intercalated (gray ovals) into the aptamer by forming noncanonical G:A base pairs.[312] Sometimes, the aptamer is also drawn as in Figure 15B. Prior to the isolation of this DNA aptamer, Sassanfar and Szostak also selected an RNA aptamer for ATP with a K_d of 0.7 μM (Figure 15C). In addition to ATP, both aptamers can also bind AMP and adenosine tightly (Figure 15D).

3.3. Fluorescent Sensors

The size of a fluorophore is usually on the order of that of a nucleotide. Fluorophores can have minimal perturbations on aptamer binding if their labeling sites are judiciously chosen, although such perturbations are sometimes purposefully introduced to probe aptamer binding. A fluorophore possesses a number of properties, including extinction coefficient, quantum yield (emission intensity), excitation/emission wavelengths, lifetime, anisotropy, and energy transfer. For aptamer based sensor design, many of these properties can be rationally applied. Fluorophores can associate with nucleic acids through a number of interactions, such as noncovalent binding, electrostatic or hydrophobic interactions, intercalation, and covalent attachment.

3.3.1. Aptamer Binding-Induced Fluorophore Local Environment Change

It is well established that aptamers "adaptively bind" target molecules, and a conformational change usually accompanies such binding events.[314] Such conformational changes may alter the local environment of associated fluorophores and, therefore, change their emission properties. To induce a large signal change, the fluorophore should be close enough to the binding site to experience a large environment change but introduce little perturbation to the aptamer binding properties. Such requirements pose significant challenges to rational design, even when crystal or NMR structures of aptamers are available.

3.3.1.1. DNA Intercalation Dyes for Signaling. Many DNA interacting dyes (e.g., YOYO, TOTO, and ethidium bromide, Figure 16) that are routinely used for DNA detection have also been employed for designing aptamer sensors. These dyes have very low quantum yields in buffer, and fluorescence enhancement can be over one-thousand-fold upon binding to double-stranded DNA. Although most aptamers are single-stranded nucleic acids, they usually contain double-stranded regions. Therefore, these intercalating dyes usually have relatively high emission intensity when mixed with free aptamers. Upon binding to target molecules, conformational changes of the aptamer may displace or release the dye molecules and decrease fluorescence intensity (Figure 16A). McGown and co-workers mixed YOYO or YO dyes (Figure 16C, D) with the 15-mer thrombin DNA aptamer (Figure 14B), and studied their fluorescence properties in the presence and absence of thrombin.[315] Addition of thrombin decreased the fluorescence intensity, which was attributed to the change the dye's local environment. While a fluorescence anisotropy increase was observed for the YO dye, thrombin had no effect on the anisotropy of the YOYO/aptamer complex because of homoenergy transfer between the two YO groups. Although no quantitative thrombin binding studies were carried out, this early work showed that a number of basic fluorescence properties of these dyes could be affected by aptamer−target interactions. Fang, Li, and co-workers mixed the TOTO dye with a DNA aptamer against the platelet-derived growth factor B chain (PDGF-BB),[51] and they observed decreased fluorescence in the presence of the target.[316] A detection limit of 0.1 nM was achieved with high selectivity. Wood and Bishop probed three L-argininamide binding aptamers with ethidium bromide (EB, Figure 16E). The authors found that each aptamer bound two EB molecules, a portion of which were released in the presence of the target molecule with decreased
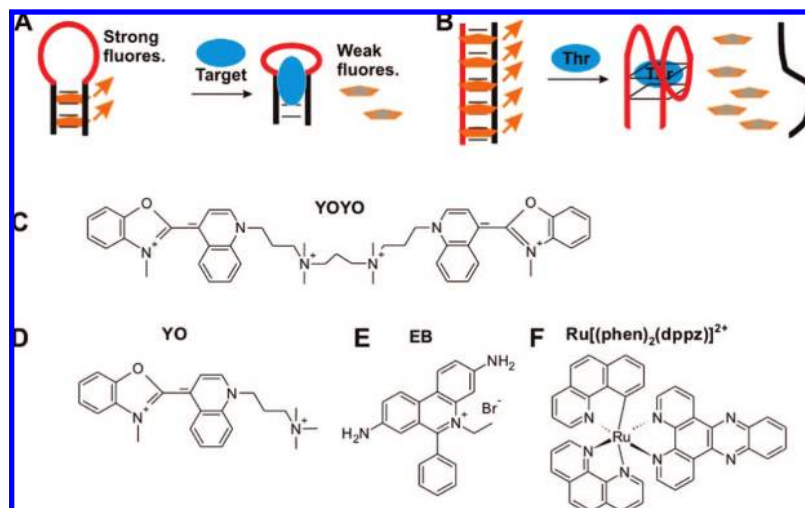
Figure 16. (A) Schematic representation of dye displacement by aptamer targets and the accompanying fluorescence decrease. A change of the dye local environment led to a fluorescence decrease. (B) An antisense DNA (in black) was used to form double-stranded DNA with the aptamer DNA (in red). Binding of thrombin (or, in general, any target) can release the antisense DNA and the EB dye.[322] Chemical structures of YOYO-1 iodide (YOYO) (C), YO-Pro-1 iodide (YO) (D), ethidium bromide (EB) (E), and a molecular light switching complex $[Ru(phen)_2(dppz)]^{2+}$ (F).

fluorescence observed.[317] Further studies on aptamer binding energies were also carried out.[318] OliGreen is a dye that binds to single-stranded DNA, and its fluorescence will increase by over 1000-fold upon DNA binding. Huang and Chang mixed OliGreen with a guanine rich DNA. In the presence of K^+, the DNA folded into a quadruplex structure to release the dye, resulting in decreased fluorescence.[319]

In addition to using organic fluorophores, Fang, Bai, and co-workers also employed a metal complex $Ru[(phen)_2(dppz)]^{2+}$ to achieve the same goal (Figure 16F).[320,321] This complex showed no luminescence in buffer but high luminescence after intercalation into nucleic acids. Different aptamer sensors for three proteins and a small molecule target were tested, and the detection limits for IgE, PDGF-BB, thrombin, and ATP were determined to be 0.1, 1.0, 0.01, and 1 nM, respectively. In this study, the RNA (instead of DNA) aptamer for thrombin was used.[311] These values were much lower compared to those of many other detection methods discussed in this review. Based on luminescence lifetime and quenching results, it was proposed that the metal complex was still bound to the aptamers after addition of target molecules.[321]

Instead of relying on disruption of intrinsic double-stranded regions in aptamers, Dong and co-workers reported a more rational design for thrombin detection (Figure 16B).[322] To maximize dye intercalation, the thrombin aptamer was first annealed to a cDNA to efficiently bind EB with strong fluorescence. Addition of thrombin caused the aptamer to bind thrombin and released its cDNA, resulting in decreased fluorescence. A detection limit of 2.8 nM was reported. This method should be generally applicable to detect many other targets. The structure switching properties of aptamers will be discussed in more detail later in the review.[225,323] Chang and co-workers have attached the PDGF aptamer to AuNPs. A fluorophore (N,N-dimethyl-2,7-diazapyrenium) was added to intercalate into the aptamer, and its emission was quenched by AuNPs. The addition of PDGF released the fluorophore, and enhanced emission was observed with a reported detection limit of 8 pM.[324]

The biggest advantage of using fluorescent DNA intercalators to signal aptamer binding is probably its label-free nature. In these systems, neither the aptamer nor the target

needs to be covalently labeled, which, in particular, makes RNA aptamer-based sensing more convenient. The sensitivity can also be very high, as demonstrated by Fang and co-workers.[320,321] In general, however, it is difficult to control the position of such fluorophores on DNA, and thus further optimization by rational design might be less straightforward. In addition, target detection was based on decreased emission in all the above systems, which left the sensors with limited room for signal change and could make the sensors prone to false positive signals generated by quenchers in environmental or clinical samples.

3.3.1.2. Cationic Conjugated Polymers as Fluorophores. Conjugated polymers possess useful optical and electronic properties and have been widely used in sensor design.[325−327] To probe negatively charged nucleic acids, cationic conjugated polymers (CCPs) have been shown to be highly effective. The construction of fluorescent sensors with CCPs is reviewed below, and their applications in colorimetric and electrochemical sensing are described later. Leclerc and co-workers prepared a water soluble CCP as shown in Figure 17A.[328,329] When free in solution, this polymer was fluorescent. Upon addition of a single-stranded probe DNA, its fluorescence intensity decreased due to the formation of a rigid polymer/DNA duplex that could further aggregate. Addition of a target DNA complementary to the probe DNA allowed recovery of fluorescence intensity, because, after formation of the rigid DNA duplex, the polymer wrapped around the DNA duplex to form a triplex, in which the polymer structure was less rigid.[328,330] The discovery that CCP can be used to probe DNA conformations has also been applied to aptamer-based detections. With the same polymer, Ho and Leclerc designed an assay for thrombin and K^+ as shown in Figure 17B.[330,331] In the absence of thrombin, for example, the aptamer associated with the polymer to form a rigid double helix with quenched fluorescence. Addition of thrombin folded the aptamer and the polymer wrapped around the folded aptamer to adopt a less rigid conformation, resulting in enhanced emission. A detection limit of 10 pM was reported. Later, the researchers labeled the thrombin aptamer with a Cy3 fluorophore and utilized fluorescence resonance energy transfer (FRET) for signal amplification.[332−334] The aptamer and polymer were initially in the aggregated
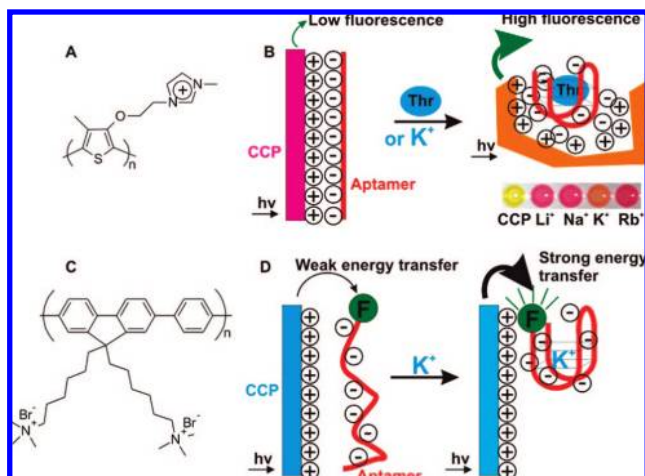
Figure 17. Sensors based on cationic conjugated polymers (CCPs). (A) Structure of the CCP used in part B. (B) Fluorescent and colorimetric detection of thrombin (Thr) or K^+.[331] CCP and aptamer are positively and negatively charged, respectively. (C) Structure of the CCP used in part D. (D) Fluorescent detection of K^+. Reprinted with permission from ref 331. Copyright 2004 American Chemical Society.

state with multiple CCPs and aptamers bundled together. Binding of thrombin recovered the polymer emission and allowed transfer of energy to multiple Cy3 dyes and also energy transfer among Cy3 dyes. In this work, the aptamer was immobilized on a glass surface. Compared with the previous solution system,[331] the surface immobilized sensor did not improve in terms of sensitivity in concentration (62 pM detection limit). However, the number of molecules that can be detected improved by ∼2 orders of magnitude, because a much smaller volume could be used for surface based detection (0.4 μL on the surface vs 200 μL in the cuvette). This signal amplification mechanism was termed superlighting. For DNA detection, a detection limit of 5 copies of DNA in 3 mL was reported, rivaling PCR sensitivity.[335,336]

Wang and co-workers employed a different CCP as shown in Figure 17C to detect K^+.[337] The authors proposed that when a fluorescein-labeled guanine rich DNA was free in solution, its electrostatic interaction with the CCP was weak because of its low charge density. Addition of K^+ folded the DNA into a more compact quadruplex structure that had higher charge density. Therefore, the folded aptamer was closer to the CCP, allowing more efficient energy transfer (Figure 17D). This system has also been applied to study DNA quadruplex to duplex transition[338] and monitor single-stranded DNA cleavage.[339]

3.3.1.3. Selection of Fluorophore Binding Aptamers. The studies mentionaed above use known DNA intercalation dyes or fluorescent cationic conjugated polymers that can bind DNA. To expand fluorophore−DNA systems for sensing applications, Kobayashi and co-workers have selected a DNA aptamer for hematoporphyrin IX (HPIX).[340] However, no fluorescence intensity change was observed upon aptamer binding. Wilson and co-workers selected RNA aptamers for sulforhodamine B, fluorescein,[341] and malachite green.[342] Tsien and co-workers reported that the malachite green aptamer can increase the dye's quantum yield by over 2000-fold upon binding.[343] This discovery has made it possible to image RNA, which was first demonstrated in vitro by Aoyama's group.[344,345] Aoyama and co-workers have isolated an RNA aptamer that can bind to a modified Hoechst
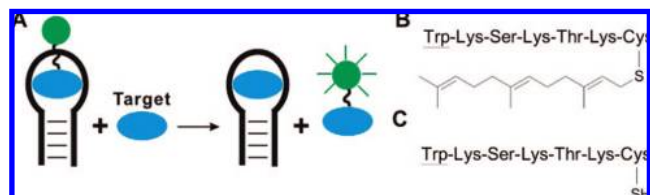

Figure 18. (A) Schematics of competitive assays with labeled target molecules. Structures of farnesylated (B) or nonfarnesylated (C) K-*ras*-based peptide.

dye with a K_d of 35 nM, and significant fluorescence enhancement was observed upon binding. By fusing the corresponding DNA sequence to a luciferase gene, the aptamer was expressed in the mRNA and thus can be used to monitor RNA transcription based on fluorescence enhancement.[345] In an earlier work, the group also obtained a DNA aptamer for the modified Hoechst dye.[344] Although direct sensing application of these dye-binding aptamers may be limited,[346] they can be conjugated to other aptamers to form allosteric aptamers (*vide infra*).[347−349]

3.3.2. Competitive Assays with Labeled Target Molecules

In addition to the aforementioned noncovalent labeling approach, Rando and co-workers covalently attached fluorophores to target molecules to develop competitive assays. For example, a pyrene fluorophore was linked to an aminoglycoside (tobramycin), and strong fluorescence quenching (over 80%) was observed upon aptamer binding.[350] Labeled and unlabeled tobramycin competed for the aptamer binding site (Figure 18A), and competitive assays were developed to determine the K_d of the aptamers. RNA aptamers for farnesylated K-*ras*-based peptide were selected by the same group (Figure 18B), which bound to nonfarnesylated peptide (Figure 18C) at least 10-fold less efficient. A tryptophan residue was placed on one end of the peptides (underlined), and strong tryptophan fluorescence enhancement (over 300%) for the farnesylated peptide was observed in the presence of an aptamer.[351] Recently, Chang and co-workers have reported an interesting system for PDGF detection. The authors used PDGF to functionalize 2 nm photoluminescent Au nanodots and a PDGF aptamer to functionalize 13 nm AuNPs. In the absence of free PDGF, the two kinds of nanoparticles were brought close to each other, resulting in quenched luminescence. Free PDGF competed with 2nm nanodot conjugated PDGF to reduce the quenching effect, and a detection limit of 80 pM was reported.[352]

3.3.3. Aptamers Modified Covalently with Fluorophores

Ellington and co-workers first explored covalent labeling of fluorophores to aptamers through a rational design approach for sensor design.[353] Based on the structure of the RNA aptamer for ATP (Figure 15C), it was determined that residue 13 was close to the binding pocket but not directly involved in binding. Labeling an acridine fluorophore (Figure 19A) at this position showed ATP-dependent fluorescence enhancement, while interestingly, labeling with fluorescein (Figure 19B) at the same position or at the terminus of the aptamer failed to generate a signal change. In the best case, the sensor was able to detect ∼10 μM ATP. The researchers also tested the strategy on the ATP DNA aptamer (Figure 15A), and a similar position was determined to be residue 7. Labeling of fluorescein at this position, however, failed to generate fluorescence change. Instead, placing a fluores-
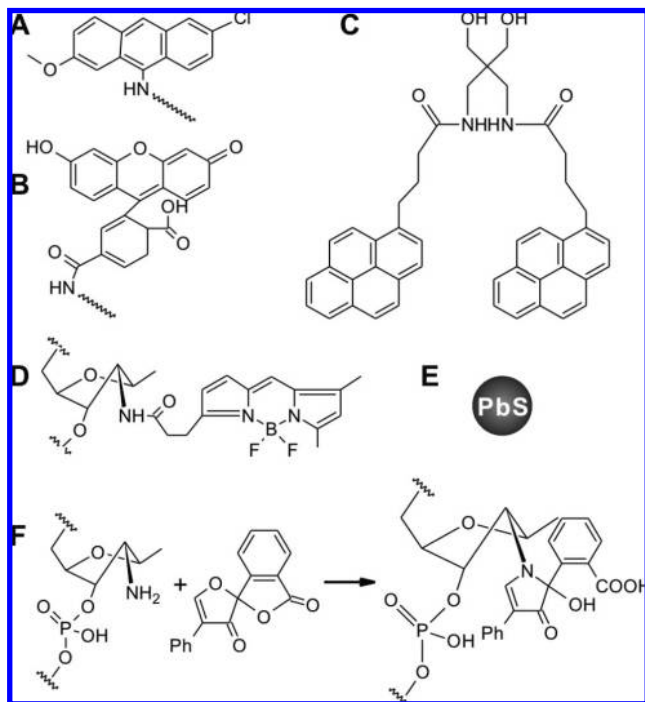
Figure 19. Structures of acridine (A), fluorescein (B), bis-pyrene (C), Bodipy-FL at the 2′-ribose cytosine residue (D), and a PbS quantum dot (E). (F) 2′-Amine substituted cytidine and its reaction with fluorescamine to form a stable fluorescent pyrrolinone.

cein between residue 7 and 8 showed ATP-dependent signal change. In this system, the fluorescence increase was less than one-fold.

Yamana and co-workers synthesized a bis-pyrene fluorophore (Figure 19C) and attached it to a number of positions on the ATP DNA aptamer (Figure 15A).[354] Only the labeling at residue 20 resulted in ATP-dependent fluorescence change, while labeling at residue 7 failed to give a signal. The same research group also labeled a pyrene at the 2′-ribose positions on the ATP aptamer. Out of the seven positions tested, two gave an ATP-dependent fluorescence increase.[355] Based on the knowledge that the 2′-ribose positions in nucleic acids are very sensitive to local chemical environments, Weeks and co-workers placed a Bodipy-FL fluorophore at the 2′-ribose of the cytosine residues on three DNA aptamers (Figure 19D).[356] For the ATP aptamer, among the three cytosine residues, positions 3 and 17 were tested. The remaining one (position 2) should have less effect than position 3 and therefore was not tested. While position 3 failed to generate a fluorescence change, fluorescence enhancement was observed at position 17. For the three positions tested on a tyrosinamide aptamer, all of them showed a fluorescence increase, and one out of three tested positions in an argininamide aptamer showed almost a 4-fold increase.

For all of the above systems, the fluorescence increase was relatively small (<4-fold). Katilius and workers showed that a much higher signal increase could be achieved by using fluorescent nucleotide analogues.[357] Based on the crystal structure of thrombin and its aptamer complex,[307] the authors first replaced the T base at position 7 of the 15-mer thrombin aptamer (Figure 14B) with a 4-amino-6-methylpteridone and a ∼30-fold fluorescence enhancement was observed upon addition of thrombin. The modified aptamer did not change its binding property, as a K_d of 12 nM was determined, which was similar to that of the native aptamer.[45] The same position

was also replaced by 2-aminopurine and 3-methylisoxanthopterin, both of which showed ∼10-fold thrombin-induced fluorescence enhancement. This method was further tested with aptamers whose 3-D structures were not available. Among all the constructs reported, the IgE and PDGF aptamers showed a 5.6- and 6.7-fold fluorescence increase in their best cases, respectively. The quantum yield of these nucleotide analogues is strongly dependent on base stacking interactions with their neighboring nucleotides, which may change significantly upon binding to target molecules and therefore give a large fluorescence change.

Dwarakanath et al. labeled semiconductor nanocrystals (quantum dots or QD) with antibodies or DNA aptamers targeting bacteria, and a change in the quantum dot emission wavelengths was observed upon binding to bacteria.[358] For example, the aptamer-conjugated Fort Orange QD had a major emission peak at 600 nm and a minor peak at 460 nm. In the presence of *E. coli*, the 600 nm peak disappeared completely while the 460 nm peak increased slightly. Although it was not clear as to the exact cause of the peak intensity changes, the authors proposed that it could be due to changes in local environmental factors such as hydrophobicity/hydrophilicity, pH, or electric charge. Strano and co-workers reported that the thrombin aptamer-functionalized PbS QDs (Figure 19E) showed quenched emission in the presence of thrombin, which was attributed to the electron transfer from functional groups on thrombin to the QD.[359] The detection limit was reported to be 1 nM, and the quenching effect was specific to thrombin.

The influence of aptamer binding on local chemical environments of aptamers was also probed by chemical reactions. Weeks and co-workers prepared DNA ATP aptamers containing single 2′-amine substituted cytidines.[360] The amine reacted with fluorescamine to form a stable fluorescent pyrrolinone (Figure 19F). It was expected that the free aptamer would have high flexibility and high reactivity, while low reactivity would be observed upon ATP binding due to constraints. Three ATP aptamers with modified cytidine residues at positions 2, 3, and 17 were tested, and the position 3 modified one showed the largest difference in reactivity. A FRET-based sensor was prepared, and the detection limit was ∼100 μM.

The above studies demonstrated that it is possible to rationally design aptamer sensors by strategically and covalently attaching fluorophores to aptamers. This method often requires knowledge of aptamer structures and a few rounds of trial-and-error. Placing a fluorophore too close to the binding site may disrupt binding, while fluorophores too far away from the binding site may not result in fluorescence changes. To overcome limitations from rational design, Ellington and co-workers employed fluorescently modified nucleotides to select for signaling aptamers.[361] The selected aptamers should possess the desired fluorescent signal changes. In related studies, the effect of aptamers on photophysical properties of different fluorophores has also been studied.[362]

The difficulties associated with the above strategy come from several aspects. First, even though aptamers usually experience conformational changes to inductively fit their targets, it is hard to predict the influence of such changes on the local environment of fluorophores. Second, labeling with bulky fluorophores may disrupt aptamer's binding properties. Third, because no external quenchers were involved, the fluorescence changes were usually small, even when such
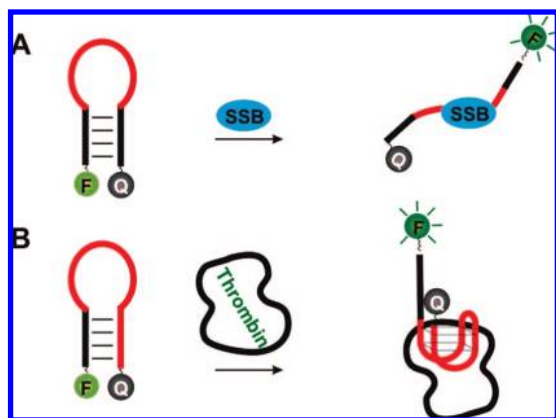
Figure 20. Aptamer beacons. (A) Application of molecular beacons to probe single-stranded DNA binding proteins (SSB).[363] (B) Detection of thrombin with an aptamer beacon. The aptamer contained an extension (in black), which formed the stem part of the hairpin. Binding to thrombin opened the hairpin and increased fluorescence.[364]

changes did occur. Fortunately, nucleic acids allow convenient incorporation of fluorophores and external quenchers, which can be positioned close to each other by taking advantage of appropriate secondary structures. A primary example is the molecular beacon used for DNA detection. To improve sensor performance, a molecular beacon type of signaling method has been introduced to construct aptamer-based sensors known as aptamer beacons.

3.3.4. The Aptamer Beacon Approach

3.3.4.1. Classic Molecular Beacon Designs. In section 2.3.1, we have mentioned classic molecular beacons, which have found important applications in DNA detection and in catalytic beacons, which use DNAzyme for sensing a variety of metal ions. Tan and co-workers have applied the molecular beacon technology to study protein−DNA interactions.[363] The single-stranded DNA binding protein (SSB) was chosen to interact with a molecular beacon (Figure 20A). In the presence of SSB, the beacon was opened and an immediate fluorescence enhancement was observed. The extent of fluorescence change was similar to that induced by the cDNA. Although no aptamers were involved in this work, the paper suggested that the molecular beacon concept could be used in aptamer-based detections. When aptamer−target interactions are involved, such molecular beacons are called aptamer beacons.

Based on the classical molecular beacon design, Stanton, Ellington, and co-workers constructed a thrombin aptamer beacon (Figure 20B).[364] One end of the thrombin aptamer was extended (extended part in black) so that a hairpin structure was forced to form. The number of base pairs in the stem of the hairpin was varied from 4 to 6, and the largest fluorescence increase was observed with five base pairs. The system could detect less than 10 nM thrombin, with a maximum fluorescence increase of 2.5-fold. The same system was also used by Stratis-Cullum et al. for thrombin detection.[365]

In a recent work by Morse, the loop region of an RNA hairpin was randomized in order to obtain a sequence that could separate the two ends of the hairpin upon target (tobramycin) binding.[366] After selection, the two ends were labeled with a fluorophore and a quencher to construct sensors. However, in the two sequences tested, the fluores-
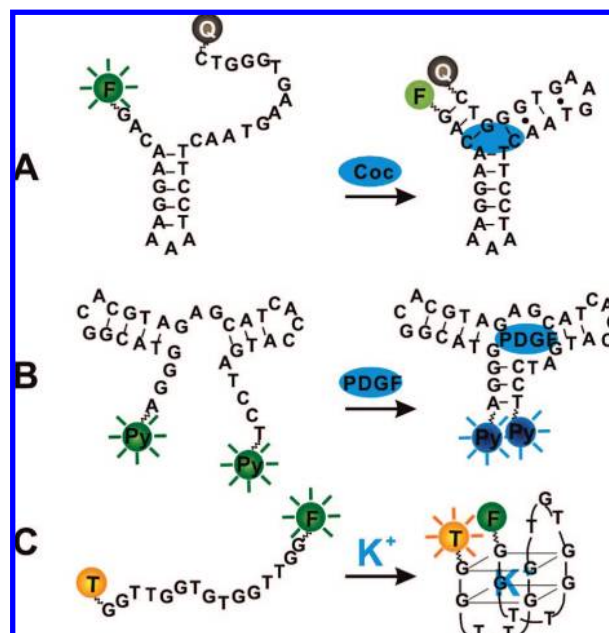

Figure 21. Aptamer beacons with nonclassical molecular beacon design. (A) An aptamer beacon for cocaine was constructed by labeling the two ends with a fluorophore and a quencher.[367] (B) Two pyrenes (Py) were labeled on the two ends of a PDGF aptamer. Shifted emission wavelength was observed in the presence of PDGF by pyrene excimer formation.[370] (C) Aptamer beacon for K^+ detection by labeling with two fluorophores: F = FAM and T = TMARA.[18]

cence increase in the presence of saturating tobramycin was only ∼10%, and a detection limit of 30 μM was reported.

3.3.4.2. Nonclassical Molecular Beacon Designs. As shown above, aptamer sensors can be made by inserting aptamer sequences into molecular beacons with the classic stem−loop structure. Forcing aptamers to be initially in such a stem−loop structure, however, may not be the best design for all aptamers because such confinements may result in decreased binding affinity. Therefore, many aptamer beacons were designed based on the fluorophore/quencher approach but did not require the formation of a hairpin structure initially. For example, the cocaine aptamer was predicted to have a binding structure of a short hairpin flanked by two single-stranded regions (Figure 21A).[367] A fluorophore and a quencher were labeled at the two ends, and high fluorescence intensity was initially observed. In the presence of cocaine, the binding structure was formed and the fluorophore was brought close to the quencher. Around 50% quenching was observed with 1 mM cocaine. Even in blood serum, 10 μM cocaine could be detected. The DNA aptamer for L-argininamide adopts a random structure in solution.[28] In the presence of the target molecule, the aptamer formed a stem−loop structure, similar to the cocaine aptamer. Ozaki et al. labeled the two ends of the aptamer with a fluorophore and a quencher and observed L-argininamide-dependent quenching.[368] Urata and co-workers constructed a number of adenosine aptamer based sensors with a fluorophore and a quencher on the two ends.[369] A decrease in fluorescence intensity was observed in the presence of adenosine. A detection limit of ∼5 μM was reported with quenching efficiency up to 67%.

Tan and co-workers labeled two pyrene molecules at the two ends of the PDGF aptamer (Figure 21B).[370] The aptamer was optimized such that the two ends were far away in the absence of PDGF while close to each other upon target
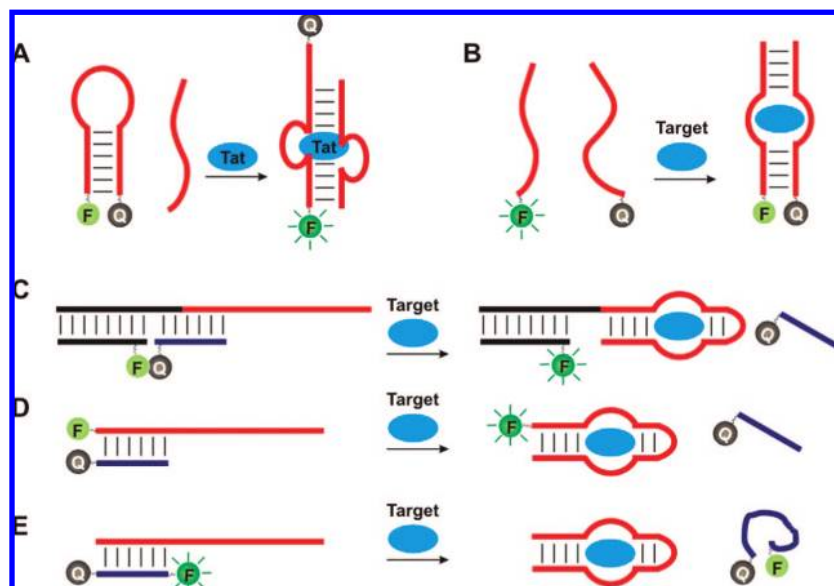
Figure 22. An aptamer beacon with the aptamer being split into two fragments for HIV Tat protein detection (A)[378] or for cocaine or ATP detection (B).[33] Different designs of aptamer beacons based on the structure switching properties of aptamers (C),[323] (D),[382] and (E).[384]

binding. When positioned close to each other, the pyrene excimer was formed, which emitted green fluorescence (480 nm) instead of the monomer's blue emission (400 nm). Such a shift in emission wavelength allowed ratiometric detection, which was less dependent on sampling conditions and system fluctuations. Less than 1 nM PDGF could be detected. Importantly, the pyrene excimer has longer fluorescence lifetimes (40 ns) than its monomers (5 ns). This property makes the system useful for sensing in complex sample matrixes such as cell media, where strong background fluorescence often makes intensity-based detection difficult.

Instead of a fluorophore and a quencher, two different fluorophores, 6-carboxyfluorescein (FAM) and 6-carboxytetramethylrhodamine (TAMRA), were attached to the two ends of a G-rich DNA by Takenaka and co-workers (Figure 21C).[18,371,372] When FAM was excited in the absence of K^+, only strong FAM emission was observed. In the presence of K^+, formation of a G-quadruplex structure brought the two fluorophores close and strong TAMRA emission resulting from energy transfer was observed. The sensor can detect 10 μM of K^+ if the ratio of the two fluorophore emissions was monitored. Two pyrene molecules were also placed at the two ends of the same DNA, and K^+-dependent excimer formation was observed.[373] The sequence used here is the same as the 15-mer thrombin DNA aptamer (Figure 14B). By labeling the two ends with a fluorophore and a quencher, or with two different fluorophores, Tan and co-workers have observed a thrombin-dependent fluorescence change with detection limits around 0.4 nM.[374] Ono and co-workers reported an interesting fluorescent sensor for Hg^{2+} detection[375] based on the fact that Hg^{2+} can be chelated between two thymine bases in DNA to stabilize the T−T mismatch.[19,376] A fluorophore and a quencher were labeled on the two ends of a thymine rich DNA. The addition of Hg^{2+} led to the formation of a DNA hairpin to cause reduced fluorescence. A detection limit of 40 nM was reported. To improve the performance of the system into a "turn-on" sensor (i.e., fluorescent increase in the presence of analyte), we designed a structural switching sensor with a detection limit of 3.2 nM.[377]

3.3.4.3. Split Aptamer Beacons. In the above work, all sensors are based on the complete aptamer sequences.

Aptamer beacons have also been constructed by splitting aptamers into two fragments. Yamamoto et al. reported such an aptamer beacon in 2000.[378] As shown in Figure 22A, a molecular beacon type of hairpin was constructed and the initial fluorescence was quenched. The aptamer sequence was divided into two parts, with one part in the hairpin and the other as a separated strand. In the presence of the target analyte (Tat protein of HIV), the two parts self-assembled to bind the analyte and thus separated the quencher from the fluorophore, resulting in increased fluorescence. In the presence of 200 nM Tat protein, a ∼14-fold increase in fluorescence intensity was observed. In a follow-up study by the same group, the use of nucleic acid array technology was investigated.[379] In this study, the Tat protein aptamer was split into two halves. One half was labeled with a fluorophore and the other with a biotin and immobilized on a streptavidin-coated surface. The surface lit up only in the presence of Tat. In the absence of Tat, the affinity between the two halves was too low because they were not complementary.

Stojanovic et al. also divided an anticocaine aptamer into two halves, and no DNA hairpin was designed (Figure 22B). As a result, the initial fluorescence signal was high. In the presence of cocaine, the two halves associated to bind the target and quenched fluorescence was observed.[33] This sensor was able to detect cocaine from 10 to 1000 μM with ∼40% quenching. Similarly, the authors also constructed an ATP sensor by splitting the ATP aptamer into two halves. The method of splitting an aptamer sequence may not be applicable to all aptamers and aptamer binding affinity may decrease by such modifications.

3.3.4.4. Structure-Switching Aptamers. Li and co-workers argued that it was difficult for all the above designs to be generalized for a broad range of aptamers, and they reported a general strategy for signaling aptamer binding based on aptamer structure-switching properties,[225,226,302,323,380,381] given the fact that an aptamer can associate either with a cDNA strand or with its target analyte, and there is a structure switching process between the two states. As shown in Figure 22C, a DNA containing an aptamer fragment was used as a template to assemble two DNAs in such a way that the labeled fluorophore and quencher were brought close to each

other, resulting in quenched fluorescence.[323] In the presence of target analytes, the aptamer fragment switched to the target-binding structure. As a result, the number of base pairs between the quencher-labeled DNA and the aptamer DNA reduced so that the quencher-labeled DNA dissociated into solution, giving increased fluorescence. Sensors for detecting thrombin and ATP were demonstrated, with detection limits of ~10 nM and 10 μM, respectively. The sensors showed instantaneous response with a very high fluorescence increase (over 15-fold for ATP). Alternatively, a two-strand system was constructed as shown in Figure 22D, in which the aptamer carried a fluorophore.[382] In a recent design reported by the Tan group, the two ends without fluorophore/quencher labels in Figure 22D were linked by a PEG chain to form a hairpin structure. In the presence of target molecules, increased fluorescence was observed.[383] Another variation was reported by Rankin and co-workers as shown in Figure 22E.[384] An RNA aptamer for theophylline was hybridized to a piece of fluorophore and quencher labeled DNA. Due to the rigidity of short double-stranded DNA, the fluorophore and quencher were well separated, giving high emission intensity. Addition of theophylline released the DNA piece, which then formed a random coil structure in solution, resulting in quenched fluorescence. Li and Ho designed a similar beacon. In the absence of the target molecule, the aptamer opened the beacon to form a duplex, giving a high fluorescence signal. In the presence of the target molecule, the aptamer dissociated from the beacon and the beacon folded into the hairpin structure with decreased fluorescence observed.[385] In addition to using organic quenchers, Zhao and co-workers employed AuNPs as quenchers for designing structure-switching aptamer sensors for protein detection.[386] In principle, there are no structural requirements (e.g., an aptamer can be divided into two pieces or needs to change its end-to-end distance upon binding) on aptamers to employ this design, and therefore, it should be generally applicable to many aptamers.

Brennan, Li, and co-workers have also studied the entrapment of the structure switching signaling aptamers in sol−gel-derived silica,[387] and they applied such systems to solid phase enzyme activity assays,[388] nanoengines,[382] and screening.[389] Linking structure switching aptamers to silica nanoparticles was also reported.[390] Ellington and co-workers proposed to employ in vitro selection to obtain structure switching signaling aptamers, and they have demonstrated such selections using an oligonucleotide as the target.[391] Li and co-workers demonstrated such selections for small molecule targets.[302] Recently, Ellington and co-workers have applied QDs to construct sensors based on the structure-switching aptamer design.[392] A thrombin aptamer was attached to QDs, and a cDNA with a quencher was hybridized to the aptamer, resulting in quenched QD emission. Addition of thrombin removed the quencher and an up to 14-fold emission increase was observed. The importance of the structure switching property of aptamers is manifested not only in designing fluorescence sensors. The inducible physical movement of aptamers has also been applied to construct other types of sensors, including colorimetric sensors and electrochemical sensors, that will be discussed later. In addition to sensing applications, this concept has been seen in nanotechnology and materials science to create stimuli responsive nanomaterials.[105,106]

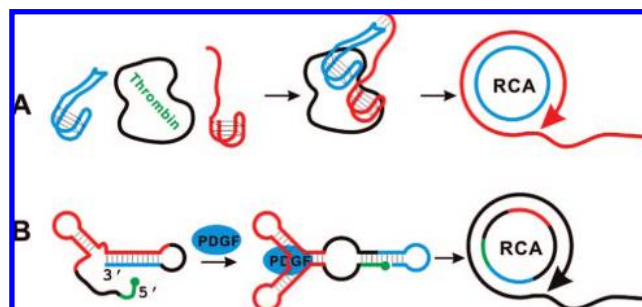For all of the above aptamer beacons, the fluorophore and quencher were attached to the aptamers. Sparano and Koide,

Figure 23. Aptamer-based detections involving PCR. (A) Detection of thrombin.[395] The aptamer concentrations were very low and will not form priming interactions without both being associated to thrombin. (B) Detection of PDGF.[402]

however, have designed a system in which both the fluorophore and the quencher were attached to the target molecule.[393,394] First, a compound displaying photoinduced electron transfer (PET) property was synthesized. An RNA aptamer targeting the quencher moiety of the PET system was selected. Mixing 100 μM aptamer with the compound increased its fluorescence by 13-fold. Although this method may have limited sensing applications (except for detecting the aptamer itself), it may be very useful for in vivo RNA imaging.

3.3.5. Detection Involving PCR

Polymerase chain reactions (PCRs) are very powerful methods for nucleic acid amplification and even a single copy of DNA can be detected. By converting the detection of small molecules or proteins into nucleic acid amplifications, sensor sensitivity can be enhanced.

King and co-workers demonstrated the use of rolling circle amplification (RCA) for thrombin detection.[395] The authors extended the heparin exosite binding aptamer (Figure 14D) and circularized it. The other aptamer for the fibrinogen recognition exosite (Figure 14B) was extended with a poly-T spacer and then a short primer complementary to the circular aptamer. In the presence of thrombin, both aptamers bound to the same thrombin and thus allowed priming for initiating RCA (Figure 23A). The reaction was monitored by real time PCR and also by incorporating a ferrocene-labeled nucleotide for electrochemical detection. A detection limit of 30 pM thrombin was reported. To increase the stability of aptamers in biological fluids, King and co-workers have also constructed many other circular aptamers where the two ends of aptamers were ligated.[396,397] A PDGF can also bind two aptamer molecules. Landegren and co-workers designed two extended PDGF aptamers, and when the two aptamers bound to the same PDGF, the extended parts were close enough to be ligated by a template DNA.[398] Through PCR amplification of the ligated product, PDGF could be detected with zeptomole sensitivity.

In a related system, although no PCR was involved, Heyduk and co-workers labeled the two different thrombin aptamers with a FRET donor and an acceptor, respectively.[399] Strong FRET was observed only in the presence of thrombin because the two aptamers were brought in close proximity to one another by binding to the same thrombin molecule. The authors optimized the fluorophore/quencher or fluorophore/fluorophore pairs, and under optimal conditions, a detection limit of < 100 pM was achieved. A similar method has also been applied to detect DNA binding proteins by the same group.[400] Xu and co-workers took advantage of

aptamer−protein binding interactions to protect aptamer DNAs from nuclease digestion.[401] The surviving aptamer was employed as a template to ligate two other pieces of DNA, and the ligated product was PCR amplified to generate a detection limit of several hundred thrombin molecules.

Ellington and co-workers designed an aptamer switch as shown in the left panel of Figure 23B.[402] The 3′-end of the DNA (in blue) was blocked by a fraction of the PDGF aptamer sequence (red). In the presence of PDGF, the aptamer switched its structure and released the 3′- end sequence of the DNA to form the binding structure. The two ends of the DNA were then brought close by the designed template sequence and ligated to form circular DNA that was amplified by RCA and detected by real time PCR. A detection limit of 0.4 nM PDGF was achieved.

3.3.6. Fluorescence Anisotropy-Based Detection

Fluorophores have many important photophysical properties, and the studies reviewed above mainly deal with steady-state fluorescence intensity, including those related to fluorophore quantum yield and energy transfer. Other fluoresence properties, such as lifetime and anisotropy, have also been used in aptamer-based detections. These parameters have the advantage of being less affected by environmental interferences, such as background fluorescence. Fluorescence anisotropy is dependent on a fluorophore's ability to produce depolarized emission when excited by a polarized light source. Small fluorophores rotate relatively fast during their excited lifetimes and, thus, can better depolarize the excitation and give a low anisotropy. When a fluorophore is associated with a large molecule (i.e., a protein), the motion of the fluorophore is confined to give relatively high anisotropy values.[403]

To achieve a large anisotropy change, it is important to have a large change in the molecular weight associated with the fluorophore during the aptamer/target binding process. Therefore, the fluorophore is usually labeled on the smaller one of an aptamer/target pair. For example, to detect small molecules, the target will be labeled with a fluopophore. In one report, addition of an aptamer to dye-labeled tobramycin resulted in an anisotropy increase.[68] To detect tobramycin in real samples, unlabeled tobramycin in the sample was mixed with the dye-labeled tobramycin/aptamer complex. The competitive binding caused the release of the dye-labeled tobramycin and, therefore, a decreased anisotropy. This method was able to measure tobramycin levels accurately in the 0−28 nM range, which was approximately 150-fold more sensitive than previous fluorescence polarization-based immunoassays for tobramycin. Yu and co-workers also used an anisotropy-based assay to study aptamer−aminoglycoside interactions.[404]

For large molecule targets such as proteins, the target's molecular weight is usually higher than that of the aptamer. Therefore, it is preferred to label the aptamer, instead of the target protein (Figure 24B). Tan and co-workers labeled a fluorescein at the 5′-end of the PDGF aptamer. Increased anisotropy upon addition of PDGF was observed, and a detection limit of 0.22 nM was reported.[405] The assay can be performed in homogeneous solutions without the need for target separation or purification. Similarly, anisotropy-based assays have been performed on the IgE aptamer.[406] Under optimized conditions, a detection limit of 350 pM was achieved. Anisotropy has also been applied to study thrombin aptamer[407] and aptamers for amyloid β-peptides,[408]
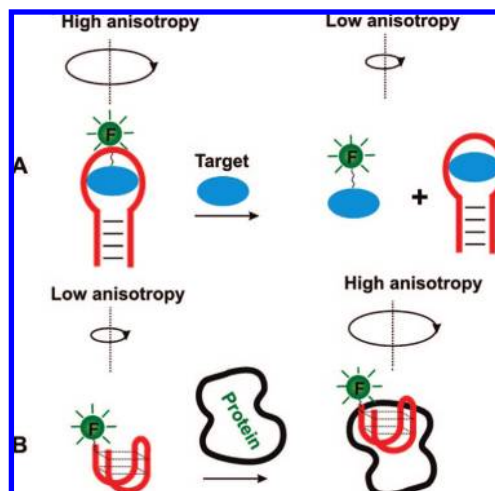

Figure 24. Fluorescence anisotropy-based aptamer sensors for detecting small molecule targets in a competitive assay format (A) or for detecting protein targets (B).

angiogenin,[409] and Hg^{2+},[410] as well as to provide complementary information to FRET-based measurements for studying protein−protein interactions.[411]

In addition to performing anisotropy measurements in the solution phase, anisotropy changes for surface attached aptamers have also been studied. Hieftje and co-workers developed a sensor for detection of thrombin.[412] The thrombin aptamer was fluorescently labeled and attached to a surface. The anisotropy signal was generated by evanescent-wave-induced fluorescence, which allowed detection of 0.7 amol of thrombin in 140 pL with a dynamic range of 3 orders of magnitude and a precision of better than 4% relative standard deviation over a range of 0−200 nM. McCauley and co-workers have made a chip-based aptamer array containing four aptamers targeting four different proteins.[413] This device was able to simultaneously detect and quantify each protein in complex sample solutions.

Screening small molecule inhibitors for proteins is a highly important tool for drug development. While direct screening small molecule binders may be difficult, high-throughput small molecule-induced displacement assays can be performed using fluorescence anisotropy or polarization techniques, because aptamers can be obtained to bind essentially any protein of choice. The Famulok group has demonstrated this concept in developing inhibitors for the cytohesin class of small guanosine exchange factors.[414,415]

3.3.7. Aptamer Sensors Based on Inspiration from Immunology

Aptamers are known as the nucleic acid equivalent of antibodies, and therefore, many assays developed for antibodies are directly transferable to aptamers. For most of the sensors introduced previously, detections were carried out in a homogeneous solution and no washing or separation steps were involved, which actually represents one of the advantages of aptamer-based sensors. Antibodies, on the other hand, lack the predictable structure changes upon analyte binding, and it is generally difficult to attach fluorophores to antibodies in a site-specific manner. As a result, most antibody-based assays require surface immobilization and washing steps. Despite the lengthy procedures, very high sensitivity and specificity can be achieved. A commonly used technique for signal amplification is to
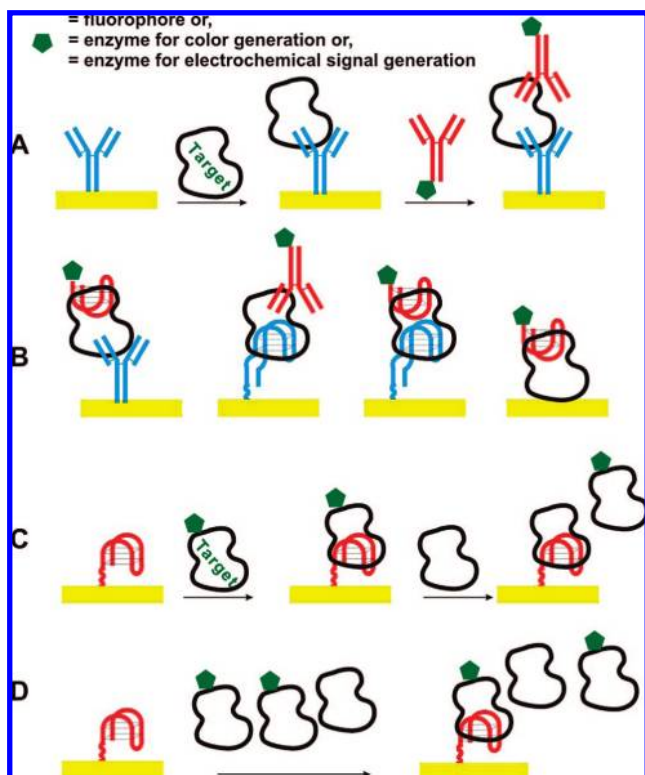
Figure 25. (A) A typical antibody-based ELISA assay. (B) Variations on ELISA involving aptamers. The primary binder on the surface (in blue) and the secondary binder (in red) can be either an antibody (shown as a Y shape, left panel) or an aptamer (shown as a curved shape, middle two panels). In the last panel, the target protein was directly immobilized onto the surface without being captured by antibodies or aptamers. Schematics of a displacement assay format (C) and a competitive assay format (D).

use an enzyme-labeled antibody for signal generation and amplification through catalytic turnovers.

3.3.7.1. Enzyme-Linked Aptamer Assays (Sandwich Format). Enzyme-linked immunosorbent assays (ELISA) have been one of the most widely used methods in medical diagnosis of many important analytes. In a typical sandwich ELISA assay, two different antibodies for the same target molecule are involved (Figure 25A). The capture antibody is first immobilized onto a surface to capture the target. Following that, a detection antibody is added to bind to a different site of the target. The detection antibody can be labeled with a signaling moiety for target detection. More commonly, however, a secondary antibody linked to an enzyme is used to bind to the detection antibody. After all the washing steps, an enzyme substrate is added so that the enzymatic reaction can generate amplified luminescence intensity, color change, or electrochemical signals. With the high binding affinity and specificity of aptamers, it is natural to employ aptamers in place of antibodies in the same assay format. Many different combinations can be made by substituting antibodies with aptamers, as shown in Figure 25B. In addition to other advantages of aptamers described previously, their smaller size compared to antibodies allows higher surface density and, thus, higher sensitivity.

In a traditional ELISA, the signaling element is usually an enzyme (commonly horseradish peroxidase, HRP) that can turnover chromogenic substrates to produce a color. Alternatively, fluorophores, fluorogenic substrates, or enzyme/substrate pairs that can generate electrochemically active species (i.e., H_2O_2) were also used to achieve much higher

sensitivity. In a novel approach, enzymes were employed to generate precipitants for enhanced surface plasmon resonance (SPR) signals.[416] The examples covered in this section are mostly fluorescence or luminescence based. Due to the similarity in the assay platform, colorimetric and electrochemical signaling methods will only be briefly mentioned in their corresponding sections.

Drolet et al. demonstrated the first enzyme-linked aptamer assay (ELAA) with an aptamer for the human vascular endothelial growth factor (VEGF).[69] In this system, an antibody for VEGF was immobilized to capture VEGF. A fluorescein-labeled VEGF aptamer was then added to sandwich VEGF.[417] Finally, an alkaline phosphatase conjugated antifluorescein Fab fragment was added to bind fluorescein and generate chemiluminescence. The performance of the aptamer-based system was comparable to traditional all antibody-based ELISA detections, and a detection limit of 25 pg/mL was reported. Recently, Chu and co-workers immobilized PDGF-BB antibodies to an electrode surface, and the PDGF aptamer with an extension was added to sandwich PDGF between the two kinds of binding molecules.[418] The extended part on the aptamer served as a primer for rolling circle amplification (RCA). A biotinylated short oligonucleotide was added to bind the segments generated by RCA, and finally streptavidin with an alkaline phosphatase label was added to generate electrochemical signals. A detection limit of 10 fM was reported. Similar designs were also used for detection of IgE by Yu and co-workers.[419] Rye and Nustad coated magnetic beads with an antithrombin antibody for thrombin capture and labeled a thrombin aptamer with biotin for detection.[420] Europium-labeled streptavidin was then added to bind to biotin, and detection was achieved through the europium luminescence. Although not for sensing applications, Gorenstein and co-workers employed a bead-based immunofluorescence assay for selection of protein-binding aptamers.[421]

To increase the binding between target analytes and aptamers, Golden and co-workers employed PhotoSELEX to isolate aptamers that could form covalent bonds with target analytes upon UV irradiation.[52,422] After target analytes were covalently captured on the surface, harsh washing conditions were employed to eliminate nonspecific binding. Signaling elements were then introduced for detection. The advantage of the photoaptamer system is that many target proteins can be detected on a single surface in parallel, which is especially valuable for detection of human protein levels in sera for disease diagnostics. Using the photoaptamer system, Bock et al. were able to construct an array to analyze 17 proteins simultaneously.[423]

The sandwich assay format was also employed to detect anthrax spores. An antianthrax aptamer was immobilized on magnetic beads for target capture, and another anthrax aptamer contained a biotin moiety. Streptavidin labeled with $Ru(bpy)_3^{2+}$ was used to generate chemiluminescence for detection. Similarly, an enzyme-linked colorimetric assay was also performed on the system.[57] Bruno and Kiel coated magnetic beads with antitoxin aptamers (aptamers against *cholera*, whole toxin, and *staphylococcal* enterotoxin B). Detection was based on chemiluminescence from $Ru(bpy)_3^{2+}$ labeled target toxins.[424] Recently, thrombin was also sandwiched between two aptamers, with one aptamer immobilized on the surface and the signaling aptamer attached to Pt nanoparticles. The signal was generated through the

peroxidase activity of Pt nanoparticles, and a detection limit of 0.4 μM was reported.[425]

Ellington and co-workers immobilized biotinylated antilysozyme aptamers on streptavidin-coated microbeads, and the beads were placed in micromachined wells to form an array.[426] The target proteins were either directly labeled with a fluorophore or indirectly through binding to a fluorophore-labeled antibody, with the latter case being in a sandwich assay format. The array was able to identify the best binder among several clones obtained from in vitro selection of antilysozyme aptamers. With the sandwich assay format, ricin was detected by an antiricin aptamer, and the detection limit (320 ng/mL) was comparable to those obtained from antibody-based assays.[426] By using labeled target proteins and attaching in vitro selected aptamers on a slide, the same group reported the detection of lysozyme over 7 orders of magnitude in concentration range with a detection limit of 1 pg/mL.[427] In another array-based study, simultaneous detection of four proteins with four different aptamers in a single buffer condition was demonstrated.[428] Similarly, Lindner and co-workers immobilized anti-IgE and antithrombin aptamers on a glass surface and demonstrated the capture and detection of fluorescently labeled target proteins. The performance was comparable and even superior to those from antibody-based detections.[71] Besides proteins, small molecules have also been detected. Kato et al. immobilized cholic acid onto an agarose matrix and modified its aptamer with a biotin. A streptavidin functionalized alkaline phosphatase and its fluorogenic substrate were used for signal generation. Cholic acid was detected with a detection limit of 10 μM.[429] Xu and co-workers functionalized AuNPs with the PDGF aptamer, while the free aptamer contained a biotin label.[430] This mixture was incubated in an avidin coated plate, and AuNPs were immobilized on the plate by sandwiching PDGF between two aptamer molecules. The immobilized AuNPs were used as catalysts to grow silver nanoparticles to increase sensitivity,[431] and a detection limit of 83 aM was reported.

3.3.7.2. Competitive Assays and Displacement Assays. Competitive and displacement assays are closely related to the sandwich assay format. Similarly, surface immobilization and washing steps are needed. A representative displacement assay is schematically shown in Figure 25C, where a surface bound labeled target was displaced by unmodified targets in solution. In a competitive assay, labeled and unlabeled target molecules are competing for limited binding sites on the surface (Figure 25D). Lee and Walt developed a competitive assay for thrombin.[432] The thrombin aptamer was immobilized on silica microspheres, which were placed at the distal end of an imaging fiber. Fluorescein-labeled and unlabeled thrombin competed for binding sites on the beads. Detection was accomplished with a fiber-optical device, giving a detection limit of 1 nM for unlabeled thrombin.

Using thrombin as the model target molecule, O'Sullivan and co-workers have systematically studied various ELAA formats.[433] For example, the capture agent and the detecting agent can be either an antibody or an aptamer. In addition to the traditional sandwich assay format, the authors also investigated other formats such as competitive assays. The highest sensitivity (<1 nM detection limit) was found in a mixed sandwich format in which the aptamer was immobilized for capture and the enzyme-labeled antibody was used for detection. However, the detection process required ~4 h. The researchers also tested a number of other assay formats, and it was found that relatively fast detection with
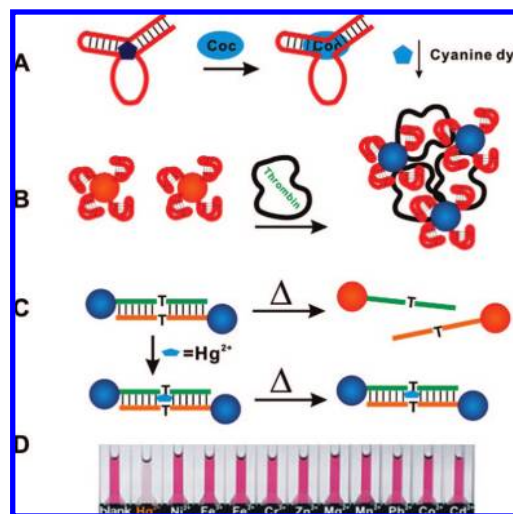
Figure 26. (A) A colorimetric cocaine sensor based on dye replacement.[435] (B) Assembly of aptamer-functionalized AuNPs by proteins that can bind two aptamer molecules.[443,444] (C) A colorimetric Hg^{2+} sensor and its color change in the presence of various metal ions (D). Reprinted with permission from ref 445. Copyright 2007 John Wiley & Sons, Inc.

high sensitivity could be achieved in a competitive assay format, in which enzyme-labeled thrombin was mixed with unlabeled thrombin to compete for binding to immobilized aptamers. The assay could be finished in 1.5 h, and a detection limit of 1.8 nM was reported.[433] It was also noticed that the aptamer had lower affinity for enzyme-labeled thrombin compared to unmodified thrombin. The difference in K_d was ~4-fold. Taking advantage of this observation, the researchers studied displacement assays systematically using thrombin as a model target. Although such a difference in K_d was not mandatory in displacement assays, it had the advantage of facilitating the displacement reaction.[434] Under optimized conditions, the displacement was finished in 10 min, and the total assay took ~30 min. Detection limits of 4.5 nM and <1 nM for optical and electrochemical-based detections respectively were reported.

3.4. Colorimetric Sensors

As mentioned in section 2.4, colorimetric sensors are desirable because in principle no equipment is neccesary for detection, making it possible for on-site and real time detection.

3.4.1. Detection Based on Dye Displacement

Stojanovic et al. screened 35 different dyes by incubating the dyes with an anticocaine aptamer and then adding cocaine to the mixture.[435] Only a cyanine dye showed differences in absorption spectra upon addition of cocaine (Figure 26A). The authors suggested that cocaine could displace the cyanine dye in the aptamer binding pocket and push the dye into solution. The dye formed dimers in solution whose absorption spectrum was different from that of the monomer, resulting in a color change. However, to visualize the color change by the naked eye, 20 μM of aptamer was used and a waiting time of 12 h was needed. It is also difficult to generalize this method for the design of other colorimetric aptamer sensors, because it is not certain whether there will be an appropriate dye for each aptamer.

3.4.2. Detection with Conjugated Cationic Polymers

Some fluorescent sensors using conjugated cationic polymers, reviewed in section 3.3.1.2, also showed color changes in the presence of target molecules.[330,331] When a conjugated polymer is in a random coil conformation in solution, the effective conjugation length is relatively short, giving a relatively short absorption maximum. In the solid state, the absorption peak shifts to longer wavelengths due to the formation of highly conjugated forms. Using the polymer in Figure 17A and K^{+} aptamer as an example, the polymer formed a stiff duplex with a the free aptamer and shifted its absorption to a longer wavelength. When the aptamer bound K^{+} and folded into a compact structure, the polymer wrapped around the aptamer and displayed an absorption maximum at a shorter wavelength. A photograph of the sensor in the presence of different monovalent ions is shown in Figure 17B. The same principle was also applied to thrombin detection with a detection limit of 100 nM. However, micromolar aptamers were still needed for visualization by the naked eye.

3.4.3. Detection Based on Analyte-Induced Assembly of Gold Nanoparticles

Compared to organic chromophores, metallic nanoparticles have much higher extinction coefficients.[436] The color of metallic nanoparticles originates from the surface plasmon effect.[437] For example, the extinction coefficients for 13 and 50 nm AuNPs were reported to be 2.7×10^8 and 1.5×10^{10}, respectively.[438] These values are 3−5 orders of magnitude higher than those of organic dyes. Therefore, only nanomolar AuNPs are needed for visual detection, as compared to the micromolar needed for organic dyes. In addition to being highly sensitive, metallic nanoparticles display distance-dependent optical properties.[439] For example, dispersed AuNPs are red, and the color changes to blue or purple upon AuNP aggregation. DNA can be conveniently attached to AuNPs via the thiol-gold chemistry, and DNA-functionalized AuNPs have been used for highly sensitive and selective colorimetric detection of nucleic acids by Mirkin and co-workers.[107,439−442] By using aptamers as the molecular recognition element, AuNPs have also been reported for sensitive colorimetric detection of a wide range of analytes beyond nucleic acids.

Willner and co-workers functionalized AuNPs with the 15-mer antithrombin aptamer via a poly-T spacer, and mixed the AuNPs with thrombin.[443] With high concentrations of thrombin, some turbidity was observed. The authors suggested that each thrombin can interact with two aptamers.[45,307,308] As a result, AuNPs were linked by thrombin to produce aggregates (Figure 26B). However, no color change was reported. For signal amplification, the aggregates were separated and used as seeds to grow larger AuNPs. A detection limit of 20 nM was reported with this method. Similarly, Chang and co-workers functionalized PDGF aptamers onto AuNPs.[444] It is known that each PDGF can bind two aptamers, and a red-to-purple color change was observed with addition of PDGF, which was again attributed to the cross-linking of AuNPs by the target protein. Interestingly, the authors noted that too much PDGF could inhibit color change, because when AuNPs were completely covered by PDGF, no aptamers were available for cross-linking. A competitive binding assay for PDGF receptor-β was developed as well. Being highly sensitive, the aggregation-based

method requires that the target molecule can bind two or more aptamers. Therefore, it is difficult to generalize this method, especially for small molecule detection.

Recently, Mirkin and co-workers reported a colorimetric sensor for Hg^{2+} detection, and the design is shown in Figure 26C.[445] Two kinds of AuNPs self-assembled through their surface DNA, and a T-T mismatch was intentionally introduced to interact with Hg^{2+}.[19,375,376] When heated to a temperature just above the melting temperature of the AuNPs, all the aggregates turned red except the one containing Hg^{2+}, which maintained a purple color (Figure 26D). A detection limit of 100 nM was reported. With a chip-based scanometric method, the detection limit could reach 10 nM.[446] For the above system to work properly, careful heating and monitoring of thermal denaturation temperature during the detection process is required. To overcome this limitation for even wider applications where no heating is required, Liu and coworkers have made significant improvement of the design, allowing one-step, room temperature colorimetric detection of Hg^{2+}.[648]

3.4.4. Detection Based on Analyte-Induced Disassembly of AuNP Aggregates

To develop a more general strategy for colormetric sensing, instead of using target molecules to form or stabilize AuNP aggregates, we tested the reverse process, using target analytes to disassemble AuNPs.[447] The sensor for adenosine detection is shown in Figure 27A. Two DNA-functionalized AuNPs (1 and 2) were assembled by a linker DNA containing an adenosine aptamer (in green). The aptamer was extended by 17 nucleotides on its 5′-end. The first 12 were complementary to the DNA on AuNP 1, while the other 5 on the extension and an additional 7 from the aptamer were complementary to the DNA on AuNP 2. In the presence of adenosine, the aptamer switched its structure to bind the target. As a result, the number of base pairs left to bind AuNP 2 decreased from 12 to 5, which could no longer hold AuNP 2 and led to dissociation of the aggregates. A color change from purple to red was observed. Unlike the relatively slow AuNP assembly process, disassembly can be finished in seconds. As shown in Figure 27D, faster color change was observed with increasing concentrations of adenosine, while other ribonucleosides did not produce any color change (Figure 27C). The sensor design is quite general. AuNPs assembled by a cocaine aptamer were also prepared (Figure 27B). A red color was produced upon addition of cocaine but not adenosine (Figure 27E). The rate of color change also varied with cocaine concentration (Figure 27F). Similarly, sensors responsive to potassium ions have also been obtained.[448]

Most sensors, including the ones described above, can detect only a specific analyte. For some applications, it may be desirable to detect multiple analytes in the same system, which has also been demonstrated in the aptamer-linked AuNP system. First, a system with high analyte cooperativity was designed. It contained two kinds of AuNPs (1 and 3) and two DNA linkers (Figure 28A).[448] AuNP 1 was functionalized with one kind of DNA and AuNP 3 with two kinds of DNA. Both the adenosine aptamer and the cocaine aptamer were used to assemble the AuNPs. To observe a color change, both adenosine and cocaine were needed, while neither molecule alone could induce a significant color change. Therefore, the two molecules were highly cooperative in disaggregating the AuNPs. As shown in Figure 28B,
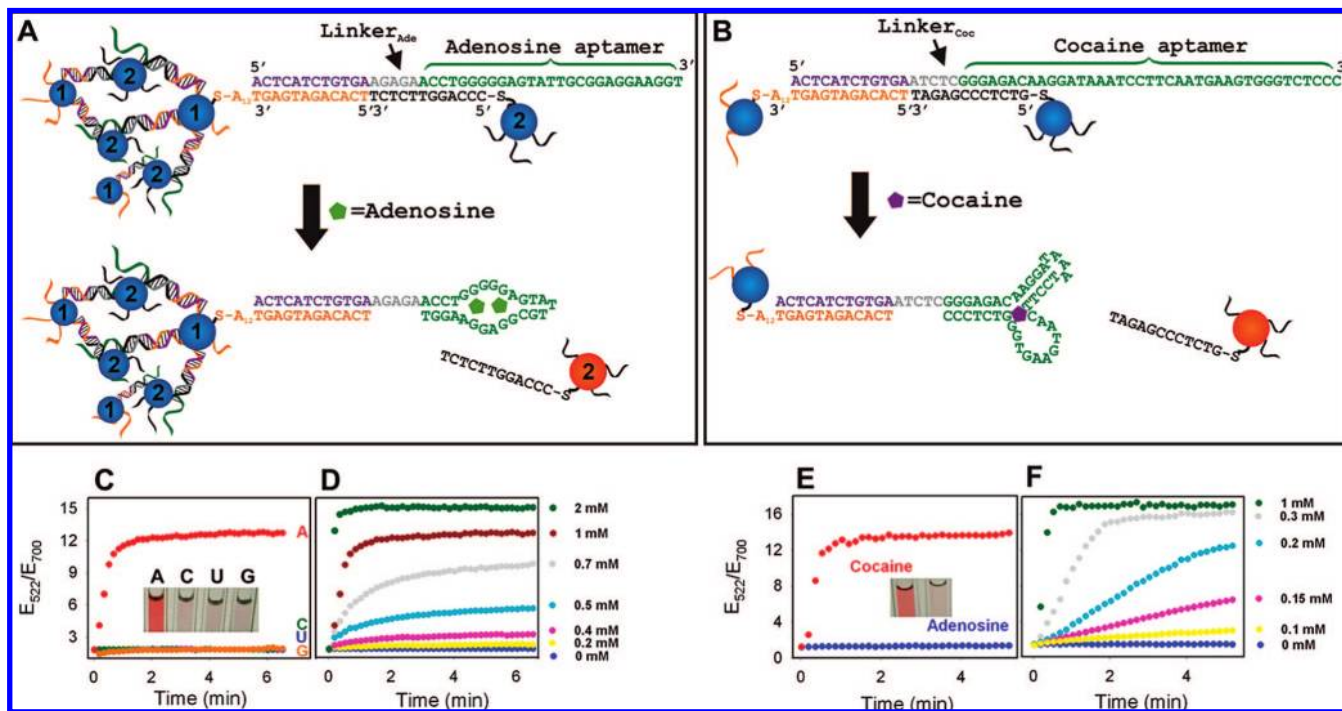
Figure 27. Colorimetric sensors based on the disassembly of AuNPs linked by an adenosine aptamer (A) or a cocaine aptamer (B). Specificity test of the adenosine (C) and cocaine (E) sensors. Insets: photographs of sensor solutions after treatment with analytes. Kinetics of sensor color change in the presence of varying concentrations of adenosine for the adenosine sensor (D), or cocaine for the cocaine sensor (F). Reprinted with permission from ref 447. Copyright 2006 John Wiley & Sons, Inc.
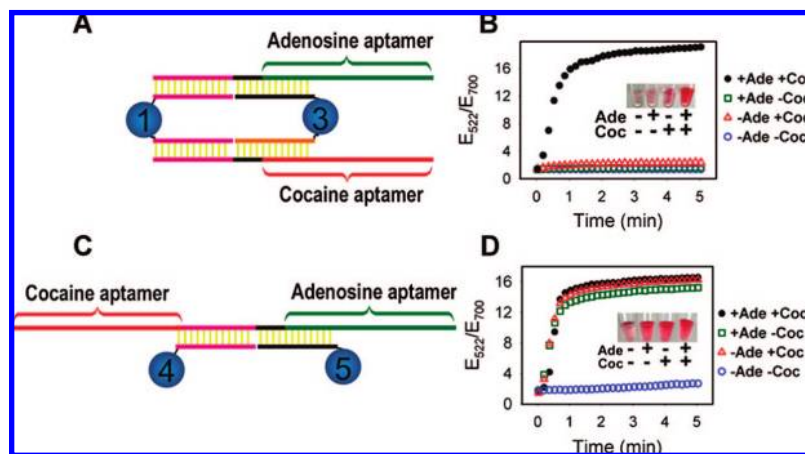
Figure 28. Colorimetric sensors that change color only when both adenosine and cocaine are present (A) or either analyte is present (C). Kinetics (B and D) of color change of the aggregates in the presence of 1 mM adenosine, 1 mM cocaine, 0.5 mM adenosine, and 0.5 mM cocaine, or no analytes in parts A and C, respectively. Insets show the colors displayed by the sensors. Reprinted with permission from ref 448. Copyright 2006 John Wiley & Sons, Inc.

fast color change was observed only when both molecules were present (black curve). The inset shows the color of the sensors when exposed to different analytes and an intense red color was observed only when both molecules were present. Using a different design, a system without analyte cooperativity was built, which contained two types of AuNPs (4 and 5) and a linker DNA flanked by the adenosine and cocaine aptamers (Figure 28C).[448] In the presence of either analyte, AuNPs were dispersed. As shown in Figure 28D, a color change was observed in the presence of either adenosine, or cocaine, or both.

In the above system, although the sensors can detect both adenosine and cocaine, one cannot determine the identity of the analytes. By incorporating QDs into the AuNP aggregates to encode for different analytes, multiplex detection was achieved (Figure 29).[449] To detect adenosine, for example,

in addition to AuNPs 1 and 2, QD Q1 (emission at 525 nm) was also used. Q1 and AuNP 2 were functionalized with the same DNA sequence, and therefore, both were linked to AuNP 1 by the adenosine aptamer linker. In the aggregated state, the emission of the QD was quenched because of energy transfer to surrounding AuNPs.[450−454] Addition of adenosine disassembled AuNPs, resulting in increased emission intensity at 525 nm. Similarly, cocaine sensors were prepared by incorporation of Q2, which emitted at 585 nm. Because different QDs can be excited at the same wavelength, when these two types of aggregates were mixed, two emission peaks at 525 and 585 nm were observed (Figure 29B, solid line), corresponding to the adenosine and cocaine sensors, respectively. Addition of cytidine and uridine (dashed line) did not change the emission intensity of either peak. Addition of adenosine alone increased only the 525

Figure 29. (A) QD-encoded and aptamer-linked nanoparticles for multiplex detection. QD emission was initially quenched. Addition of target analytes allowed recovery of QD emission. (B−E) Luminescence spectra of mixed sensors in the presence of different analytes. Reprinted with permission from ref 449. Copyright 2007 American Chemical Society.
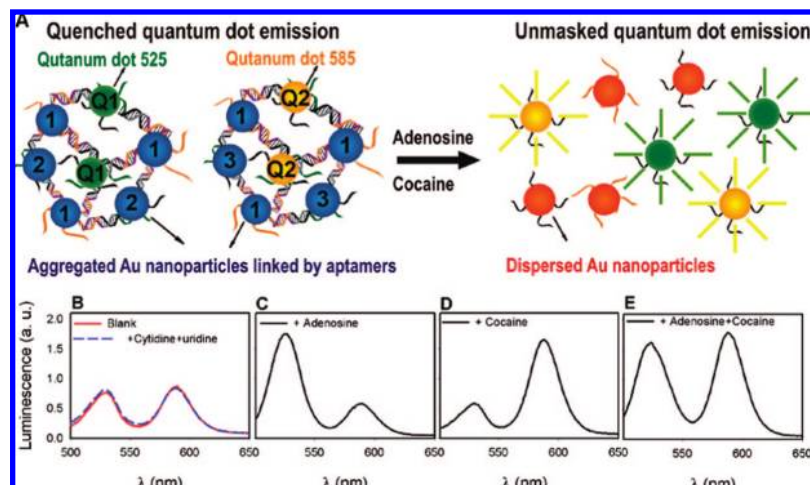
nm peak (Figure 29C); addition of cocaine alone only increased the 585 nm peak (Figure 29D); and addition of both analytes resulted in enhancements of both peaks (Figure 29E). This result shows the feasibility of using aptamer-linked nanoparticles for one-pot simultaneous detection of multiple analytes.

3.4.5. Detection Based on Non-Cross-Linking DNA

In the above AuNP-based colorimetric sensors, the color change was due to the cross-linking of AuNPs by DNA hybridization. Interestingly, it has been shown that non-DNA-cross-linking based AuNP aggregation is also useful for developing colorimetric aptamer sensors. The stability of AuNPs is dependent on the concentration of electrolytes in solution, and high concentrations of salt can induce aggregation of colloids, giving a similar red-to-blue color change. A schematic of such a process is shown in Figure 30A. AuNPs are usually made from reduction of HAuCl$_4$ by sodium citrate. However, AuNPs protected by the citrate ligand are relatively unstable. They tend to aggregate irreversibly in tens of millimolar NaCl. DNA-functionalized AuNPs on the other hand, are much more stable and can survive even molar concentrations of NaCl.[439] Nanoparticle stability against salt is also dependent on the state of DNA. For example, single-stranded, double-stranded, folded, unfolded, short, long, thiolated, and nonthiolated DNA all give different AuNP stabilities, which provides another useful means for signaling aptamer binding. Because such aggregation processes are not induced by DNA hybridization, they are usually called non-cross-linking AuNP aggregation. The first report on this method was by Sato et al.[455] They attached thiol-modified 15-mer single stranded DNA to AuNPs. These nanoparticles were highly stable and remained dispersed and red in color even in 2.5 M NaCl (Figure 30B, the left panel). There were over 100 DNAs on each AuNP, but only one is drawn here. In the presence of the cDNA, the salt stability of the AuNPs decreased, and purple colored precipitant was observed at 0.5 M NaCl concentration (middle panel). If the duplex DNA contained a single mismatch at the end, the AuNPs could also survive 2.5 M NaCl and remained red in color. This system, however, required a target DNA/AuNP ratio of 200:1 to induce aggregation, which led to a limited sensitivity of 500 nM. The difference in AuNP stability was attributed to the rigidity of double-stranded DNA.
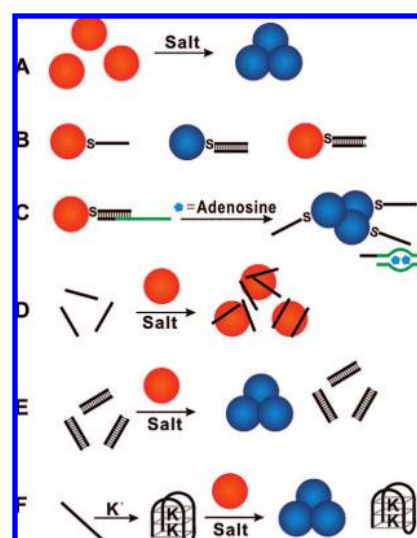
Figure 30. Colorimetric sensors based on non-cross-linking DNA. (A) Schematics of AuNP aggregation induced by electrolytes. (B) Different stabilities of AuNPs with different DNAs in high salt buffers.[455] (C) Colorimetric detection of adenosine.[456] There are ~100 DNAs on each AuNP, but only one is shown for clarity. Nonthiol modified single-stranded DNA can also protect AuNPs from aggregation (D), but not double-stranded DNA (E).[460] (F) Colorimetric detection of K$^+$.[462]

Li and co-workers also functionalized AuNPs with short thiol-modified DNA and hybridized an adenosine DNA aptamer to the DNA. The stability of AuNPs was so high that they were stable in 500 mM MgCl$_2$. Such high salt concentrations were undesirable to carry out aptamer binding and structure switching reactions. AuNP stability was then tuned down by treating with 6-mercaptohexanol (MCH). It was found that the number of thiol DNAs dropped from ~150 to ~100 after MCH treatment, and 90% of them were hybridized to the adenosine DNA aptamer. These AuNPs were stable in 35 mM MgCl$_2$ for more than 1 min. Addition of adenosine led to structure switching of the aptamer and its dissociation from AuNPs (Figure 30C). The salt stability of the AuNPs then decreased, giving a red to purple color change. Such color changes could be observed in 1 min, and a detection limit of 10 μM was reported.[456,457] Chang and co-workers functionalized AuNPs with an ATP aptamer, and such nanoparticles have relatively low stability in high salt
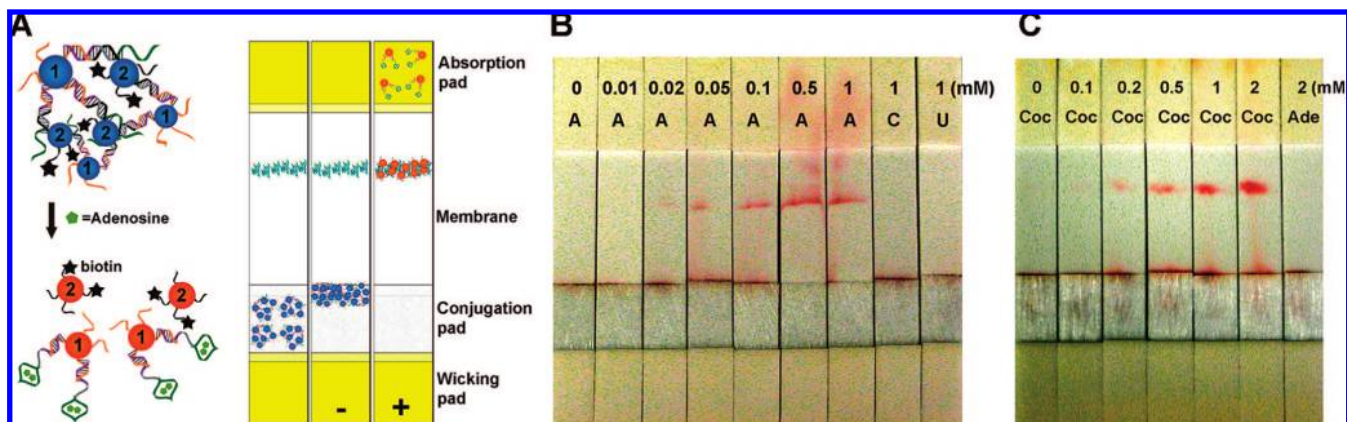
Figure 31. Aptamer/AuNP-based lateral flow device. (A) Left: adenosine-induced disassembly of AuNPs. Biotin is denoted as a black star. Right: schematics of lateral flow devices loaded with assembled nanoparticles (on the conjugation pad) and streptavidin (on the membrane in cyan) before use (left strip), in a negative (middle strip), or a positive (right strip) test. (B) Test of the adenosine device with varying concentrations of nucleosides. A = adenosine, C = cytidine, U = uridine. (C) Test of the cocaine device with varying concentrations of cocaine in undiluted human blood serum. Coc = cocaine, Ade = adenosine. Reprinted with permission from ref 468. Copyright 2006 John Wiley & Sons, Inc.

solutions. In the presence of ATP, the aptamer folded into a more compact structure with increased charged density and stability. A detection limit of 10 nM ATP was reported.[458]

Instead of using thiol-modified DNA to functionalize AuNPs, Rothberg and co-workers found that nonthiolated short single-stranded DNA can also be adsorbed onto AuNP surface with protection effects (Figure 30D).[459−461] The kinetics of DNA adsorption was dependent upon the length of DNA and temperature. Shorter DNA (10−20 nucleotides) and higher temperatures gave faster adsorption.[460] Long or double-stranded DNA could not be associated with AuNPs effectively, making the AuNPs susceptible to salt-induced precipitation (Figure 30E). Along this line, Fan and co-workers designed a colorimetric sensor for K^+ detection.[462] A piece of guanine rich DNA could form a G-quadruplex structure in the presence of K^+. Similar to double-stranded DNA, this folded DNA could not be effectively adsorbed onto the AuNP surface, and therefore, the AuNPs aggregated in the presence of NaCl (Figure 30F). This sensor system was able to detect ~1 mM K^+. Similar designs were also reported for the detection of thrombin by Dong and co-workers[463] and the detection of Hg^{2+} by the Willner group.[464] The Fan group has also split the cocaine aptamer into two halves. In the absence of cocaine, the DNA fragments can protect AuNPs from aggregation, while cocaine caused assembly of the aptamer into a rigid binding structure, which could not protect nanoparticle aggregation.[465] A colorimetric sensor for ATP was also reported by the group based on the generation of single-stranded DNA from an aptamer-containing double-stranded DNA in the presence of ATP.[466] These sensors did not need thiol-modified DNA for AuNP functionalization, which can reduce the cost associated with sensor production and simplify the experimental protocol. This very reason, however, also contributes to relatively low AuNP stability, even with protection from short single-stranded DNA. For example, thiol DNA protected AuNPs can survive 2.5 M NaCl, but this number goes down 10-fold for nonthiolated DNA protected AuNPs. Therefore, high ionic strength samples or the presence of high valent cations may give false positive results, while the presence of other single-stranded DNA or protecting polymers may give false negative results.

Since both cross-linking (also called labled sensor) and non-cross-linking (also called lable-free) systems have been

used for colorimetric sensing, we have carried systematic study and comparison of pros and cons of each system using a UO_2^{2+}-dependent DNAzyme as a test system.[278] For all non-cross-linking systems, a common advantage is fast color change kinetics. The assembly of AuNPs by DNA base pairing interactions usually takes several minutes to hours because the AuNPs have negative charges from the DNA phosphate backbone and repel each other. DNA hybridization needs to overcome such repulsive forces. For non-cross-linking systems, on the other hand, the negative charges on DNA are screened by high salt concentrations and aggregation is driven by van der Waals forces.[455,456] Usually color changes in such systems can be observed in 1 min. The cross-linking system has higher stability and is simpler to use, as it requires only the addition of target analytes once the sensor is prepared. On the other hand, the non-cross-linking system has better sensitivity, shorter operation time, and lower costs. If operation requires a very low detection limit, the label-free system should be a better choice. When the detection limit is adequate, such as in the case of uranyl sensing, the labeled method should be used due to turn-on sensing and high stability of the system that allows operation under a variety of conditions.

3.4.6. "Dipstick" Colorimetric Tests

Even though colorimetric sensors can eliminate the use of analytical instruments, one limitation that prevents their practical application is the need for laboratory techniques, such as transferring microliter volumes of solutions, which makes the sensors difficult to use for most people without proper equipments and skills. One of the most successful methods to convert antibody-based assays to user-friendly test kits is the lateral flow technology, and a well-known example is the pregnancy test kit. Despite their wide applications in antibody assays, lateral flow devices based on nucleic acids were seen only for DNA detection.[467] We have recently employed this technology for aptamer-based detection.[468]

The sensing method shown in Figure 27A was applied to the lateral flow device platform. Some AuNPs were labeled with biotinylated DNA (black stars in Figure 31A) so that they could be captured by streptavidin to form a colored band. The lateral flow device contained four overlapping pads

placed on a backing (Figure 31A). The four pads (from top to bottom) were as follows: absorption pad, membrane, glass fiber conjugation pad, and wicking pad. The aptamer-assembled AuNPs were spotted on the conjugation pad while streptavidin was applied on the membrane (Figure 31A, left strip). For adenosine detection, the strips were dipped into samples containing various nucleoside species at different concentrations (Figure 31B). Higher adenosine concentrations resulted in bands with more intense red color, and the detection limit was ~20 μM. For other ribonucleosides, no red bands were observed. Similarly, cocaine sensitive strips were also prepared and tested in undiluted blood serum (Figure 31C). These results demonstrate that the device can be used in biological samples, making applications in medical diagnostics possible.

3.4.7. Detection Based on Structural Color Change

Even in the absence of any color reporting groups, color can still be generated through interference, diffraction, scattering, or a combination thereof. Termed structural colors, they are possessed by many species in Nature, such as butterflies. Kinoshita et al. constructed a polypeptide multilayer Langmuir−Blodgett (LB) film on a silicon surface and demonstrated that the color of the film changed with the thickness of the peptide layer.[469] The authors further designed an aptamer-based colorimetric sensor by immobilizing an RNA aptamer for bacteria, *Sphingobium yanoikuyae*, onto a poly lysine film. On a precolored silicon surface, the system displayed a yellow color. In the presence of the bacteria (1 × 10^5 cfu/mL), the film turned orange due to changes in the thickness of the film.[470]

3.5. Electrochemical Sensors

While aptamer-based optical sensors have been used since over a decade ago, electrochemical detection with aptamers appeared in the literature only in the last four years.[471] The number of publications on this topic, however, is increasing rapidly. Part of the reason could be that many designs and concepts of optical sensors can be readily transferred to electrochemical sensing. As can be observed from the following examples, many aptamer-based electrochemical sensors can be regenerated with minimal loss of sensor performance, and most of these sensors do not require the addition of extra reagents and are thus called "reagentless sensors". The possibility of detecting targets in a complex matrix such as blood serum has also been demonstrated. In a recent review by Xiao and Plaxco,[472] electrochemical aptamer sensors have been categorized into three classes: sandwich type assays, impedance based assays, and aptamer structure switching-based assays. The former two have been seen in antibody assays while the last one is unique to aptamers.

3.5.1. Sandwich Electrochemical Assays

This assay format has been covered previously in the fluorescent sensor section (section 3.3.7). By replacing fluorophores or fluorogenic enzymes with redox active labels or enzymes that can generate a redox active species (i.e., H_2O_2), electrochemical assays can be designed. As shown previously in this review, there are two different aptamer binding sites on thrombin (Figure 14). Ikebukuro and co-workers took advantage of this fact and developed a
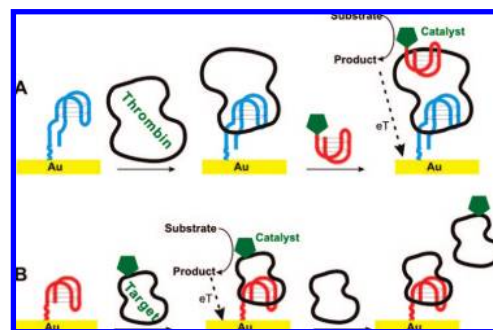
Figure 32. (A) Sandwich assays for electrochemical thrombin detection. (B) Competitive assays based on electrochemical aptamer sensors.

sandwich type assay as shown in Figure 32A.[473,474] The 29-mer thrombin aptamer was immobilized onto a gold electrode. After binding thrombin to the surface, a glucose dehydrogenase (GDH)-conjugated 15-mer thrombin aptamer was added to bind to the other site on thrombin. Oxidation of GDH was monitored by the increase of current through the electrode, and a detection limit of 10 nM thrombin was reported. Mascini and co-workers employed thrombin aptamer-functionalized magnetic beads to capture thrombin, whereby a biotinylated secondary aptamer was applied to sandwich thrombin. Finally, alkaline phosphatase conjugated streptavidin was added to bind biotin for signal generation. The magnetic beads were collected on the electrode surface containing the magnetic core. This system allowed highly sensitive thrombin detection with a detection limit of 0.5 nM in buffer and 5 nM in serum and plasma.[475]

Similarly, Willner et al. sandwiched thrombin between an electrode-immobilized thrombin aptamer and a thrombin aptamer attached to a Pt nanoparticle,[476] and the Pt catalyzed reduction of H_2O_2 to H_2O was monitored. A detection limit of 1 nM was reported. In this work, however, only the 15-mer thrombin aptamer was used, suggesting that this aptamer has affinity for different sites on the protein. Katakis and co-workers sandwiched thrombin between a surface immobilized aptamer and an aptamer bearing a linkage to horseradish peroxidase (HRP), which was detected through its enzymatic reaction, and a detection limit of 80 nM was reported.[477]

The examples above used thrombin as a model target. Since thrombin is unique in that it contains two aptamer binding sites, it is difficult to judge the generality of this sandwich approach because many target analytes only have one aptamer binding site. Variations of the sandwich assay format can be made by replacing the capture aptamer by a simple adsorption event, while keeping the signaling aptamer.[477,478] Alternatively, Hianik et al. kept the immobilized capturing aptamer but replaced the signaling aptamer with free redox-active labels such as methylene blue (MB) that can bind thrombin.[479] However, because MB can also nonspecifically bind to DNA and streptavidin, the background signal and signal variations were high and the sensitivity was relatively low (detection limit 10 nM). Other proteins, such as IgG, also gave significant signal changes.[479] Recently, Yu and co-workers immobilized the lysozyme aptamer onto an electrode and incubated it with a redox cation $[Ru(NH_3)_6]^{3+}$.[480] Binding of lysozyme to the aptamer reduced the number of $[Ru(NH_3)_6]^{3+}$ molecules associated with the aptamer, thereby decreasing the electrochemical signal. A detection limit of 0.5 μg/mL was reported. He,

Fang, and co-workers immobilized the thrombin aptamer onto an electrode, and a cDNA strand attached to $(Ru(bpy)_3^{2+}$-doped silica nanoparticles was added. In the presence of thrombin, the labeled strand was displaced, resulting in decreased electrochemiluminescence signals. A detection limit of 1 fM was reported. This high sensitivity was the result of each silica nanoparticle being able to contain many $Ru(bpy)_3^{2+}$ labels.[481] Shao and co-workers immobilized the anti-AMP aptamer onto an electrode, and a short piece of DNA complementary to part of the aptamer sequence was added to form a double stranded region. Positively charged $[Ru(NH_3)_6]^{3+}$ was added to bind DNA through electrostatic interactions. In the presence of AMP, the short strand was displaced due to the structure-switching property of aptamers, resulting in a decrease in the electrochemical signal associated with $[Ru(NH_3)_6]^{3+}$.[482]

As a serine protease, thrombin can catalyze the hydrolysis of a peptide (β-Ala-Gly-Arg-p-nitroaniline) to produce p-nitroaniline. The bound peptide and free p-nitroaniline have different redox potentials. Katakis and co-workers immobilized the thrombin aptamer onto a substrate. In the presence of thrombin and the peptide, the redox peak corresponding to free p-nitroaniline was observed, while, in the absence of thrombin, only the bound peptide peak was observed. This method could produce a signal in 5 min. Even though p-nitroaniline has a yellow color, 3 hours were required to generate a visible color change.[477] As covered previously, Baldrich and co-workers immobilized the thrombin aptamer onto an electrode surface and developed a displacement assay where the unmodified thrombin was used to displace enzyme-labeled thrombin captured by immobilized aptamers (Figure 32B), producing changes in electrochemical signals.[434]

3.5.2. Electrochemical Impedance Spectroscopy-Based Detection

Electrochemical impedance spectroscopy (EIS) is a useful technology for studying biomolecular interactions. It is based on a change in electrode dielectric properties induced by ligand binding interactions.[483] Under high frequency alternative current (AC) conditions, the migration rate of redox species to the electrode surface becomes rate limiting, and factors that block their access to the electrode surface can generate a frequency dependent phase lag between the AC voltage and the current. The analytical method based on this phenomenon is EIS. EIS has been applied to construct sensors to detect a number of reactions, including DNA hybridization and antibody−antigen binding.[483] Recently, EIS has also been applied to construct aptamer-based sensors. As it is not necessary to introduce external functional groups for signal generation, EIS represents another label-free detection method.

Wang and co-workers immobilized a biotinylated DNA aptamer for lysozyme on an indium−tin oxide (ITO) electrode coated with streptavidin and polymer.[484] Because the aptamer was negatively charged, access of $[Fe(CN)_6]^{3-/4-}$ to the electrode surface was hindered. As a result, the interfacial electron transfer between this redox pair and the electrode was not efficient. At pH 7.0, lysozyme is positively charged (pI = 11). Binding of lysozyme to the negatively charged aptamer gradually increased the positive charge on the electrode surface, causing the electron transfer resistance to decrease. Based on this observation, the authors were able to detect 14 nM of lysozyme in 10 μL with high
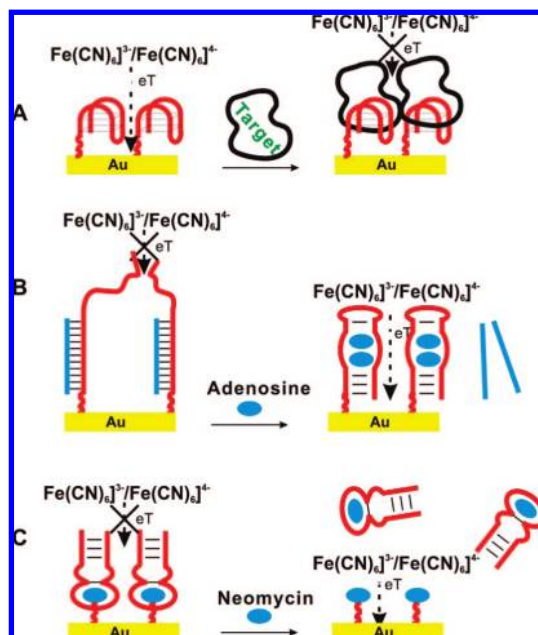
Figure 33. Electrochemical impedance-based detection. (A) Protein detection based on electrode surface blocking upon protein binding. (B) Relief of surface blocking upon adenosine binding. (C) A displacement assay used to relieve blocking from aptamers for neomycin detection.

reproducibility. For EIS-based sensors, it is unusual to observe decreased resistance upon binding to target proteins, because such binding always blocks the access of redox probes. In the lysozyme system, the authors purposefully carried out experiments at a pH value 4 units below the pI of the protein to make the protein positively charged.

In a similar system, Radi et al. immobilized the thiol-modified thrombin aptamer onto a gold electrode, and $[Fe(CN)_6]^{3-/4-}$ was also used for probing electron transfer.[485] The interfacial electron transfer resistance increased upon addition of thrombin, which was attributed to the blocking effect of thrombin (Figure 33A). The detection limit was estimated to be 2 nM, and regeneration of the sensor was demonstrated. Hsing and co-workers also reported an impedance-based thrombin detection system, and a detection limit of 0.1 nM was observed.[486] Xu et al. reported an amplified impedance detection method similar to that shown in Figure 33A. After capturing thrombin onto the electrode surface by the aptamer, the protein was denatured by a high concentration of guanidine hydrochloride, which expanded the area covered by thrombin on the electrode, making it a better blocking agent. The authors observed a surprisingly low detection limit of 10 fM, which is over 6 orders of magnitude below the K_d of this aptamer.[487] Recently, Liao and Cui applied the method to detect PDGF, and a detection limit of 40 nM was reported.[488]

Xu et al. fabricated a gold film deposited electrode array and immobilized thiol-modified IgE aptamers.[489] An IgE-dependent increase of impedance was observed with a detection limit of 0.1 nM. Importantly, the authors were able to show that they could place different DNA sequences onto different electrodes in the array, and increased impedance was observed only for the native aptamer, but not its mutants. This work indicates that the method can be used to construct arrays capable of detecting multiple proteins simultaneously.

Because the sensitivity of impedance-based sensors increases with decreasing electrode separation, Löhndorf,

Schlecht, and co-workers fabricated nanometer-gap impedance sensors whose working frequency was higher than 1 GHz.[490,491] The authors immobilized an antibody and an RNA aptamer for thrombin and showed that both ligands were able to detect thrombin specifically.[491] The researchers also compared impedance sensors of different sizes and geometries based on the performance for HIV Rev peptide detection. It was found that 3-D nanogap sensors had higher sensitivity than 2-D planar sensors with micrometer gaps.[492]

In addition to protein detection, aptamer impedance sensors have also been successfully applied to detect small molecules, which is generally difficult for antibodies. Radi and O'Sullivan immobilized a guanine rich DNA that could fold into a DNA quadruplex structure in the presence of K^+. Such a conformational change made the DNA a good blocking agent, and this system could detect 0.1 mM K^+.[493] Willner and co-workers applied the structure switching mechanism of aptamers and constructed a sensor for AMP (Figure 33B).[494] The AMP aptamer was immobilized onto the electrode surface, and a short piece of antisense DNA complementary to a small fraction of the aptamer was added. In this state, the device had high impedance. Addition of AMP switched the aptamer to its binding structure and released the antisense DNA, giving decreased impedance. This system had a detection limit of 2 μM. With similar designs, the Willner group also reported the detection of two analytes with a single sensor by rational incorporation of two different aptamers.[495] Tuñón-Blanco and co-workers designed an impedance-based competition assay for neomycin, as shown in Figure 33C.[496] Neomycin was first covalently attached to the electrode surface, and its aptamer was added to bind neomycin and block the electrode, giving high impedance. In the presence of free neomycin molecules, the aptamers were displaced from the surface, thereby reducing the impedance. This system was able to detect neomycin from 0.75 to 500 μM in buffer and 25 to 2500 μM in milk.

3.5.3. Electrochemical Detection Based on Aptamer Structural Changes

This class of electrochemical sensors is unique to aptamers because antibodies do not possess controllable structure changes that can generate predictable signals. Using the aptamer beacon concept, Kim and co-workers have constructed a hairpin containing the thrombin aptamer sequence in a similar way as shown in Figure 20B, except that no fluorophore or quencher was present.[497] The 5′-end of the hairpin was immobilized onto a gold electrode. Methylene blue (MB) could intercalate into the stem region of the hairpin. In the presence of thrombin, the hairpin was opened to form a G-quadruplex structure to bind thrombin, thus releasing intercalated MB and decreasing the electrochemical signal. The method has a detection limit of 11 nM thrombin.

Leclerc and co-workers introduced a ferrocene substituent into the monomer of a cationic polymer to make the polymer a large electroactive label.[72] A thrombin aptamer was immobilized onto a gold electrode. In the presence of thrombin, the cationic polymer did not have access to the aptamer because the aptamer was bound to thrombin, and low signal intensity was observed. In the absence of thrombin, the cationic polymer was able to bind the DNA aptamer and an electrochemical signal from ferrocene was observed. Under experimental buffer conditions, however, this system suffered from signal saturation and could not offer quantitative results. In a second system reported by
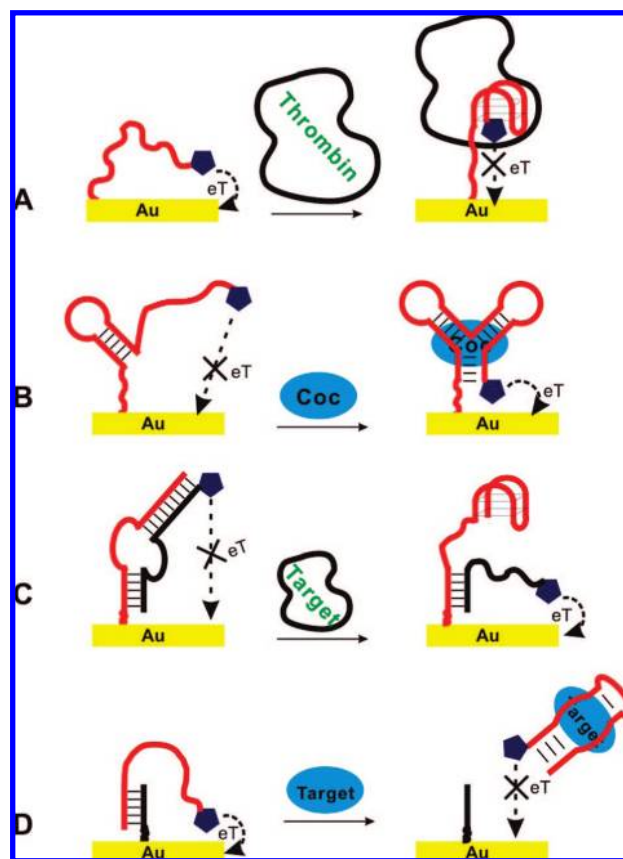
Figure 34. Electrochemical aptamer sensors based on aptamer structure change upon target binding. (A) Binding of thrombin moved the redox label away from the electrode surface.[498] (B) Binding of cocaine pulled the label closer to the surface.[501] The same design also worked for PDGF detection.[504] (C) The label was in a DNA strand that formed two duplex regions with an aptamer. Addition of the target switched the aptamer structure and released the redox label to enhance electron transfer.[506] (D) Binding of the target forced the label to be away from the electrode surface and decreased electron transfer.[507]

the authors, a PNA complementary to the thrombin aptamer was immobilized, and a nuclease digestion reaction was first carried out in solution.[72] In the presence of thrombin, the aptamer was protected from nuclease by binding to thrombin, and the surviving aptamers reacted with the immobilized PNA to form a double helix, which then associated with the cationic polymer to generate a signal. In the absence of thrombin, the aptamer was digested and PNA (neutral charge) alone could not bind the cationic polymer. With this indirect method, quantitative analysis was performed and a detection limit of 75 nM was reported.

Compared to using noncovalent labels as above, sensor performance has been significantly improved by covalent attachment of electroactive labels to aptamers. These sensors are called electronic aptamer-based (E-AB) sensors by the authors.[498] For example, a 31-mer DNA was modified with a 5′-thiol, and the 3′-end of the DNA contained a thrombin aptamer that was terminated by linking to MB (Figure 34A).[498] In the absence of thrombin, the DNA unfolded and the MB group had a high probability of colliding with or even weakly binding to the electrode surface. Addition of thrombin, however, inhibited electron transfer because the aptamer part folded into a G-quadruplex structure, and only half of the DNA strand remained flexible. One disadvantage associated with this detection method is its "turn off" nature, which means electron transfer decreases in the presence of

thrombin. The detection limit was 6.4 nM, with a dynamic range up to 768 nM.[498] The sensor was capable of detecting thrombin in human blood serum, suggesting high specificity. The binding kinetics, however, was relatively slow. It took more than 3 h to reach signal saturation.

Interestingly, in another report on the same thrombin aptamer system, the 15-mer DNA aptamer was directly attached to the electrode and no single-stranded spacer was involved.[499,500] The electroactive label was a ferrocene (Fc) instead of MB. In the absence of thrombin, the Fc group was held away from the surface by the DNA chain. Addition of thrombin forced the aptamer to fold into a G-quartet to bind thrombin, and the Fc group was pointed down toward the surface. As a result, enhanced electron transfer was observed, making it a "turn on" sensor. Because all the linkages were covalent in the system, the sensor could be regenerated by washing with denaturants. The results obtained from 25 regeneration cycles had a standard deviation of only 5.4%, suggesting that the system was very robust. This method could detect up to 35 nM thrombin with a detection limit of 0.5 nM.

Similar strategies have been applied to design a cocaine sensor.[501] A cocaine aptamer was attached to a gold electrode directly, without additional DNA sequences serving as a spacer (Figure 34B). The aptamer was proposed to have a short hairpin structure flanked by two single-stranded regions in the absence of cocaine, and the MB group was away from the surface. Binding of cocaine completely folded the aptamer, forcing the MB group to be close to the surface. This sensor was able to detect cocaine in a number of biological fluids, such as blood serum and saliva. The sensor could also be regenerated and the response time was fast, with 97% of the total signal observed in 80 s. The detection limit was lower than 10 μM, and the sensor could detect up to 500 μM cocaine before signal saturation. Systematic optimization has also been performed on this sensor.[502] Using Ru(bpy)$_2$(dcbpy)NHS as a label, Zhang and co-workers designed an electrochemiluminescence sensor based on a similar design, and a detection limit of 1 nM was reported for cocaine detection.[503] This method has also been applied to construct an electrochemical sensor for PDGF by Plaxco, Heeger, and co-workers with a detection limit of 1 nM in undiluted blood serum and 50 pM in 2-fold diluted serum.[504] Recently, the detection of theophylline based on the structure change of an RNA aptamer was also reported.[505]

It can be seen from the above examples that knowledge of the secondary structure of DNA aptamers and the interactions between DNA and gold surfaces is crucial for sensor design. Single-stranded DNAs are usually very flexible, and it is difficult to predict their interactions with solid surfaces. Nonspecific interactions between DNA and surfaces can lead to high background or low signal change, thus limiting the sensitivity. In an effort to improve the thrombin sensor and minimize nonspecific interactions with the surface, double-stranded DNAs were introduced (Figure 34C).[506] The thrombin aptamer DNA formed two double-stranded regions with another piece of DNA labeled with MB. The rigidity of the double-stranded DNA kept MB away from the surface. Addition of thrombin opened one of the double-stranded regions and liberated the DNA with MB for enhanced electron transfer. The sensor had a detection limit of 3 nM and a dynamic range linear up to 100 nM. Since the structure of the DNA complex is more predictable, this design should be generally applicable to the construction of

many other aptamer-based electrochemical sensors. This method also had the advantage of making "turn on" sensors, with increased electron transfer in the presence of the target. Compared to "turn off" sensors,[498] the signal change was much greater. However, because only one of the two DNA strands was covalently attached to the electrode, the sensor was not reusable.

Recently, Shen, Yu, and co-workers developed another scheme for detecting analytes based on the structure switching properties of aptamers (Figure 34D). A short DNA was immobilized onto a gold electrode surface, and an adenosine aptamer containing an end-labeled ferrocene was hybridized to the short piece of DNA to give a strong electron transfer signal. Addition of adenosine switched the aptamer to its binding structure, pulling it away from the surface, which resulted in decreased electron transfer.[507] A detection limit of 20 nM was reported. In a similar report by Mao and co-workers, the label was placed on the complmentary strand, which was immobilized on the electrode. The presence of target analytes released the aptamer strand, and the label on the complementary strand was brought to the electrode surface.[508] Such electronic sensors based on target-induced strand release were also reported by Yamana and co-workers.[509]

3.5.4. Detection Based on Electrochemical Stripping

Other than using electroactive labels to detect electron transfer, electrochemical stripping methods have also been tested.[510] QDs were attached to target proteins, and the targets were captured by immobilized aptamers. This assay was designed to be a displacement reaction format. In the presence of the target protein, the QD-labeled protein was displaced, and the number of QDs left on the surface decreased. After dissolving the remaining QDs on the surface, the metal species and its concentration were detected and quantified by electrochemical stripping, which was correlated to the concentration of target proteins in solution. Owing to the amplification effect originated from dissolving QDs and the highly sensitive nature of electrochemical stripping detection, the sensitivity of this method was very high. A detection limit of 0.54 pM was achieved for thrombin detection, which was even more sensitive than PCR-based detection of thrombin.[395] Importantly, different aptamers can be immobilized onto the same gold substrate to target different analytes, taking advantage of the fact that QDs with different cation compositions (i.e., CdS, ZnS, CuS, and PbS) can be attached to different protein targets. As demonstrated by the authors, thrombin and lysozyme were labeled with CdS and PbS, respectively, and both proteins were detected on a single gold substrate (Figure 35). Instead of encoding target analytes based on their optical properties,[449] here the QD encoding was based on their elemental compositions.

Oxidation of tyrosine and tryptophan residues in proteins can be used to detect trace amounts of proteins by chrono-potentiometric stripping analysis (CPSA).[511] Such intrinsic electrochemical properties of proteins combined with the specific recognition provided by aptamers were applied by Wang et al. to construct label-free sensors for protein detection.[512] The lysozyme aptamer was immobilized onto magnetic beads through biotin−avidin interactions, and the functionalized beads were able to bind lysozyme and be captured by a magnet. After releasing lysozyme into solution, CPSA was used to detect the protein, and a detection limit of 7 nM was reported.
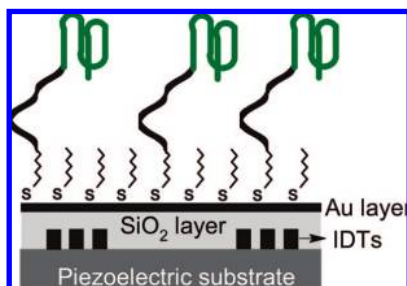
Figure 35. Thrombin and lysozyme were labeled with CdS and PbS QDs, respectively. The labeled proteins were captured by immobilized aptamers for displacement assays. In the presence of unlabeled free target proteins, the labeled proteins were displaced. After dissolving the QDs, the metal species were detected by electrochemical stripping.[510]

3.5.5. Detection Based on Nanotube Field Effect Transistors (FETs)

Carbon nanotubes and semiconductor nanowires have previously been chemically modified with antibodies and peptide nucleic acids (PNAs).[513−515] These functionalized one-dimensional nanomaterials can be incorporated into nanoscale electronic devices. In the presence of target analytes, the electric properties of these devices will change upon binding to target analytes. Recently, aptamers were also immobilized onto single-walled carbon nanotubes using carbonyldiimidazole-Tween (CDI-Tween) as a bifunctional linker.[516] The Tween hydrophobically interacted with the nanotube side wall, and the CDI reacted with the 3′-amine group of the DNA aptamer. Addition of thrombin decreased the conductance of the nanotubes, while addition of elastase had a much smaller effect. The thrombin detection limit was reported to be 10 nM. Recently, a polymer nanotube-based field effect transistor sensor for thrombin detection was also reported.[517]

3.6. Aptamer Sensors Based on Mass Difference upon Binding

Differing from optical or electrochemical methods, detections based on mechanic devices do not need the labeling of external functional groups. Therefore, perturbations to the aptamer properties should be minimal and no complicated chemical modifications are needed. Instead, signal generation comes from binding-induced mass change and the subsequent change of the resonance frequency of supporting materials. Usually, very small mass changes can be detected, resulting in high sensitivities.

Figure 36. IgE aptamers labeled with an amine group (A) or a biotin (B) for surface attachment. (C) IgE aptamer with an extended stem.[70]

3.6.1. Quartz Crystal Microbalance (QCM) Based Detection

A QCM can measure very small masses via change of its resonance frequency, and a linear relationship exists between the two factors. For instance, in a study carried out to compare the binding between antibodies and aptamers, a gold-coated quartz crystal was designed to face a flow-through chamber.[70] Under constant flow conditions, the crystal oscillated at its resonance frequency. If the target protein (IgE) was present, binding of the protein would increase the mass of the crystal and thus decrease the resonance frequency. Several different attachment methods have been employed to immobilize the IgE aptamer onto the gold surface. When the amine-modified aptamer (Figure 36A) was directly attached to the gold surface through a small molecule linker (3,3′-dithiopipropionic acid-di(*N*-succinimidylester)), even though specific binding to IgE was observed, the dissociation rate was too high, which was attributed to the denaturation of the IgE aptamer under the flow conditions. By using a biotinylated aptamer (Figure 36B) to interact with streptavidin-modified gold surfaces, the dissociation rate was greatly reduced. The binding, however, was still weaker than that of the antibody ($K_d = 1.9$ nM and 8.4 nM for immobilized antibody and aptamer, respectively). Since the IgE aptamer has a stem−loop structure, it was proposed that the stem could be unstable and release the bound protein, giving a weaker K_d. Elongating the stem by addition four G-C base pairs should significantly enhance the stability of the stem (Figure 36C). Indeed, the K_d changed to 3.6 nM using this modification. With this engineered aptamer, the detection limit was the same as that obtained from antibody-based detection (0.5 nM). The dynamic range, however, was 1 order of magnitude wider for the aptamer (0.5−50 nM), which was attributed to the higher surface density achieved from nucleic acid immobilization. Furthermore, aptamer-immobilized surfaces were able to survive multiple cycles of regeneration (<5% loss of signal after 10 cycles of regeneration), while antibody-modified surfaces lost more than 50% signal in the first regeneration. Aptamer-modified surfaces could even withstand harsh denaturing conditions, such as washing by strong acids, 6 M urea, and storing at 100 °C for 30 min. Because of the high selectivity, the device could detect IgE in complex protein matrices, such

Figure 37. Scheme of an aptamer sensor based on the change in surface acoustic waves. The aptamer is shown in green and is attached to the gold surface via a DNA spacer (in black).[524]

as meat extract, bouillon, and milk. QCM has also been applied to aptamer-based detection of the HIV-1 Tat protein[518] and thrombin.[479] Similarly, biotinylated aptamers were immobilized through biotin–avidin interactions and the detection limits were determined to be 0.25 ppm and 1 nM for the Tat protein and thrombin, respectively. More recently, Mascini and co-workers performed comprehensive studies on the thrombin aptamer with QCM in terms of variations in experimental procedures. The authors concluded that even simple experimental steps needed to be optimized to improve sensor performance. The authors also compared the detection of thrombin in buffer and in complex sample matrixes such as plasma.[519] In a different report, Hianik et al. studied the effect of ionic strength, pH, and aptamer configuration on sensor performance.[520]

3.6.2. Surface Acoustic Wave-Based Detection

To detect a change of mass, acoustic wave sensors have proven to be highly sensitive. The commonly used Rayleigh wave devices are not compatible with detection in solution because of high energy loss. Pioneering work in this area has overcome a number of difficulties associated with using surface acoustic waves (SAWs) to detect analytes in the liquid phase, and antibody-based detections have been successfully carried out.[521,522] In addition, SAW devices have been used to detect aptamer–protein interactions. Furtado et al. employed this method to study the binding between HIV-1 trans-activation response element (TAR) RNA and the trans-activator of the transcription (Tat) protein, where the RNA was immobilized onto the sensor surface.[523] In work reported by Famulok and co-workers,[524,525] the sensor device was made of interdigital transducers (IDTs) on a piezoelectric material (i.e., quartz) and sealed with SiO_2 to avoid direct contact with liquid (Figure 37). IDTs are metal electrodes for generating and receiving acoustic waves, through which electric signals and acoustic waves can interconvert. The SiO_2 layer also served waveguide purposes. A gold layer was deposited onto the SiO_2 layer for electric shielding and for attaching thiol-modified aptamers. The device had a thrombin detection limit of 72 pg/cm^2. In a follow-up work, the SAW-based device was used to monitor complex formation in the blood-coagulation cascade with both DNA and RNA aptamers for thrombin.[525] Gronewold and co-workers also attached the RNA aptamer for thrombin detection using SAW.[526]

3.6.3. Microfabricated Cantilever-Based Detection

Microfabricated cantilevers have previously been applied to antibody-based detections.[527] Adsorption of proteins induces a change in the surface stress of a cantilever, which can bend the cantilever, and such bending can be conve-

niently monitored with a laser beam. Aptamers have also been recently attached to such cantilevers for protein detection.[528] The protein target chosen for this study was the Taq DNA polymerase.[529] The sensor was built in such a way that there were two cantilevers in the same device; one was used as the sensor, and the other was used as a reference. Aptamers were attached to the sensor cantilever via gold–thiol interactions, and a nonaptamer single-stranded DNA was attached to the other cantilever to act as a reference, such that nonspecific interactions can be eliminated. The obtained Taq polymerase binding curve was similar to that obtained in solution, suggesting that the method did not disrupt the aptamer binding property. Since the aptamer has a very high affinity for the polymerase ($K_d = 9$ pM in solution), the sensitivity of the cantilever-based device was also very high (detection limit less than 10 pM). It was also demonstrated that the device could be used in a complex matrix such as *E. coli* lysate. Importantly, the method can be scaled up so that multiple detections can be performed at the same time.

3.6.4. Surface Plasmon Resonance-Based Detection

Surface plasmon resonance (SPR) occurs when plane-polarized light interacts with a metal film under total internal reflection conditions. At a certain angle of incoming light, the intensity of the reflected light is reduced.[530] The resonance angle is dependent on the properties of the metal film. Keeping all the other conditions constant, binding of a molecule to the surface can change the refractive index of the media on the film and thus change the resonance angle. Although SPR is not a direct measurement of mass, an SPR signal is proportional to the mass concentration close to the surface. Therefore, SPR-based sensing is placed in this section. SPR has become a well-established and widely used method to probe molecular binding interactions, mainly because there is no need to label either the binding molecule or the target molecule, and the detection is in real time.[531] Mascini and co-workers employed SPR to study the binding of drugs with immobilized DNA.[532] Because of the small change in mass, care was taken to minimize nonspecific effects. The same group employed SPR to detect the HIV-1 Tat protein binding to an RNA aptamer. As low as 0.12 ppm of Tat protein was detected.[533] Other examples include the study of RNA aptamers binding to aminoglycosides,[534] S-adenosylhomocysteine,[535] HIV-1 Tat protein in the presence of Zn^{2+},[536] DNA aptamers binding to tubulin,[537] adenosine,[538] thrombin, and thyroid transcription factor 1.[539] Localized surface plasmon resonance-based optical sensors for studying aptamer–protein interactions have also been reported.[540]

3.7. Liquid Chromatography and Capillary Electrophoresis for Separation and Detection of Aptamer Binding

Affinity chromatography utilizes affinity probes immobilized on the separation column to capture the target of interest in a complex mixture. Using aptamers as the capturing molecules in liquid chromatography has been demonstrated by the Drolet, Peyrin, and Kennedy groups.[102,541–543] In these reports, aptamers were immobilized on the column as the stationary phase. Target analytes were retained by interactions with aptamers, which resulted in an increased retention time and subsequent target identification. By using a stereospecific aptamer, even the D-enantiomer of an oligopeptide

was able to be separated and distinguished from its L-counterpart.[542]

Capillary electrophoresis (CE) is a powerful analytical tool for separation and analysis of affinity interactions. CE separation based on antigen/antibody complex formation has been widely used. However, antibodies are heterogeneous under electrophoretic conditions, and it is difficult to observe a sharp peak. Labeling with fluorophores may affect binding, and there could be multiple reactive sites on antibodies for labeling. Aptamers, on the other hand, can be labeled with a single fluorophore at any position of choice, generating a single sharp peak in the capillary.[102]

Kennedy and co-workers first studied the use of aptamers as ligands in CE.[544] A DNA aptamer for IgE was labeled with fluorescein so that the aptamer could be detected by laser-induced fluorescence. The aptamer and IgE were incubated, and the mixture contained free aptamers, free IgE and their complex. For a typical CE trace, two peaks corresponding to free aptamer and IgE/aptamer complex were observed. IgE detection was achieved either by monitoring the increase of the complex peak or by the decrease of the free aptamer peak. To minimize dissociation of the complex, vacuum was applied to increase flow rate and the separation distance was set to be only 7 cm. The assay could be performed in human serum without any major interference, and the detection limit was determined to be 46 pM. The effects of buffer conditions, electric field, and time on separation and detection have also been studied.[545] Similar CE-based assays have been performed on other protein targets, such as the HIV type 1 reverse transcriptase,[546−548] thrombin,[549] and ricin.[550] Le and co-workers have coupled CE separation with PCR by separating the protein/aptamer complex and performing PCR on the aptamer. As few as 180 molecules of HIV-1 RT could be detected.[551] Recently, Dong and co-workers employed CE and chemiluminescence for detecting cocaine and hemin.[552,553] Peyrin and co-workers developed an affinity capillary electrophoresis-based competitive assay. As low as 0.01% of the minor enantiomer could be detected in a nonracemic mixture.[554] Aptamers have also been shown to be useful for protein analysis in CE. The CE trace of proteins often suffers from peak broadening. Binding of a highly negatively charged DNA aptamer to proteins can help focus the protein in the capillary, thus improving the resolution. As shown by Le and co-workers, the sensitivity improved 70- to 120-fold for detection of HIV-1 RT with the aptamer-driven focusing technique.[547]

For most CE-based detection, it is desirable that the aptamer has a high affinity to the target protein; otherwise, the complex may dissociate during migration, resulting in a decrease or loss of the complex peak. To minimize the effect of dissociation, the running time can be shortened or the decrease of free aptamer peak is monitored as an indirect method of analysis. Krylov and co-workers have developed a novel technique known as nonequilibrium capillary electrophoresis of equilibrium mixture (NECEEM) to study low affinity aptamers with CE.[294,555,556] Aptamers and proteins were first allowed to reach equilibrium, and the equilibrium complex was injected into the capillary. Due to separation, the complex was no longer in equilibrium with free aptamer or protein, and an exponential decay of the complex was observed as peak tailing, from which the monomolecular decay rate constant k_{-1} was obtained. Besides the decayed part, the CE trace also contained peaks for free aptamers and remaining complexes. By comparing the area under the

peaks, K_d could be obtained. The thrombin detection limit with this method was determined to be 60 nM, similar to those reported with equilibrium methods. Similarly, Nishikawa et al. employed microchip electrophoresis to assay the binding of an RNA aptamer to proteins.[557]

3.8. Detection with Mass Spectrometry

Mass spectrometry is a useful analytical technique for identification of molecules. Coupled with the specific recognition properties of aptamers, several mass spectrometry-based detection methods have been developed. Dick and McGown immobilized the thrombin aptamer onto a sample chip for MALDI-MS (matrix-assisted laser desorption/ionization mass spectrometry) and demonstrated that thrombin could be specifically retained on the surface while other proteins were washed away.[558] After lowering the pH to denature the aptamer, the retained thrombin was analyzed by mass spectrometry. Capture of thrombin and prothrombin from human plasma was shown. Because the aptamer was covalently linked to the surface, the authors demonstrated that the surface could be regenerated for multiple usages. This technique was also applied to study the binding between an insulin-linked polymorphic region (a G-rich repeat unit) and insulin.[559] Harrison and co-workers functionalized magnetic nanoparticles with the aptamer for D-vasopressin and used the nanoparticles to capture the target peptide. After collecting the nanoparticles with a magnet and mixing with liquid matrix, MALDI-MS was performed to detect the peptide.[560] Kim and co-workers functionalized magnetic beads with an aptamer targeting hepatitis C virus (HCV) RNA polymerase via a photocleavable linker.[561] In this way, the captured protein could be released by UV irradiation, minimizing contamination from traditional chemical elution procedures. Because the bead was part of an affinity chromatography chip, less than 1 μL of volume was needed and the detection limit was estimated to be 9.6 fmol. Huang and Chang employed ATP aptamer-functionalized AuNPs to capture ATP, followed by release of ATP onto unlabeled AuNPs as laser desorption/ionization (LDI) matrixes for mass spectrometry analysis. A detection limit of 0.48 μM ATP was reported, and its application in human cell lysate analysis was also demonstrated.[562]

Electrospray ionization mass spectrometry (ESI-MS) has been used to study chemical and biological binding interactions, as this technique is relatively gentle and can at least partially preserve noncovalent interactions. It has been demonstrated that some protein/aptamer complexes can survive ESI-MS.[563,564] Ellington and co-workers employed ESI-MS to study the binding between small molecules and aptamers.[565] The binding affinity data for tobramycin and its aptamer correlated well with solution assay data, although deviations were observed for ATP, FMN, and their aptamers, suggesting that care should be taken when interpreting binding data from mass spectrometry.

3.9. Blotting Assays

Nucleic acids have been used to probe DNA/RNA-binding proteins, such as in Southwestern and Northwestern blots. Since aptamers can be selected against almost any protein of choice, these blotting methods can now be used for detecting proteins that do not usually interact with nucleic acids, and aptamers can replace antibodies for such applications. Conrad and Ellington immobilized protein kinase C

isozymes onto a nitrocellulose membrane and employed radiolabeled aptamers to bind the immobilized enzymes.[566] The enzyme was quantified by the amount of radioactivity on the membranes, and the detection limit was ~0.5 pmol. Dong and co-workers have immobilized thrombin on a nitrocellulose membrane. Aptamer-functionalized AuNPs could be retained on the surface, and with a silver enhancement method, a detection limit of 14 fmol was reported.[567] Recently, Ying and co-workers also demonstrated the detection of immobilized proteins based on aptamer-functionalized nanoparticles on a nitrocellulose strip.[568]

3.10. Detection Based on Charge Transfer

Fahlman and Sen employed charge transfer to probe aptamer conformational changes induced by analyte binding.[196] The oxidant anthraquinone was covalently attached to one end of the adenosine aptamer. Binding of adenosine facilitated internal stacking of the aptamer loop and charge transfer, resulting in more oxidative DNA cleavage. Two different designs were tested, and the systems were sensitive to adenosine down to low micromolar levels. However, the detection was based on radioisotope labeling and gel electrophoresis. Very recently, the group has demonstrated the detection of thrombin and the construction of a laboratory-on-a-chip type of immobilized sensor with picomolar sensitivity.[569]

3.11. Detection Based on Fourier Transform Infrared Attenuated Total Reflection (FTIR-ATR)

FTIR-ATR is a technique for probing surface adsorption and reactions, and it is also a label-free method. A number of biological processes have been monitored by FTIR-ATR, such as adsorption of protein or cells.[570] Zhao et al. recently employed this technique to study aptamer—protein interactions.[571] The IR light migrated in a total reflecting manner, and the absorption of the evanescent wave by the surface was recorded. The thrombin aptamer was covalently attached to a Si surface, and absorption in the $3550-2800$ cm^{-1} window ($N-H$ and CH_2 bands) was monitored at varying thrombin concentrations. A detection limit of 10 nM was reported.

3.12. Detection Based on Magnetic Resonance Imaging

Magnetic resonance imaging (MRI) is a powerful medical imaging technique for noninvasive 3-dimensional visualization of the structure and function of the human body. It reveals the localized relaxation properties of protons (usually of water) in a strong magnetic field. Many contrast agents have been developed to improve MRI signals, among which, superparamagnetic iron oxide nanoparticles can efficiently diphase the spins of neighboring water protons and generate a change in the spin—spin relaxation time (T2).[572,573] Analyte sensing based on MRI is of particular interest because it can easily realize detection under in vivo conditions, which remains challenging for most other sensing techniques. Weissleder and co-workers used cDNA to link oligonucleotide-functionalized, cross-linked dextran-coated superparamagnetic iron oxide nanoparticles (CLIOs), and they found that the CLIO clusters had very different magnetic properties than dispersed CLIOs. The clusters decreased the T2 relaxation time more effectively and produced darker T2-

weighted MR images.[574−576] Based on this principle, the authors demonstrated detection of nucleic acid and protein targets as well as biological interactions. We incorporated aptamers into CLIOs and developed a MRI sensor for adenosine.[577] Similar to the scheme illustrated in Figure 27A, the AuNPs were replaced by CLIO. Addition of adenosine disrupted the linkage between CLIOs and led to a clear brightness increase in MRI images. The sensor was further shown to be functional even with 10% human serum. Recently, the detection of thrombin was also demonstrated.[578]

3.13. Allosteric Aptamers

Allosteric enzymes are commonly seen in proteins in which an enzyme contains several subunits, and binding of a molecule to one subunit can affect the binding or catalytic activity of the others. Similar concepts have been applied to nucleic acids, where a DNA or RNA contains several aptamer or enzyme units and binding of one aptamer can affect the binding or catalytic property of others. In the case when binding is allosterically affected, the system is called an allosteric aptamer. When catalytic activity is affected, it is called an allosteric DNA/RNAzyme or aptazyme, which will be discussed later. Allosteric aptamers are useful in sensing applications, and there are some unique features that cannot be easily achieved by single aptamers. For example, when an aptamer sensor is optimized, attaching other aptamers to make allosteric aptamers could help transfer the current detection method to a broader range of analytes. It should be noted that merely containing two aptamers in a DNA strand does not necessarily comprise an allosteric aptamer, and one such example is known in the literature.[579] In other words, the two aptamers have to have some kind of communication, and the two target molecules need to have some cooperativity, either positive or negative. Here, allosteric aptamers are classified into two categories: binding of a first aptamer induces weakening or enhancement of the binding of a second aptamer.

Wu and Curran applied in vitro selection to search for aptamers that could target either Cibacron blue or cholic acid.[580] First, selections for each target were carried out separately. Then the two pools were fused to form longer DNA, which was again selected against Cibacron blue and then eluted by cholic acid. One of the resulting DNAs displayed mutually exclusive binding for the two molecules. The aptamer bound to the Cibacron blue column could be eluted by cholic acid and vice versa. This work demonstrates that aptamer binding can be controlled through allosteric interactions. A scheme showing the process is presented in Figure 38A. Beal and co-workers attempted to regulate protein activity through allosteric aptamers.[581] They performed a selection for sequences that bound a DNA repair enzyme (Fpg) and only collected those eluted by neomycin. An RNA capable of inhibiting Fpg activity completely at 100 nM concentration was isolated, and the enzyme activity was rescued by neomycin.

In a broader sense, the structure switching signaling aptamer developed by Li and co-workers can also be considered an allosteric aptamer.[225,302,323,380] For comparison, one such aptamer is shown in Figure 38B. The aptamer first binds a small piece of antisense DNA. In the presence of its target, the aptamer switches its structure and releases the antisense DNA to bind the target molecule. Therefore, the aptamer can be considered to have two binding regions, one
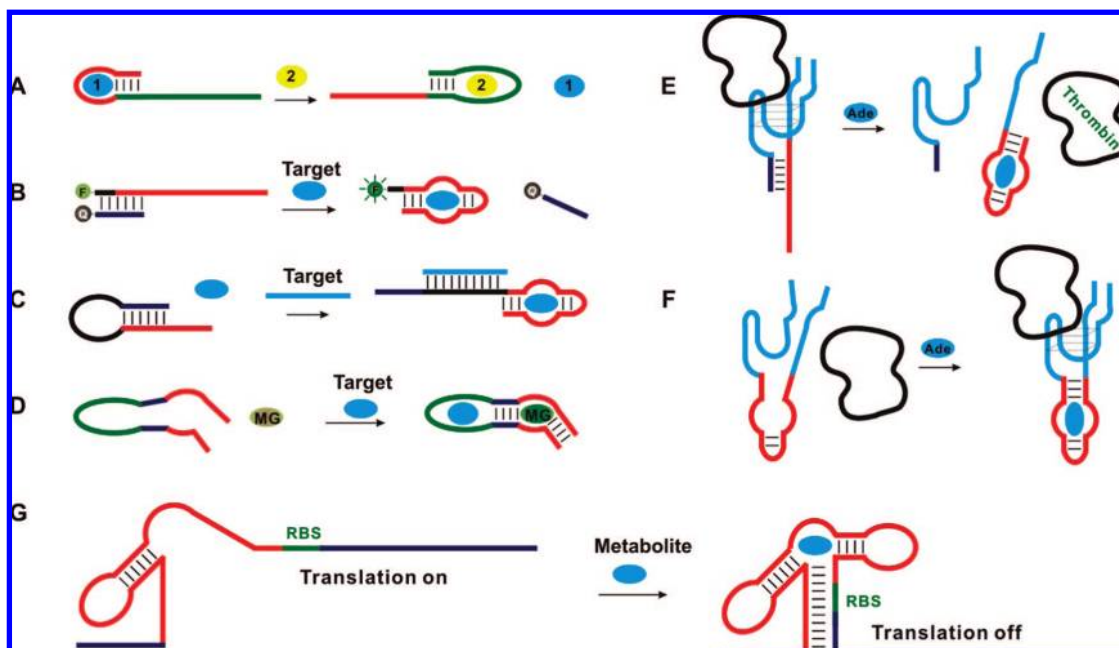
Figure 38. Allosteric aptamers. (A) A nucleic acid contains two aptamer regions, and binding of one aptamer weakens the binding of the other.[580] (B) The structure switching aptamer beacon can also be considered an allosteric aptamer.[323,382] (C) An allosteric aptamer with a hairpin structure for nucleic acid detection.[582] (D) Binding of one aptamer strengthens the binding of the other.[347] Allosteric aptamers with adenosine-induced weakening (E) or enhancement (F) of thrombin binding.[583] (G) Schematic of a riboswitch that shows metabolite-dependent mRNA translational control.[14,587]

for the antisense DNA and one for its target molecule, which represents a negative cooperative effect.

Similarly, Cong and Nilsen-Hamilton constructed a DNA hairpin with an overhang. An ATP aptamer was designed in the overhang and the stem region of the hairpin (Figure 38C).[582] The hairpin structure inhibited ATP binding, as part of the aptamer sequence was used to form a duplex stem. In the presence of the cDNA, the hairpin was forced to open, freeing the aptamer for ATP binding. Ikebukuro and co-workers have constructed allosteric thrombin aptamers regulated by adenosine with two separated DNA strands.[583] A scheme of this design is shown in Figure 38E. In the presence of adenosine, the strand in red bound adenosine and dissociated from the allosteric aptamer complex, which also disrupted the formation of the active thrombin aptamer.

Russell's viper venom factor X activator (RVV-X) can trigger the blood coagulation cascade, which results in visible precipitants in the presence of polystyrene microspheres, and therefore, it provides a useful means of constructing optical sensors. A DNA aptamer was selected by Chelyapov to bind and inhibit RVV-X, and the aptamer was fused to an aptamer for human vascular endothelial growth factor (VEGF$_{165}$) to construct an allosteric aptamer.[584] Upon addition of VEGF$_{165}$, the allosteric aptamer was incapable of binding to RVV-X. Therefore, the RVV-X activity was restored, and visible precipitation was generated by the coagulation-related enzymes in the presence of microspheres. With the naked eye, 5 fmol of VEGF$_{165}$ could be detected in 1 h. In the same paper, Chelyapov also demonstrated another system for detection of tyrosine phosphatase based on the same design. Compared to traditional ELISA-based assays, which take 4.5 h, the allosteric aptamer-based assays are faster (~1 h) and the sensitivities of the two methods are comparable.

In addition to designing negative cooperativities, positive cooperativities have also been used in some allosteric aptamers. Sen and co-workers selected a DNA that could bind hemin and cytochrome c at the same time, with cytochrome c binding enhanced by hemin.[585] An RNA aptamer for malachite green (MG) was reported to increase the fluorophore's quantum yield by over 2000-fold.[343] Stojanovic and Kolpashchikov have designed several allosteric aptamers as shown in Figure 38D. The target binding aptamers were fused with the MG aptamer through a communication module, and MG binding was significantly enhanced upon target binding.[347,586] Fluorescent sensors for ATP, FMN, and theophylline have been demonstrated based on this design, showing the generality of the approach. Later, Kolpashchikov also applied this strategy for nucleic acid detection.[348] Similarly, Ikebukuro and co-workers designed allosteric aptamers as shown in Figure 38F, whose thrombin binding was enhanced by binding of adenosine at an allosteric site.[583]

All the above examples of allosteric aptamers are obtained either by in vitro combinatorial selection or by rational design. Interestingly, Nature has also utilized such aptamers to control gene expression, called riboswitch by Breaker and co-workers.[12,14,15,587] An example of a riboswitch is shown in Figure 38G. In this case, the switch controls mRNA translation. Normally the ribosome binding site (RBS) is free and translation is able to proceed. In the presence of a certain metabolite, the aptamer binding structure is formed to confine the RBS within the structure so that translation is terminated. Other riboswitch mechanisms such as transcriptional control are also known.

While natural riboswitches may not generate physically detectable signals upon metabolite binding, a number of artificial riboswitches and allosteric aptamers have been engineered inside cells to regulate the expression of reporter proteins such as green fluorescence protein or β-galactosidase for sensing applications. For example, Werstuck and Green inserted a Hoechst dye 33258 aptamer into the 5′-untranslated region of a β-galactosidase expression plasmid, and the expression was shown to be reduced by 90% with the addition of the dye molecule.[588] Gallivan and co-workers
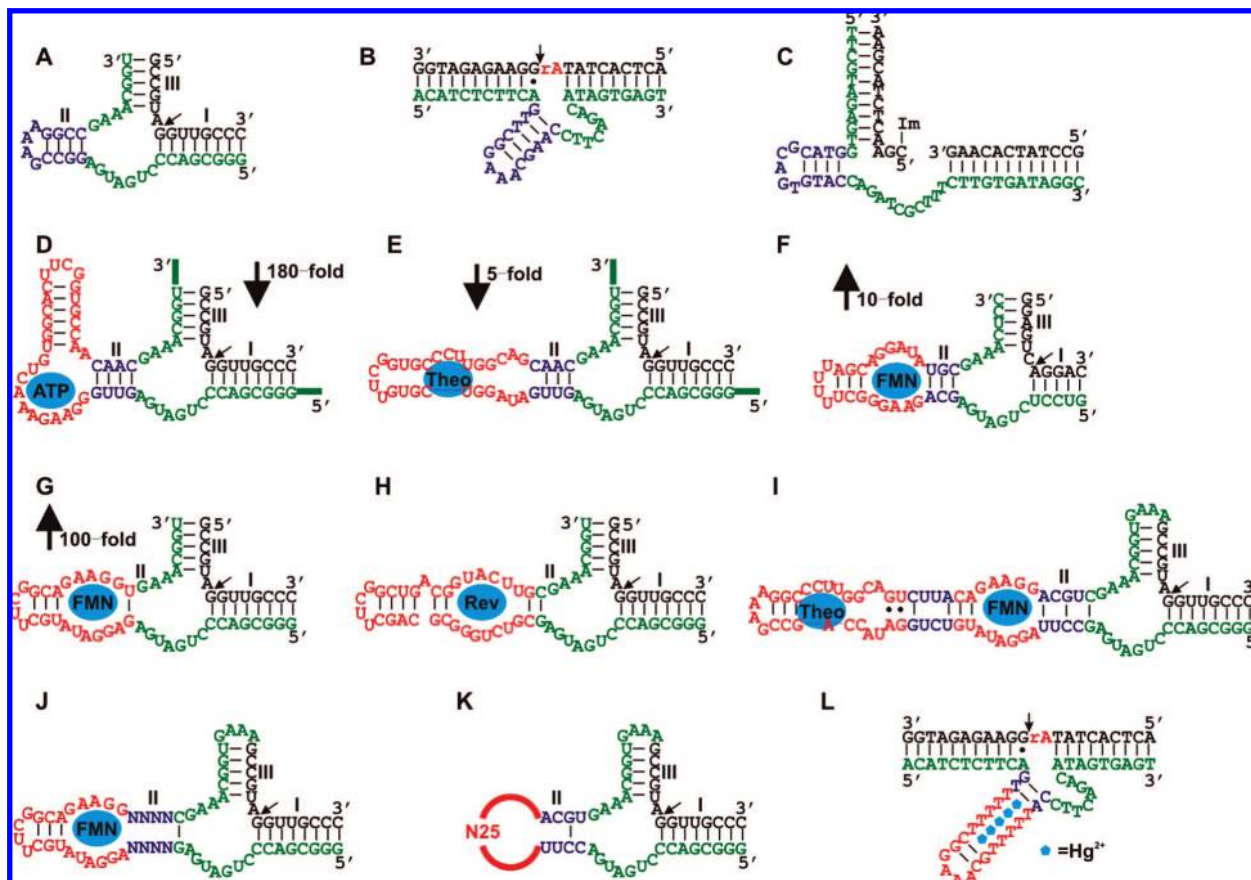
Figure 39. (A−C) Examples of NAEs with replaceable hairpins (in blue) in the enzyme strand. (D−H) Examples of aptazymes based on appending aptamers to stem II of the hammerhead ribozyme. (I) An aptazyme activated by both theophyllilne and FMN with cooperativity. Optimization of aptazymes with in vitro selections by randomizing the communication module (J) or the aptamer (K). (L) A Hg^{2+}-activated aptazyme based on a UO_2^{2+}-specific DNAzyme.[623]

have inserted the theophylline aptamer sequence into the plasmid for β-galactosidase expression of *E. coli* and showed theophylline dependent color signals through the enzyme catalyzed X-gal conversion.[589,590] Recently, the use of small molecules to control the movement of bacteria has also been shown by the same group, which was also based on aptamer mediated control of protein expression.[591] Liu and co-workers have constructed aptamer switches that could stimulate gene expression by small molecules.[592,593] In the above in vivo riboswitches, the aptamer and mRNA were in the same strand and, therefore, aptamers were acting in a cis-form. Bayer and Smolke also demonstrated trans-acting allosteric aptamers, in which a piece of antisense RNA was released or blocked by aptamers binding to small molecules.[594]

4. Aptazyme-Based Sensors

NAE-based metal sensors are highly sensitive, which is due in part to catalytic signal amplification. Aptamers can recognize a wide range of target molecules. To take advantage of the high sensitivity of NAEs for detection of a broad range of analytes, aptamers have been coupled with NAEs, and these enzymes are usually termed allosteric DNA/RNAzymes or aptazymes.[13,91,112,113,595−598] This section first reviews the methods used to obtain aptazymes. Because the signaling methods for NAEs are quite adaptable to aptazymes, they are summarized briefly toward the end.

4.1. Aptazyme Construction

Many methods have been developed to couple aptamers to nucleic acid enzymes, and we categorized them into the following three classes. Although many of these methods are considered general, their applications still depend strongly on the structural characteristics of each NAE and aptamer.

4.1.1. From NAEs with a Replaceable Hairpin

To be called a true NAE, the substrate(s) and the enzyme should be in separate strands, and a single enzyme molecule should be able to turnover multiple substrates. In many cases, the enzyme contains a stem loop or hairpin that only plays a structural role to fold the enzyme, which can be replaced by other hairpins with different sequences.[22,166,255,599−602] If the hairpin is replaceable, aptamers can be inserted into the enzyme in a relatively straightforward manner. Several examples of NAEs with replaceable hairpins are shown in Figure 39A−C. One of the model systems frequently used for aptazyme design is the hammerhead ribozyme (Figure 39A). Its trans-cleaving form contains a substrate (in black) and an enzyme (in green and blue), and the cleavage site is indicated by an arrow. The substrate/enzyme complex contains three stems. Stems I and III are used for substrate binding, and the stability of stem II has been shown to be important for the enzyme activity.[599,600] We recently reported a UO_2^{2+}-dependent RNA-cleaving DNAzyme (Figure 39B) that also contains a replaceable hairpin shown in blue.[22] Such
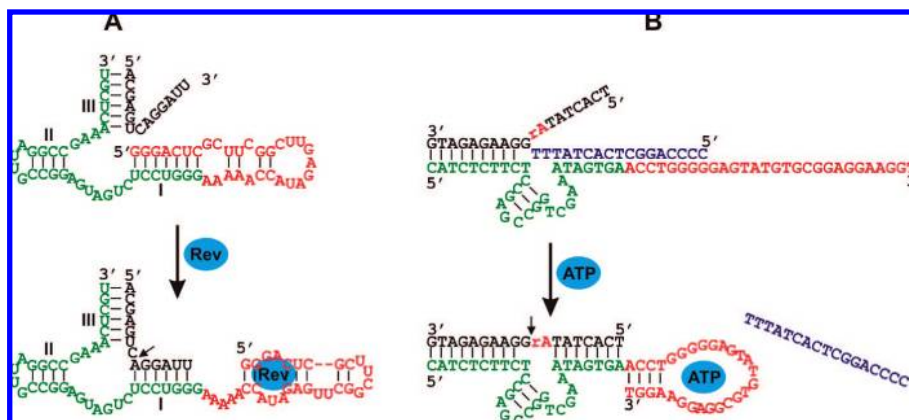
Figure 40. Aptazymes based on antisense blocking of the substrate binding regions. (A) A Rev-dependent aptazyme based on the hammerhead ribozyme. (B) An ATP-dependent aptazyme based on the 8−17 DNAzyme.

stem−loop structures are also present in many other NAEs, including the hairpin ribozyme (not shown) and the DNA ligase isolated by Cuenoud and Szostak (Figure 39C) that joins two DNA substrates (in black) into a long one.[166]

Tang and Breaker reported the first aptazyme by rational design.[603] An RNA aptamer for ATP was appended to stem II of the hammerhead ribozyme, as shown in Figure 39D. Therefore, stem II served as a communication module between the aptamer and the ribozyme. In the presence of ATP, the ribozyme activity was inhibited by ∼180-fold, which was attributed to the steric conflict between the ATP bound aptamer and the ribozyme.[604] By introducing multiple G•U mismatches into stem II, a 5- to 10-fold activity increase with ATP was observed.[603] In the same paper, the authors further demonstrated a theophylline aptamer with the hammerhead ribozyme through the same communication module, and a 5-fold inhibition by theophylline was observed (Figure 39E).[603] Araki and co-workers appended a flavin mononucleotide (FMN) aptamer through stem II of the hammerhead ribozyme and showed that the ribozyme activity increased by 10-fold in the presence of FMN (Figure 39F).[605,606] Soukup and Breaker further shortened the communication module to one G•U wobble pair and achieved over 100-fold activity enhancement with FMN (Figure 39G) and ∼40-fold enhancement with theophylline.[607] Famulok and co-workers demonstrated, as shown in Figure 39H, that binding of the HIV-1 Rev protein inhibited the ribozyme activity, but activity could be recovered by protein inhibitors that could displace Rev from the aptazyme.[381] Wang and Sen also incorporated HIV-1 Tat protein aptamers into stem II of the hammerhead in a similar way to obtain aptazymes for Tat,[608] and Yamazaki and co-workers have made a HIV-1 RT-dependent aptazyme.[609] Furthermore, Breaker and co-workers demonstrated that, by inserting both the FMN and theophylline aptamers in a sequential manner into stem II, the hammerhead ribozyme activity could be modulated by both molecules in a cooperative manner (Figure 39I).[610] When both molecules were present, the activity enhancement could be as high as 300-fold.

The rational design of aptazymes by appending aptamers to NAEs is a trial-and-error process. Before obtaining desired aptazymes, many designs have to be tested. The designed aptazymes also suffer from lower activities compared to the case of unmodified enzymes. In addition, the level of activation or inhibition is relatively low (usually around several hundred folds or less). These problems can be circumvented by employing in vitro selection. For example,

Breaker and co-workers randomized the communication module between an FMN aptamer and stem II of the hammerhead ribozyme (Figure 39J, blue region in stem II). Selections can be directed toward either ligand induced activation or inhibition. The same communication modules can be adapted to connect other aptamers including ATP and theophylline, and 40- to 600-fold activation or inhibition was reported.[611] With the same selection method, aptazymes with up to 3000-fold theophylline-activation were also isolated.[612] Diener and co-workers first isolated an ADP aptamer and appended it to stem II of the hammerhead ribozyme. After selection with randomized nucleotides on stem II, ADP-dependent aptazymes were obtained.[248] With the optimized communication bridge, Breaker and co-workers further explored the selection of a series of aptazymes by randomizing the aptamer motif (Figure 39K, N25 region).[613] By introducing different effector molecules, aptazymes specific for many different analytes have been obtained, including cGMP and cAMP,[613] Co^{2+},[614] other divalent metal ions,[615] doxycyline,[616,617] caffeine and aspartame[247] and peptides.[618]

In addition to the hammerhead ribozyme, many other nucleic acid enzymes have also been employed as scaffolds for aptazymes. For example, we have replaced the hairpin in the UO_2^{2+}-dependent DNAzyme shown in Figure 39B with a thymine rich stem loop shown in Figure 39L. The five T-T mismatches acted as aptamers for Hg^{2+}.[19,375,376] For this particular enzyme, over 150-fold Hg^{2+}-induced activity enhancement was observed. Ellington and co-workers reported a number of aptazymes based on DNAzyme ligases.[601,602,618−621] In addition to rational design and in vitro selection, computer-aided "selections" have also been carried out.[622] The authors decided to use the slip structure model for the aptazyme where a different set of base pairs were formed upon target binding. The FMN aptamer was joined with stem II of the hammerhead ribozyme, and the six nucleotides (three on each side) in the communication module were randomized. The best hit showed 60-fold activation.

4.1.2. Interfering Substrate Binding

Usually, NAEs recognize their substrates through two substrate binding arms. If one or both of these arms are blocked by antisense oligonucleotides, enzyme activity is inhibited. Incorporation of aptamers into the antisense strands may modulate the inhibition. Famulok and co-workers extended stem I of the enzyme strand of the hammerhead

ribozyme to include a Rev aptamer (in red, Figure 40A).[381] The sequence was designed such that the end of the aptamer could fold back to block substrate binding. Addition of the Rev protein removed the blocking sequences and activated the enzyme. Li and co-workers extended the enzyme strand of the 8−17 DNAzyme (Figure 40B), and an external antisense DNA was used to block the substrate binding region.[624] Addition of ATP removed the aptamer and activated the DNAzyme.

4.1.3. Other Methods To Modulate NAE Structures

Besides the two classes of approaches introduced previously, a number of other methods have been developed to interfere with NAE activity through aptamer ligand binding. For example, as shown in Figure 41A, Li and co-workers employed an ATP aptamer (in red) to join the substrate (in black) and enzyme (in green) into a cis-cleaving or self-cleaving DNAzyme.[158] The original trans-cleaving DNAzyme is shown in Figure 8B. In the aptazyme (Figure 41A), the left part of the substrate bound the enzyme through a Watson−Crick base pair region. The right part, however, did not bind the enzyme very well because the aptamer had a random structure in the absence of ATP, giving a low enzyme activity. Binding to ATP established the other substrate binding arm and restored activity. This method should be applicable to many other NAEs by using an aptamer stem loop to link the enzyme and the substrate.

Sen and co-workers reported a number of aptazymes by inserting aptamers into one of the substrate binding arms.[625] The NAEs tested included the 10−23 and 8−17 DNAzymes and the hammerhead ribozyme, and the aptamers tested included DNA aptamers for adenosine and RNA aptamers for ATP and FMN. One example is given in Figure 41B.[197,625] The adenosine aptamer (in red) was split into two halves, resulting in two enzyme strands. In the absence of adenosine, the enzyme active site could not form due to the weak interaction between the two enzyme halves. Binding of adenosine restored the enzyme active site and an activity increase of ∼222-fold was reported.[625] Instead of inserting aptamers into just one of the substrate binding arms, Cho et al. found that inserting aptamers into both arms could further suppress background cleavage.[626] The authors tested aptamers for the HCV replicase and helicase and inserted them into stems I and III of the hammerhead ribozyme simultaneously.

Famulok and co-workers designed stem II of the hammerhead ribozyme in such a way that a thrombin aptamer (in red, Figure 41C) could hybridize to it and inhibit the enzyme activity.[381] Addition of thrombin released the aptamer and restored the ribozyme activity. Allosteric hairpin ribozyme was also made by using the thrombin aptamer as antisense DNA to hybridize to the bridge region of the hairpin ribozyme. Alternatively, an FMN aptamer was placed on the bridge region of the hairpin ribozyme. An antisense DNA was then added to inhibit ribozyme activity, which was recovered by addition of FMN.[627]

Instead of using external antisense oligonucleotides, Li and co-workers designed internal antisense elements into the pH6DZ1 DNAzyme (Figure 41D).[255] This DNAzyme already contained a fluorophore and a quencher flanking the cleavage site. Part of the catalytic core (in green) formed a base pairing region with the ATP aptamer. Addition of ATP induced formation of the aptamer binding structure and release of important nucleotides to restore enzyme activity.

Aptazymes that can utilize non-nucleic acid substrates have also been demonstrated. For example, Amontov and Jäschke appended a theophylline aptamer (Figure 41E, in red) on the stem of a ribozyme that can catalyze Diels−Alder reactions[137−139] in such a way that when the aptamer was in the binding conformation, the aptazyme was active (right part of Figure 41E).[628] In the absence of theophylline, another set of base pairing interactions was formed and the ribozyme was inactive (left part of Figure 41E). The substrate was an anthracene that was covalently attached to the 5′-end of the aptazyme. The active enzyme catalyzed the Diels−Alder reaction to add a maleimide group to anthracene. Similar methods have also been applied to design aptazymes for tobramycin and a specific mRNA sequence. Around 50- to 2100-fold rate enhancement was obtained depending on the different systems.

4.1.4. Oligonucleotides as Special Effectors

A nucleic acid can be considered an aptamer for its complementary strand, and nucleic acids have been widely used as effectors to modulate NAE activity.[198−200,629−633] The use of antisense sequences for controlling NAEs has been previously covered, as shown in Figures 40 and 41C. In those cases, however, the antisense strands were still aptamers. In this section, the antisense strands are merely simple nucleic acids that can only bind their complementary strands. Stojanovic and co-workers have reported a number of systems where the substrate binding arms of NAEs were blocked by antisense interactions and such blocking effects were relieved by the addition of their cDNAs.[198−200] The use of antisense DNAs to block enzyme active sites has also been demonstrated.

Several recent examples are reviewed here. Sando and co-workers constructed a cis-cleaving (self-cleaving) "8−17" DNAzyme that could not fold into an active structure by itself. Based on the mfold program,[212] the DNAzyme folded in an inactive structure shown on the left side of Figure 42A. In the presence of the target DNA, the two ends of the DNAzyme formed a double-helical structure, facilitating the formation of the active catalytic core (Figure 42A).[634] Similarly, Famulok and co-workers engineered a hairpin ribozyme by disrupting formation of domain A of the enzyme. In the presence of the target RNA, domain A was reformed, resulting in an active enzyme (Figure 42B).[635] Burke and co-workers extended the 3′-end of the hammerhead ribozyme as the antisense strand to inhibit its catalytic core. In the presence of the target strand, the ribozyme was activated (Figure 42C).[636] Recently, Kossen and co-workers used the target RNA to activate a ligation ribozyme to detect very low copies of viral RNA. Without the target strand (Figure 42D, in red), the ribozyme was inhibited. The target strand activated the ribozyme structure and showed a ∼3 billion-fold increased ligation rate, allowing a zeptomole detection limit.[637] With the aid of computers, a number of oligonucleotide-sensitive aptazymes have been constructed by Penchovsky and Breaker.[638]

4.2. Fluorescent Aptazyme Sensors

Since aptazymes are essentially NAEs, the signaling methods developed for NAEs can be applied to aptazyme sensors. Almost all the fluorescent signaling methods shown in Figure 3 have been demonstrated in aptazymes, and therefore, aptazyme sensors are only briefly covered here.
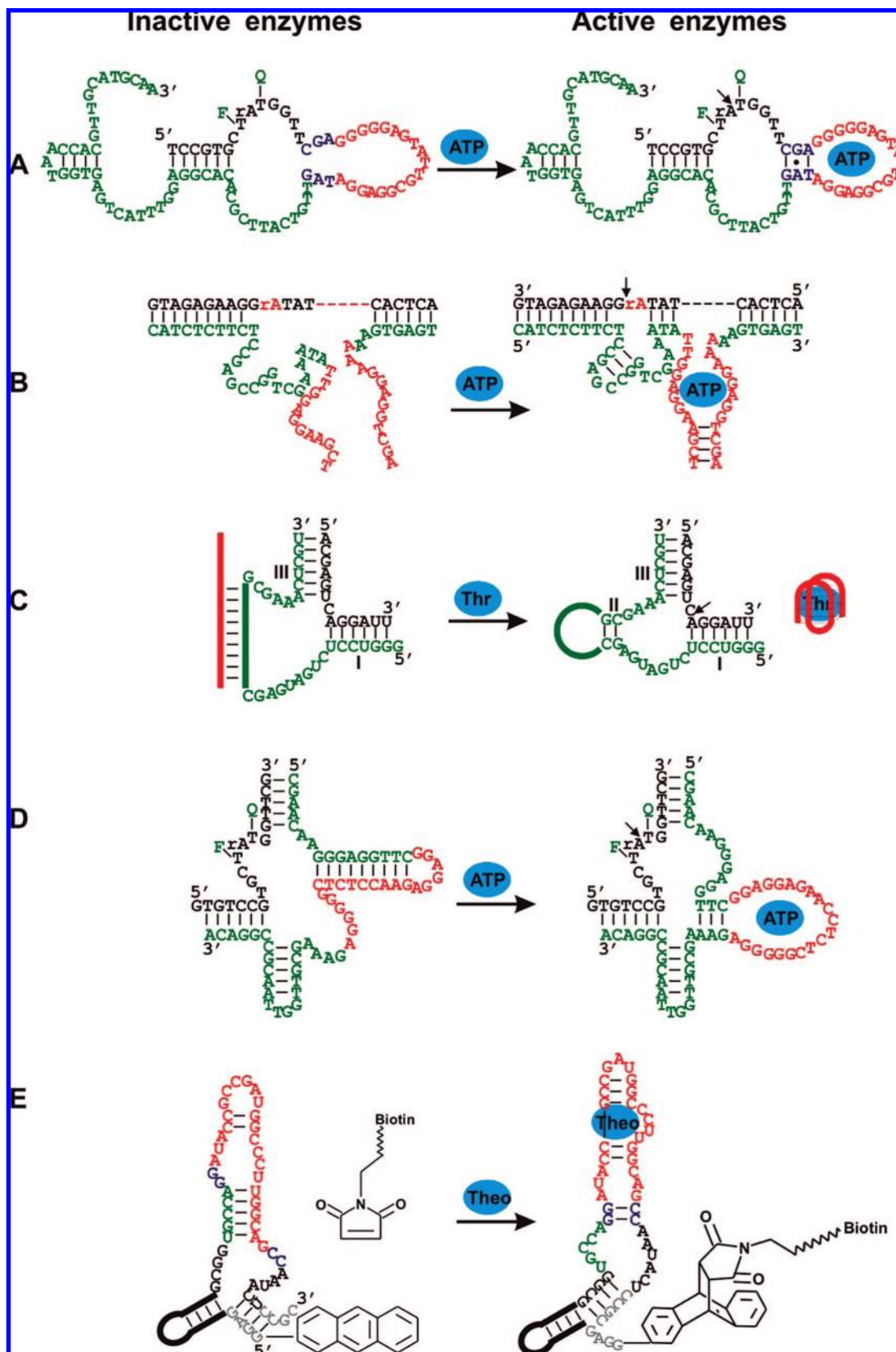
Figure 41. Other methods used to modulate NAE structures to design aptazymes. (A) An aptazyme based on a bridging aptamer to connect the substrate and enzyme. (B) Aptazymes based on inserting aptamers into substrate binding arms. (C) Aptamers as antisense DNAs to block enzyme active sites. Design of internal antisense interactions to obtain aptazymes based on an RNA-cleaving DNAzyme (D) and a Diels−Alderase (E).

Several NAEs isolated by Li and co-workers already contained fluorophore/quencher pairs during in vitro selections (Figure 8). Aptazymes generated from this process are sensors by themselves. A scheme of signal generation with

the aptazyme shown in Figure 41A is presented in Figure 43A. This ATP-dependent aptazyme showed a ~20-fold enhancement in fluorescence signaling rate in the presence of ATP.[158] In another similar aptazyme sensor reported by
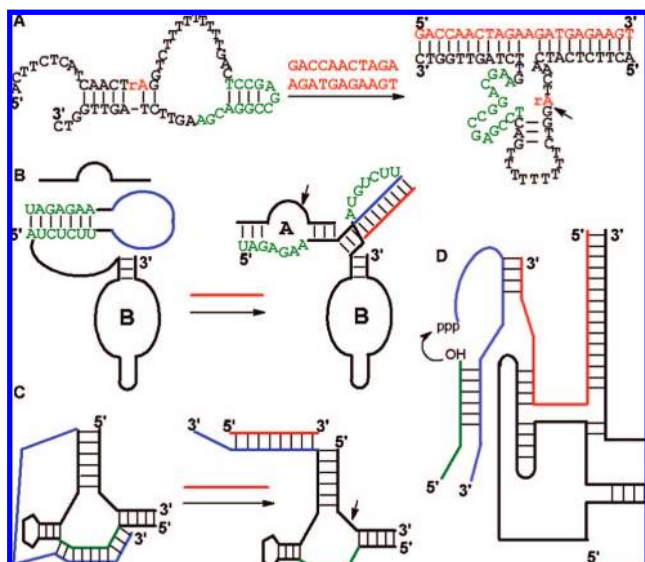
Figure 42. DNA/RNAzymes activated by oligonucleotides. (A) Activation of the 8−17 DNAzyme;[634] (B) the hairpin RNAzyme;[635] and (C) the hammerhead RNAzyme.[636] The cleavage sites are indicated by black arrows. (D) Activation of a ligase ribozyme.[637] The position of ligation is indicated by the arrow. The oligonucleotide effectors for activation are drawn in red.

the same group, the ATP aptamer was inserted through rational design and a 15-fold rate enhancement in fluorescence was observed.[255]

A number of aptazymes employed substrates labeled with fluorophore/quencher pairs on their two ends as shown in Figure 43B.[381,639] For example, Walter and co-workers labeled the hammerhead substrate ends with Cy3 and Cy5 as FRET donor (F) and acceptor (Q), respectively.[639] Decreased FRET efficiency was observed upon substrate cleavage and dissociation, and theophylline was able to accelerate the process by ~12-fold. Famulok and co-workers appended a Rev protein aptamer to the hammerhead ribozyme through stem II and labeled the two ends of the substrate. Interestingly, Rev binding inhibited activity and no fluorescence change was observed. Addition of small molecules that could bind Rev displaced Rev from the aptamer, leading to restored aptazyme activity and increased fluorescence.[381] In the same paper, end labeling of the hammerhead substrate was also applied to the aptazymes shown in Figures 40A and 41C. Capable of protein recognition and fluorescence signal generation, such systems are useful for screening protein inhibitors and studying protein−protein interactions. The signaling method in Figure 43C has been demonstrated for detection of a number of molecules, including ADP, with a detection limit down to 1 μM and greater than 100-fold selectivity over ATP,[248] and caffeine and aspartame, with a detection range from 0.5 to 5 mM in 5 min.[247] In these systems, the aptazymes were in the self-cleaving form, and therefore, the sequences were relatively long. Putting the quencher on a separate strand may help shorten the sequence and increase the synthesis yield. We have recently designed a fluorescent aptazyme sensor for Hg^{2+} detection as shown in Figure 43D. Addition of Hg^{2+} could stabilize the T-T mismatches,[19,375,376] thus restoring activity. This sensor has a detection limit of 2.4 nM, the lowest among known Hg^{2+} sensors based on small molecules or macromolecules.

In addition to using fluorescence energy transfer, immobilized aptazymes have also been prepared. Ellington and

co-workers immobilized a ligation aptazyme as shown in Figure 43E.[621] The aptazyme was activated upon binding to ATP, and the substrate was circularized by the ligation reaction. Addition of the Phi29 DNA polymerase allowed rolling circle amplification along the circular DNA template. The resulting long DNA served as a template to hybridize with Cy3-labeled short DNA to generate a fluorescence signal. This system was able to detect 1 μM ATP.

Willner and co-workers reported a special aptazyme sensor shown in Figure 43F. An aptamer for target recognition and an aptamer that can bind hemin to form a peroxidase DNAzyme were linked to a single-stranded DNA. Both aptamer regions were partially blocked by a piece of antisense DNA. Addition of the target released the antisense DNA, and hemin binding occurred to produce an active DNAzyme for signal generation. The detection limits for AMP and lysozyme were determined to be 4 μM and 0.1 pM, respectively.[640]

4.3. Colorimetric Aptazyme Sensors

Not surprisingly, signaling methods for designing colorimetric NAE sensors have also been applied to aptazymes. We chose to use an aptazyme designed by Sen and co-workers[625] to assemble AuNPs. The core sequence of the aptazyme is shown in Figure 41B.[197] The aptazyme was built on the Pb^{2+}-specific DNAzyme catalytic core, and the substrate was extended to bind AuNPs. In the absence of adenosine, the aptazyme had low activity. The substrate was uncleaved and could assemble nanoparticles. In the presence of adenosine, the enzyme was activated to cleave the substrate, resulting in a red color from dispersed AuNPs. As seen on the TLC plate in Figure 44A, only the sample with adenosine showed a red color, while other ribonucleosides gave blue colors. We also appended the adenosine aptamer onto the replaceable hairpin of the ligation E47 DNAzyme, and a ligation-based aptazyme was prepared (Figure 44B, Liu and Lu, unpublished results). With the ligation product designed to be a linker for AuNP assembly, colorimetric sensors for adenosine were prepared. In this sensor, adenosine produced a blue color instead of red because of the ligation (rather than cleavage) reaction.

4.4. Other Detection Methods

As introduced in 3.6.1, a quartz crystal microbalance (QCM) can also be used for aptazymes, as demonstrated by Ellington and co-workers.[641] Both ligation and cleavage aptazymes were reported. In the ligation aptazyme, one piece of the substrate was immobilized onto a gold surface (Figure 45A). The ligase contained an aptamer motif that could bind the HIV-1 Rev peptide. In the presence of this 500 nM Rev, the ligase was activated to join the substrate with the ligase and an increase in mass was observed. The authors also showed an RNA-cleaving aptazyme in the same paper (Figure 45B). A theophylline-dependent aptazyme was immobilized onto a gold surface, and in the presence of theophylline, mass decrease was observed due to cleavage.

Ogawa and Maeda have recently constructed an aptazyme and a blocking sequence into an mRNA that encodes for a reporter protein (luciferase or β-galactosidase).[642] The aptazyme was based on the hammerhead ribozyme appended with the theophylline aptamer. In the absence of theophylline, gene expression was suppressed because the ribosome binding site was base paired with the blocking sequence. In the presence
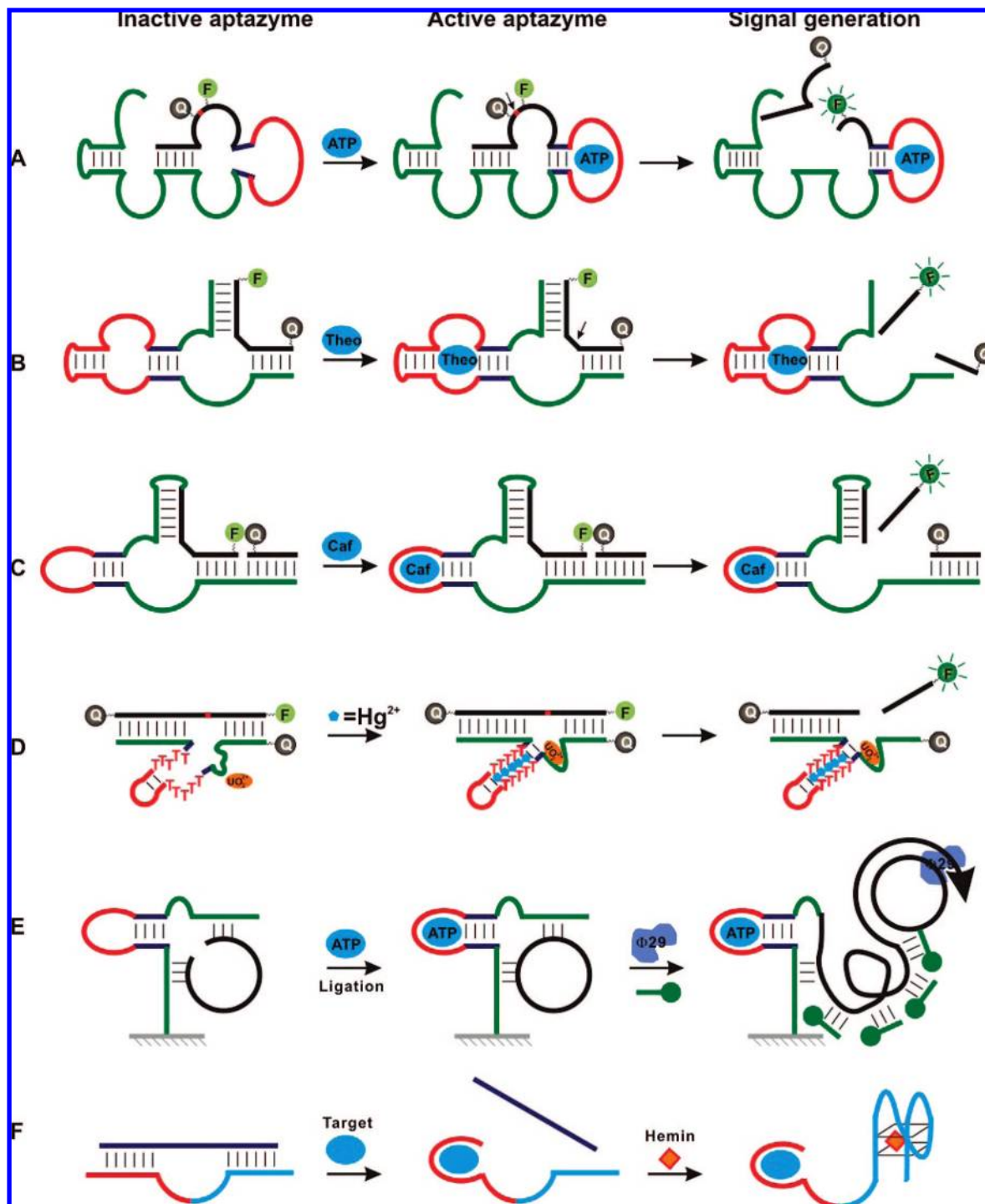
Figure 43. Signaling methods for designing fluorescent aptazyme sensors. Fluorophore and quencher flanking the cleavage site (A); on the ends of the substrate (B); brought close by extended enzyme strands as a template (C); or in a dual quencher format (D). (E) Signal generation from a surface immobilized aptazyme through rolling circle amplification and templated fluorophore immobilization. (F) An aptazyme with peroxidase activity.

of theophylline, the aptazyme cleaved off the blocking region, allowing gene expression to proceed. With both reporter genes, theophylline could be detected down to 0.1 mM.

5. Conclusions and Outlook

Since their first appearance in the literature about 20 years ago, FNAs have taken an increasingly prominent role in many important biotechnological fields. This review mainly centers upon the molecular recognition and sensing aspects of the FNAs. FNAs are generally believed to be able to target

any analyte of choice. On top of that, various efficient and practical signaling strategies have been successfully developed to transduce FNA recognition events into physically detectable signals. In addition, the rapid development of the FNA sensing field is also a result of FNA's superior properties as excellent sensors, including high stability, low cost, and ease of synthesis and modification. However, the sensing and diagnostic market is still largely dominated by antibodies, and commercially available aptamer-based sensors are limited. On one hand, the difficulties come from
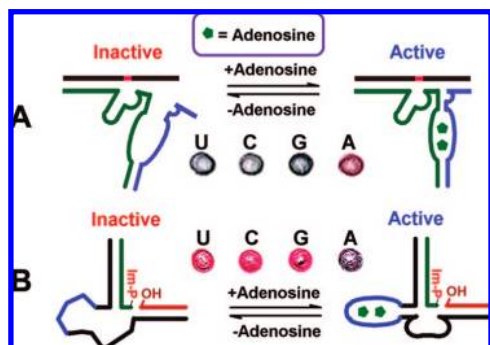
Figure 44. Colorimetric aptazyme sensors for adenosine based on RNA-cleaving enzymes (A) and DNA ligation enzymes (B). Reprinted with permission from ref 197. Copyright 2004 American Chemical Society.

the limited information (in terms of both aptamer sequences and characterizations) available for many targets of interest. This can be seen from the fact that most sensing work using FNAs has been performed on model systems for proof-of-concept emphasis, while few clinically relevant targets have actually been tested. On the other hand, most FNA sensors were developed and tested in buffer systems under well-controlled laboratory settings. For real medical diagnosis and field environmental monitoring, significant sample matrix effects need to be carefully evaluated. As has been shown multiple times in this review, the performance of an aptamer sensor could decrease considerably in serum or plasma. Therefore, it will take more research and technological efforts to optimize the sensors and eliminate matrix effects for practically useful sensitivity and specificity. Finally, to bring a technology to the market, it is essential to design easy-to-use, accurate, and cost-effective test instruments or kits. This technological platform has already matured for antibody-based diagnosis. We believe that, given enough time, FNA-based platforms will eventually catch up. Another important issue is that current methods are mostly developed for in vitro detection. To accomplish in vivo sensing, novel methods and materials for signal transduction are needed. For example, fluorophores, QDs, and other materials that

have near IR emissions could be very useful. Materials with magnetic properties can also be used for magnetic resonance imaging (MRI). We envision that one promising area for FNA sensors is to target small molecules such as metal ions and metabolites in biological systems and in the environment, because it has been very difficult to obtain highly specific antibodies for small molecules due to challenges in eliciting immune responses for small molecules. Therefore, rather than competing with antibody-based diagnostics, directing efforts toward technological gaps in antibodies may be a viable road to success for FNA sensors.

In addition to the above discussions on practical applications of FNAs, there is still room to improve the selection technology itself. Ellington and co-workers have devoted research efforts to develop automated parallel selection of both aptamers and NAEs. Using CE as a separation tool, high quality aptamers can be isolated even with only one round of selection. On the other hand, with an increasing number of aptamers being developed, the biochemical characterization of these molecules becomes more pressing and labor intensive. A conventional sensor development process includes (in order): selection, characterization, and sensor design and validation. As demonstrated by the Ellington and Li groups, when the sensor design step is incorporated into the selection process, the selected nucleic acids will be stand-alone functional sensors.[158,159,302,361] Although only fluorescent signaling methods were explored in these reports, further developments in such predesigned selections are expected to both advance fluorescent sensing and incorporate other signaling means. Despite a number of innovations and developments, in vitro selection or SELEX is by no means simple, and it is still difficult to obtain excellent aptamers, particularly DNA aptamers, with high affinity for any molecules of interest, particularly clinically important targets. With the research on FNAs in the past 20 years, however, scientists now have a much better understanding about their capability, and such understanding has fueled the development of new methods to address its limitations. One solution is to extend the chemical functionality of nucleic acids beyond the four natural nucleobases
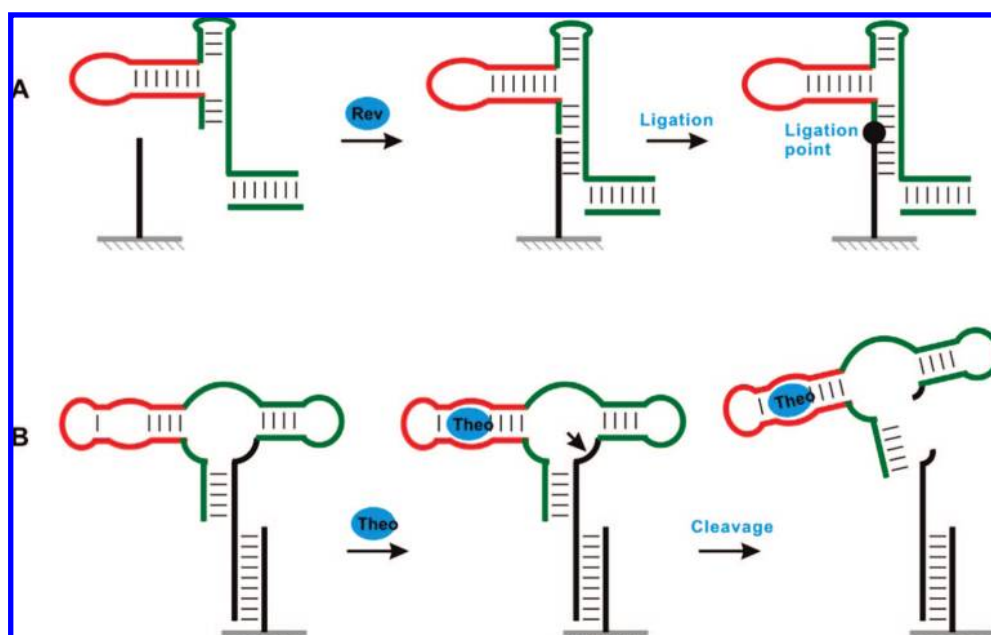

Figure 45. QCM-based aptazyme sensors with a ligation aptazyme for the HIV-1 Rev peptide (A) or an RNA-cleaving aptazyme for theophylline (B).

so that more functional groups can be introduced into FNAs for highly specific binding. In this way, highly specific Zn^{2+}-dependent DNAzymes were obtained using DNAs containing imidazole modified deoxyuridine, taking advantage of the high affinity between Zn^{2+} and imidazole ligand.[25] Along the same line, 8-histaminyl-dA and 5-aminoallyl-dU modified DNAs were used to obtain divalent metal-independent and Hg^{2+}-dependent DNAzymes. In the former case, both electrostatic and acid/base catalysis similar to that in the RNase A may be responsible for the catalysis,[156] while, in the latter case, the soft ligand binding to soft Hg^{2+} favored the catalysis.[643] Similarly, boronic-acid-labeled thymidines have been synthesized to target the carbohydrate part of glycoproteins, taking advantage of the reversible binding between boronic acid and sugars.[644,645] These examples suggest that incorporating noval chemical functionalities into nucleic acids based on the rational understanding of target molecules may further improve the molecular recognition capability of FNAs.

Once a sufficient number of sensors are obtained, the next significant advancement of the FNA sensing field would be the development of sensor arrays for more sophisticated target analysis.[71,413,423,426−428,432,614,646,647] The benefits of the sensor arrays come from two aspects. First, simultaneous detection of multiple targets is possible, which provides the capability of high-throughout analysis of complex samples. Second, the selectivity of a single sensor may not be enough for reliable target identification. Similarly, one target may induce different responses from sensors on an array, thus forming a unique signal pattern. By reading such signal "fingerprints", it is expected that target identification with unparallel accuracy could be achieved. The fabrication of sensor arrays can be accomplished by immobilizing FNAs on a solid support, or organizing sensors on a multiwell titer plate. For example, Breaker and co-workers have constructed an aptazyme array that used radioisotopes for detection.[614] As mentioned previously, Bock and co-workers were able to detect 17 analytes with a photoaptamer array.[423] Ellington and co-workers have conducted research to optimize aptamer immobilization and buffer conditions, and they demonstrated aptamer arrays for a number of protein targets including lysozyme, ricin, IgE, and thrombin.[426−428,647] Li and co-workers have recently entrapped several signaling DNAzymes into gels and demonstrated their application in metal detection.[195] Even though array development has been progressing gradually, more research efforts are still needed to improve surface conjugation chemistry, aptamer stability, reproducibility, and data processing to match or even exceed the performance of DNA microarrays.

In addition to detection of target analytes, FNA sensors can also be useful tools for many research fields and practical applications, such as in basic biological studies, high throughput drug screening, disease diagnosis, nanotechnology, and materials science. Given the increasing demand for convenient, economical, yet effective sensors, we will witness continued and rapid development and advancement of the FNA sensing field in the future.

6. Acknowledgments

7. References

(1) Tsien, R. Y. In *Fluorescnct Chemosensors for Ion and Molecule Recognition*, 538 ed.; Czarnik, A. W., Ed.; American Chemical Society: Washington, DC, 1993.
(2) Czarnik, A. W. *Chem. Biol.* **1995**, *2*, 423.
(3) Iqbal, S. S.; Mayo, M. W.; Bruno, J. G.; Bronk, B. V.; Batt, C. A.; Chambers, J. P. *Biosens. Bioelectron.* **2000**, *15*, 549.
(4) *Optical Biosensors: Present and Future*; Ligler, F. S., Rowe Taitt, C. A., Eds.; Elsevier Science B.V.: Amsterdam, 2002.
(5) Robertson, D. L.; Joyce, G. F. *Nature* **1990**, *344*, 467.
(6) Tuerk, C.; Gold, L. *Science* **1990**, *249*, 505.
(7) Ellington, A. D.; Szostak, J. W. *Nature* **1990**, *346*, 818.
(8) Wilson, D. S.; Szostak, J. W. *Annu. Rev. Biochem.* **1999**, *68*, 611.
(9) Gold, L.; Polisky, B.; Uhlenbeck, O.; Yarus, M. *Annu. Rev. Biochem.* **1995**, *64*, 763.
(10) Bunka, D. H. J.; Stockley, P. G. *Nat. Rev. Microbiol.* **2006**, *4*, 588.
(11) O'Sullivan, C. K. *Anal. Bioanal. Chem.* **2002**, *372*, 44.
(12) Winkler, W.; Nahvi, A.; Breaker, R. R. *Nature* **2002**, *419*, 952.
(13) Breaker, R. R. *Nature* **2004**, *432*, 838.
(14) Tucker, B. J.; Breaker, R. R. *Curr. Opin. Struct. Biol.* **2005**, *15*, 342.
(15) Winkler, W. C.; Breaker, R. R. *Annu. Rev. Microbiol.* **2005**, *59*, 487.
(16) Brody, E. N.; Willis, M. C.; Smith, J. D.; Jayasena, S.; Zichi, D.; Gold, L. *Mol. Diagn.* **1999**, *4*, 381.
(17) Lee, J. F.; Hesselberth, J. R.; Meyers, L. A.; Ellington, A. D. *Nucleic Acids Res.* **2004**, *32*, D95.
(18) Ueyama, H.; Takagi, M.; Takenaka, S. *J. Am. Chem. Soc.* **2002**, *124*, 14286.
(19) Miyake, Y.; Togashi, H.; Tashiro, M.; Yamaguchi, H.; Oda, S.; Kudo, M.; Tanaka, Y.; Kondo, Y.; Sawa, R.; Fujimoto, T.; Machinami, T.; Ono, A. *J. Am. Chem. Soc.* **2006**, *128*, 2172.
(20) Santoro, S. W.; Joyce, G. F. *Proc. Natl. Acad. Sci. U.S.A.* **1997**, *94*, 4262.
(21) Brown, A. K.; Li, J.; Pavot, C. M. B.; Lu, Y. *Biochemistry* **2003**, *42*, 7152.
(22) Liu, J.; Brown, A. K.; Meng, X.; Cropek, D. M.; Istok, J. D.; Watson, D. B.; Lu, Y. *Proc. Natl. Acad. Sci. U.S.A.* **2007**, *104*, 2056.
(23) Carmi, N.; Balkhi, H. R.; Breaker, R. R. *Proc. Natl. Acad. Sci. U.S.A.* **1998**, *95*, 2233.
(24) Rajendran, M.; Ellington, A. D. *Anal. Bioanal. Chem.* **2008**, *390*, 1067.
(25) Santoro, S. W.; Joyce, G. F.; Sakthivel, K.; Gramatikova, S.; Barbas, C. F., III *J. Am. Chem. Soc.* **2000**, *122*, 2433.
(26) Ellington, A. D.; Szostak, J. W. *Nature* **1992**, *355*, 850.
(27) Wilson, C.; Szostak, J. W. *Chem. Biol.* **1998**, *5*, 609.
(28) Harada, K.; Frankel, A. D. *EMBO J.* **1995**, *14*, 5798.
(29) Vianini, E.; Palumbo, M.; Gatto, B. *Bioorg. Med. Chem.* **2001**, *9*, 2543.
(30) Huizenga, D. E.; Szostak, J. W. *Biochemistry* **1995**, *34*, 656.
(31) Boiziau, C.; Dausse, E.; Yurchenko, L.; Toulme, J.-J. *J. Biol. Chem.* **1999**, *274*, 12730.
(32) Li, Y.; Geyer, C. R.; Sen, D. *Biochemistry* **1996**, *35*, 6911.
(33) Stojanovic, M. N.; de Prada, P.; Landry, D. W. *J. Am. Chem. Soc.* **2000**, *122*, 11547.
(34) Kato, T.; Takemura, T.; Yano, K.; Ikebukuro, K.; Karube, I. *Biochim. Biophys. Acta* **2000**, *1493*, 12.
(35) Saitoh, H.; Nakamura, A.; Kuwahara, M.; Ozaki, H.; Sawai, H. *Nucleic Acids Res. Suppl.* **2002**, *2*, 215.
(36) Shoji, A.; Kuwahara, M.; Ozaki, H.; Sawai, H. *J. Am. Chem. Soc.* **2007**, *129*, 1456.
(37) Kim, Y. S.; Jung, H. S.; Matsuura, T.; Lee, H. Y.; Kawai, T.; Gu, M. B. *Biosens. Bioelectron.* **2007**, *22*, 2525.
(38) Yang, Q.; Goldstein, I. J.; Mei, H.-Y.; Engelke, D. R. *Proc. Natl. Acad. Sci. U.S.A.* **1998**, *95*, 5462.
(39) Mehedi Masud, M.; Kuwahara, M.; Ozaki, H.; Sawai, H. *Bioorg. Med. Chem.* **2004**, *12*, 1111.
(40) Williams, K. P.; Liu, X.-H.; Schumacher, T. N. M.; Lin, H. Y.; Ausiello, D. A.; Kim, P. S.; Bartel, D. P. *Proc. Natl. Acad. Sci. U.S.A.* **1997**, *94*, 11285.
(41) Ogawa, A.; Tomita, N.; Kikuchi, N.; Sando, S.; Aoyama, Y. *Bioorg. Med. Chem. Lett.* **2004**, *14*, 4001.
(42) Mendonsa, S. D.; Bowser, M. T. *J. Am. Chem. Soc.* **2005**, *127*, 9382.
(43) Tang, J.; Xie, J.; Shao, N.; Yan, Y. *Electrophoresis* **2006**, *27*, 1303.
(44) Tang, J.; Yu, T.; Guo, L.; Xie, J.; Shao, N.; He, Z. *Biosens. Bioelectron.* **2007**, *22*, 2456.
(45) Bock, L. C.; Griffin, L. C.; Latham, J. A.; Vermaas, E. H.; Toole, J. J. *Nature* **1992**, *355*, 564.
(46) Lin, Y.; Padmapriya, A.; Morden, K. M.; Jayasena, S. D. *Proc. Natl. Acad. Sci. U.S.A.* **1995**, *92*, 11044.

(47) Yakimovich, O. Y.; Alekseev, Y. I.; Maksimenko, A. V.; Voronina, O. L.; Lunin, V. G. *Biochemistry (Moscow)* **2003**, *68*, 228.
(48) Andreola, M.-L.; Pileur, F.; Calmels, C.; Ventura, M.; Tarrago-Litvak, L.; Toulme, J.-J.; Litvak, S. *Biochemistry* **2001**, *40*, 10087.
(49) Mallikaratchy, P.; Stahelin, R. V.; Cao, Z.; Cho, W.; Tan, W. *Chem. Commun.* **2006**, 3229.
(50) Mosing, R. K.; Mendonsa, S. D.; Bowser, M. T. *Anal. Chem.* **2005**, *77*, 6107.
(51) Green, L. S.; Jellinek, D.; Jenison, R.; Oestman, A.; Heldin, C.-H.; Janjic, N. *Biochemistry* **1996**, *35*, 14413.
(52) Golden, M. C.; Collins, B. D.; Willis, M. C.; Koch, T. H. *J. Biotechnol.* **2000**, *81*, 167.
(53) Bassett, S. E.; Fennewald, S. M.; King, D. J.; Li, X.; Herzog, N. K.; Shope, R.; Aronson, J. F.; Luxon, B. A.; Gorenstein, D. G. *Biochemistry* **2004**, *43*, 9105.
(54) Wiegand, T. W.; Williams, P. B.; Dreskin, S. C.; Jouvin, M. H.; Kinet, J. P.; Tasset, D. *J. Immunol.* **1996**, *157*, 221.
(55) Jeon, S. H.; Kayhan, B.; Ben-Yedidia, T.; Arnon, R. *J. Biol. Chem.* **2004**, *279*, 48410.
(56) Koch, T. H.; Smith, D.; Tabacman, E.; Zichi, D. A. *J. Mol. Biol.* **2004**, *336*, 1159.
(57) Bruno, J. G.; Kiel, J. L. *Biosens. Bioelectron.* **1999**, *14*, 457.
(58) Blank, M.; Weinschenk, T.; Priemer, M.; Schluesener, H. *J. Biol. Chem.* **2001**, *276*, 16464.
(59) Wang, C.; Zhang, M.; Yang, G.; Zhang, D.; Ding, H.; Wang, H.; Fan, M.; Shen, B.; Shao, N. *J. Biotechnol.* **2003**, *102*, 15.
(60) Lee, Y. J.; Lee, S.-W. *J. Microbiol. Biotechnol.* **2006**, *16*, 1149.
(61) Shangguan, D.; Li, Y.; Tang, Z.; Cao, Z. C.; Chen, H. W.; Mallikaratchy, P.; Sefah, K.; Yang, C. J.; Tan, W. *Proc. Natl. Acad. Sci. U.S.A.* **2006**, *103*, 11838.
(62) Chen, H. W.; Medley, C. D.; Sefah, K.; Shangguan, D.; Tang, Z. W.; Meng, L.; Smith, J. E.; Tan, W. H. *ChemMedChem* **2008**, *3*, 991.
(63) Raddatz, M. S. L.; Dolf, A.; Endl, E.; Knolle, P.; Famulok, M.; Mayer, G. *Angew. Chem., Int. Ed.* **2008**, *47*, 5190.
(64) Ruckman, J.; Green, L. S.; Beeson, J.; Waugh, S.; Gillette, W. L.; Henninger, D. D.; Claesson-Welsh, L.; Janjic, N. *J. Biol. Chem.* **1998**, *273*, 20556.
(65) Pagratis, N. C.; Bell, C.; Chang, Y.-F.; Jennings, S.; Fitzwater, T.; Jellinek, D.; Dang, C. *Nat. Biotechnol.* **1997**, *15*, 68.
(66) Jenison, R. D.; Gill, S. C.; Pardi, A.; Polisky, B. *Science* **1994**, *263*, 1425.
(67) Geiger, A.; Burgstaller, P.; von der Eltz, H.; Roeder, A.; Famulok, M. *Nucleic Acids Res.* **1996**, *24*, 1029.
(68) Wang, Y.; Killian, J.; Hamasaki, K.; Rando, R. R. *Biochemistry* **1996**, *35*, 12338.
(69) Drolet, D. W.; Moon-McDermott, L.; Romig, T. S. *Nat. Biotechnol.* **1996**, *14*, 1021.
(70) Liss, M.; Petersen, B.; Wolf, H.; Prohaska, E. *Anal. Chem.* **2002**, *74*, 4488.
(71) Stadtherr, K.; Wolf, H.; Lindner, P. *Anal. Chem.* **2005**, *77*, 3437.
(72) Le Floch, F.; Ho, H. A.; Leclerc, M. *Anal. Chem.* **2006**, *78*, 4727.
(73) Ciesiolka, J.; Gorski, J.; Yarus, M. *RNA* **1995**, *1*, 538.
(74) Ciesiolka, J.; Yarus, M. *RNA* **1996**, *2*, 785.
(75) Wrzesinski, J.; Ciesiolka, J. *Biochemistry* **2005**, *44*, 6257.
(76) Doherty, E. A.; Doudna, J. A. *Annu. Rev. Biophys. Biomol.* **2001**, *30*, 457.
(77) Doudna, J. A.; Cech, T. R. *Nature* **2002**, *418*, 222.
(78) Lilley, D. M. J. *Curr. Opin. Struct. Biol.* **2005**, *15*, 313.
(79) Breaker, R. R. *Nat. Biotechnol.* **1997**, *15*, 427.
(80) Breaker, R. R. *Curr. Opin. Chem. Biol.* **1997**, *1*, 26.
(81) Sen, D.; Geyer, C. R. *Curr. Opin. Chem. Biol.* **1998**, *2*, 680.
(82) Lu, Y. *Chem.—Eur. J.* **2002**, *8*, 4588.
(83) Achenbach, J. C.; Chiuman, W.; Cruz, R. P. G.; Li, Y. *Curr. Pharm. Biotechnol.* **2004**, *5*, 312.
(84) Silverman, S. K. *Org. Biomol. Chem.* **2004**, *2*, 2701.
(85) Silverman, S. K. *Chem. Commun.* **2008**, 3467.
(86) Hobartner, C.; Silverman, S. K. *Biopolymers* **2007**, *87*, 279.
(87) Navani, N. K.; Li, Y. *Curr. Opin. Chem. Biol.* **2006**, *10*, 272.
(88) Silverman, S. K. *Nucleic Acids Res.* **2005**, *33*, 6151.
(89) Willner, I.; Shlyahovsky, B.; Zayats, M.; Willner, B. *Chem. Soc. Rev.* **2008**, *37*, 1153.
(90) Robertson, M. P.; Werner, M.; Ellington, A. D. *Nucleic Acids Symp. Ser.* **1999**, *41*, 1.
(91) Famulok, M. *Curr. Opin. Mol. Ther.* **2005**, *7*, 137.
(92) Knudsen, S. M.; Ellington, A. D. In *Aptamer Handbook*; Klussmann, S., Ed.; Wiley-VCH: Weinheim, 2006.
(93) Sullenger, B. A.; Gilboa, E. *Nature* **2002**, *418*, 252.
(94) Nimjee, S. M.; Rusconi, C. P.; Sullenger, B. A. *Annu. Rev. Med.* **2005**, *56*, 555.
(95) Lee, J. F.; Stovall, G. M.; Ellington, A. D. *Curr. Opin. Chem. Biol.* **2006**, *10*, 282.
(96) Becker, K. C. D.; Becker, R. C. *Curr. Opin. Mol. Ther.* **2006**, *8*, 122.
(97) Famulok, M.; Hartig, J. S.; Mayer, G. *Chem. Rev.* **2007**, *107*, 3715.
(98) Cho, E. J.; Rajendran, M.; Ellington, A. D. *Top. Fluoresc. Spectrosc.* **2005**, *10*, 127.
(99) Famulok, M.; Verma, S. *Trends Biotechnol.* **2002**, *20*, 462.
(100) Blank, M.; Blind, M. *Curr. Opin. Chem. Biol.* **2005**, *9*, 336.
(101) Famulok, M.; Mayer, G. *ChemBioChem* **2005**, *6*, 19.
(102) Ravelet, C.; Grosset, C.; Peyrin, E. *J. Chromatogr., A* **2006**, *1117*, 1.
(103) Ravelet, C.; Peyrin, E. *J. Sep. Sci.* **2006**, *29*, 1322.
(104) Peyrin, E. In *Aptamer Handbook*; Klussmann, S., Ed.; Wiley-VCH: Weinheim, 2006.
(105) Lu, Y.; Liu, J. *Acc. Chem. Res.* **2007**, *40*, 315.
(106) Lu, Y.; Liu, J. *Curr. Opin. Biotechnol.* **2006**, *17*, 580.
(107) Storhoff, J. J.; Mirkin, C. A. *Chem. Rev.* **1999**, *99*, 1849.
(108) Katz, E.; Willner, I. *Angew. Chem., Int. Ed.* **2004**, *43*, 6042.
(109) Feldkamp, U.; Niemeyer, C. M. *Angew. Chem., Int. Ed.* **2006**, *45*, 1856.
(110) Baum, D. A.; Silverman, S. K. *Cell. Mol. Life Sci.* **2008**, *65*, 2156.
(111) Famulok, M.; Mayer, G.; Blind, M. *Acc. Chem. Res.* **2000**, *33*, 591.
(112) Rajendran, M.; Ellington, A. D. *Comb. Chem. High Throughput Screening* **2002**, *5*, 263.
(113) Hesselberth, J.; Robertson, M. P.; Jhaveri, S.; Ellington, A. D. *Rev. Mol. Biotechnol.* **2000**, *74*, 15.
(114) Breaker, R. R. *Curr. Opin. Biotechnol.* **2002**, *13*, 31.
(115) Guthrie, J. W.; Hamula, C. L. A.; Zhang, H.; Le, X. C. *Methods* **2006**, *38*, 324.
(116) Yang, L.; Ellington, A. D. *Fluoresc. Sens. Biosens.* **2006**, 5.
(117) Song, S. P.; Wang, L. H.; Li, J.; Zhao, J. L.; Fan, C. H. *TrAC, Trends Anal. Chem.* **2008**, *27*, 108.
(118) Zhao, W.; Brook, M. A.; Li, Y. *ChemBioChem* **2008**, *9*, 2363.
(119) *Functional Nucleic Acids for Analytical Applications*; Li, Y., Lu, Y., Eds.; Springer: New York, NY, 2009.
(120) Kruger, K.; Grabowski, P. J.; Zaug, A. J.; Sands, J.; Gottschling, D. E.; Cech, T. R. *Cell* **1982**, *31*, 147.
(121) Guerrier-Takada, C.; Gardiner, K.; Marsh, T.; Pace, N.; Altman, S. *Cell* **1983**, *35*, 849.
(122) Symons, R. H. *Annu. Rev. Biochem.* **1992**, *61*, 641.
(123) Cech, T. R. *Cell* **1983**, *34*, 713.
(124) Ban, N.; Nissen, P.; Hansen, J.; Moore, P. B.; Steitz, T. A. *Science* **2000**, *289*, 902.
(125) Pan, T.; Uhlenbeck, O. C. *Biochemistry* **1992**, *31*, 3887.
(126) Pan, T.; Uhlenbeck, O. C. *Nature* **1992**, *358*, 560.
(127) Bartel, D. P.; Szostak, J. W. *Science* **1993**, *261*, 1411.
(128) Ekland, E. H.; Szostak, J. W.; Bartel, D. P. *Science* **1995**, *269*, 364.
(129) Chapman, K. B.; Szostak, J. W. *Chem. Biol.* **1995**, *2*, 325.
(130) Curtis, E. A.; Bartel, D. P. *Nat. Struct. Mol. Biol.* **2005**, *12*, 994.
(131) Huang, F.; Yarus, M. *Biochemistry* **1997**, *36*, 6557.
(132) Ekland, E. H.; Bartel, D. P. *Nature* **1996**, *382*, 373.
(133) Sun, L. L.; Cui, Z. Y.; Gottlieb, R. L.; Zhang, B. L. *Chem. Biol.* **2002**, *9*, 619.
(134) Zhang, B.; Cech, T. R. *Nature* **1997**, *390*, 96.
(135) Tsukiji, S.; Pattnaik, S. B.; Suga, H. *J. Am. Chem. Soc.* **2004**, *126*, 5044.
(136) Tsukiji, S.; Pattnaik, S. B.; Suga, H. *Nat. Struct. Biol.* **2003**, *10*, 713.
(137) Tarasow, T. M.; Tarasow, S. L.; Eaton, B. E. *Nature* **1997**, *389*, 54.
(138) Seelig, B.; Jaschke, A. *Chem. Biol.* **1999**, *6*, 167.
(139) Agresti, J. J.; Kelly, B. T.; Jaschke, A.; Griffiths, A. D. *Proc. Natl. Acad. Sci. U.S.A.* **2005**, *102*, 16170.
(140) Fusz, S.; Eisenfuehr, A.; Srivatsan, S. G.; Heckel, A.; Famulok, M. *Chem. Biol.* **2005**, *12*, 941.
(141) Sengle, G.; Eisenfuhr, A.; Arora, P. S.; Nowick, J. S.; Famulok, M. *Chem. Biol.* **2001**, *8*, 459.
(142) Conn, M. M.; Prudent, J. R.; Schultz, P. G. *J. Am. Chem. Soc.* **1996**, *118*, 7012.
(143) Lohse, P. A.; Szostak, J. W. *Nature* **1996**, *381*, 442.
(144) Jenne, A.; Famulok, M. *Chem. Biol.* **1998**, *5*, 23.
(145) Suga, H.; Cowan, J. A.; Szostak, J. W. *Biochemistry* **1998**, *37*, 10118.
(146) Suga, H.; Lohse, P. A.; Szostak, J. W. *J. Am. Chem. Soc.* **1998**, *120*, 1151.
(147) Illangasekare, M.; Sanchez, G.; Nickles, T.; Yarus, M. *Science* **1995**, *267*, 643.
(148) Illangasekare, M.; Yarus, M. *Proc. Natl. Acad. Sci. U.S.A.* **1999**, *96*, 5470.
(149) Wiegand, T. W.; Janssen, R. C.; Eaton, B. E. *Chem. Biol.* **1997**, *4*, 675.
(150) Nieuwlandt, D.; West, M.; Cheng, X.; Kirshenheuter, G.; Eaton, B. E. *ChemBioChem* **2003**, *4*, 651.
(151) Chapple, K. E.; Bartel, D. P.; Unrau, P. J. *RNA* **2003**, *9*, 1208.
(152) Lau, M. W. L.; Cadieux, K. E. C.; Unrau, P. J. *J. Am. Chem. Soc.* **2004**, *126*, 15686.
(153) Breaker, R. R.; Joyce, G. F. *Chem. Biol.* **1994**, *1*, 223.
(154) Breaker, R. R.; Joyce, G. F. *Chem. Biol.* **1995**, *2*, 655.
(155) Geyer, C. R.; Sen, D. *Chem. Biol.* **1997**, *4*, 579.

(156) Perrin, D. M.; Garestier, T.; Helene, C. *J. Am. Chem. Soc.* **2001**, *123*, 1556.

(157) Sidorov, A. V.; Grasby, J. A.; Williams, D. M. *Nucleic Acids Res.* **2004**, *32*, 1591.

(158) Mei, S. H. J.; Liu, Z.; Brennan, J. D.; Li, Y. *J. Am. Chem. Soc.* **2003**, *125*, 412.

(159) Liu, Z.; Mei, S. H. J.; Brennan, J. D.; Li, Y. *J. Am. Chem. Soc.* **2003**, *125*, 7539.

(160) Chiuman, W.; Li, Y. *Chem. Biol.* **2006**, *13*, 1061.

(161) Schlosser, K.; Gu, J.; Sule, L.; Li, Y. F. *Nucleic Acids Res.* **2008**, *36*, 1472.

(162) Carmi, N.; Shultz, L. A.; Breaker, R. R. *Chem. Biol.* **1996**, *3*, 1039.

(163) Flynn-Charlebois, A.; Wang, Y.; Prior, T. K.; Rashid, I.; Hoadley, K. A.; Coppins, R. L.; Wolf, A. C.; Silverman, S. K. *J. Am. Chem. Soc.* **2003**, *125*, 2444.

(164) Hoadley, K. A.; Purtha, W. E.; Wolf, A. C.; Flynn-Charlebois, A.; Silverman, S. K. *Biochemistry* **2005**, *44*, 9217.

(165) Purtha, W. E.; Coppins, R. L.; Smalley, M. K.; Silverman, S. K. *J. Am. Chem. Soc.* **2005**, *127*, 13124.

(166) Cuenoud, B.; Szostak, J. W. *Nature* **1995**, *375*, 611.

(167) Sreedhara, A.; Li, Y.; Breaker, R. R. *J. Am. Chem. Soc.* **2004**, *126*, 3454.

(168) Wang, Y.; Silverman, S. K. *J. Am. Chem. Soc.* **2003**, *125*, 6880.

(169) Wang, Y.; Silverman, S. K. *Biochemistry* **2005**, *44*, 3017.

(170) Coppins, R. L.; Silverman, S. K. *Nat. Struct. Mol. Biol.* **2004**, *11*, 270.

(171) Wang, W.; Billen, L. P.; Li, Y. *Chem. Biol.* **2002**, *9*, 507.

(172) Li, Y.; Liu, Y.; Breaker, R. R. *Biochemistry* **2000**, *39*, 3106.

(173) Sheppard, T. L.; Ordoukhanian, P.; Joyce, G. F. *Proc. Natl. Acad. Sci. U.S.A.* **2000**, *97*, 7802.

(174) Burmeister, J.; von Kiedrowski, G.; Ellington, A. D. *Angew. Chem., Int. Ed.* **1997**, *36*, 1321.

(175) Chinnapen, D. J. F.; Sen, D. *Proc. Natl. Acad. Sci. U.S.A.* **2004**, *101*, 65.

(176) Li, Y.; Sen, D. *Nat. Struct. Biol.* **1996**, *3*, 743.

(177) Travascio, P.; Bennet, A. J.; Wang, D. Y.; Sen, D. *Chem. Biol.* **1999**, *6*, 779.

(178) Takagi, Y.; Warashina, M.; Stec, W. J.; Yoshinari, K.; Taira, K. *Nucleic Acids Res.* **2001**, *29*, 1815.

(179) Bevilacqua, P. C.; Brown, T. S.; Nakano, S.-i.; Yajima, R. *Biopolymers* **2004**, *73*, 90.

(180) Doudna, J. A.; Lorsch, J. R. *Nat. Struct. Mol. Biol.* **2005**, *12*, 395.

(181) Fedor, M. J.; Williamson, J. R. *Nat. Rev. Mol. Cell Biol.* **2005**, *6*, 399.

(182) Kurz, M.; Breaker, R. R. *Curr. Top. Microbiol. Immunol.* **1999**, *243*, 137.

(183) Breaker, R. R. *Science* **2000**, *290*, 2095.

(184) Joyce, G. F. *Annu. Rev. Biochem.* **2004**, *73*, 791.

(185) Peracchi, A.; Bonaccio, M.; Clerici, M. *J. Mol. Biol.* **2005**, *352*, 783.

(186) Li, J.; Lu, Y. *J. Am. Chem. Soc.* **2000**, *122*, 10466.

(187) Liu, J.; Lu, Y. *J. Am. Chem. Soc.* **2003**, *125*, 6642.

(188) Liu, J.; Lu, Y. *Anal. Chem.* **2003**, *75*, 6666.

(189) Liu, J. W.; Lu, Y. *J. Fluoresc.* **2004**, *14*, 343.

(190) Liu, J.; Lu, Y. *Chem. Mater.* **2004**, *16*, 3231.

(191) Liu, J.; Lu, Y. *J. Am. Chem. Soc.* **2004**, *126*, 12298.

(192) Liu, J.; Lu, Y. *J. Am. Chem. Soc.* **2005**, *127*, 12677.

(193) Liu, J.; Lu, Y. *Methods Mol. Biol.* **2006**, *335*, 275.

(194) Liu, J.; Lu, Y. *Org. Biomol. Chem.* **2006**, *4*, 3435.

(195) Shen, Y.; Mackey, G.; Rupcich, N.; Gloster, D.; Chiuman, W.; Li, Y.; Brennan, J. D. *Anal. Chem.* **2007**, *79*, 3494.

(196) Fahlman, R. P.; Sen, D. *J. Am. Chem. Soc.* **2002**, *124*, 4610.

(197) Liu, J.; Lu, Y. *Anal. Chem.* **2004**, *76*, 1627.

(198) Stojanovic, M. N.; Mitchell, T. E.; Stefanovic, D. *J. Am. Chem. Soc.* **2002**, *124*, 3555.

(199) Stojanovic, M. N.; Stefanovic, D. *J. Am. Chem. Soc.* **2003**, *125*, 6673.

(200) Stojanovic, M. N.; Semova, S.; Kolpashchikov, D.; Macdonald, J.; Morgan, C.; Stefanovic, D. *J. Am. Chem. Soc.* **2005**, *127*, 6914.

(201) Chen, Y.; Wang, M.; Mao, C. *Angew. Chem., Int. Ed.* **2004**, *43*, 3554.

(202) Tian, Y.; He, Y.; Chen, Y.; Yin, P.; Mao, C. *Angew. Chem., Int. Ed.* **2005**, *44*, 4355.

(203) Liu, J.; Wernette, D. P.; Lu, Y. *Angew. Chem., Int. Ed.* **2005**, *44*, 7290.

(204) Bruesehoff, P. J.; Li, J.; Augustine, A. J.; Lu, Y. *Comb. Chem. High Throughput Screening* **2002**, *5*, 327.

(205) Ewing, G. W. *Analytical Instrumentation Handbook*; Marcel Dekker: New York, 1997.

(206) Czarnik, A. W. *Acc. Chem. Res.* **1994**, *27*, 302.

(207) Wang, J. *Trends Anal. Chem.* **2002**, *21*, 226.

(208) Manz, A.; Eijkel, J. C. T. *Pure Appl. Chem.* **2001**, *73*, 1555.

(209) Khandurina, J.; Guttman, A. *J. Chromatogr., A* **2002**, *943*, 159.

(210) Sooter, L. J.; Riedel, T.; Davidson, E. A.; Levy, M.; Cox, J. C.; Ellington, A. D. *Biol. Chem.* **2001**, *382*, 1327.

(211) Williams, K. P.; Bartel, D. P. *Nucleic Acids Res.* **1995**, *23*, 4220.

(212) Zuker, M. *Nucleic Acids Res.* **2003**, *31*, 3406.

(213) Peracchi, A. *ChemBioChem* **2005**, *6*, 1316.

(214) Faulhammer, D.; Famulok, M. *Angew. Chem., Int. Ed.* **1996**, *35*, 2837.

(215) Peracchi, A. *J. Biol. Chem.* **2000**, *275*, 11693.

(216) Li, J.; Zheng, W.; Kwon, A. H.; Lu, Y. *Nucleic Acids Res.* **2000**, *28*, 481.

(217) Cruz, R. P. G.; Withers, J. B.; Li, Y. *Chem. Biol.* **2004**, *11*, 57.

(218) Liu, J.; Lu, Y. *J. Am. Chem. Soc.* **2002**, *124*, 15208.

(219) Kim, H.-K.; Liu, J.; Li, J.; Nagraj, N.; Li, M.; Pavot, C. M. B.; Lu, Y. *J. Am. Chem. Soc.* **2007**, *129*, 6896.

(220) Kim, H. K.; Rasnik, I.; Liu, J. W.; Ha, T. J.; Lu, Y. *Nat. Chem. Biol.* **2007**, *3*, 762.

(221) Carmi, N.; Breaker, R. R. *Bioorg. Med. Chem.* **2001**, *9*, 2589.

(222) Liu, J.; Lu, Y. *J. Am. Chem. Soc.* **2007**, *129*, 9838.

(223) Chiuman, W.; Li, Y. *J. Mol. Biol.* **2006**, *357*, 748.

(224) Nelson, K. E.; Brueshoff, P. J.; Lu, Y. *J. Mol. Evol.* **2005**, *61*, 216.

(225) Nutiu, R.; Li, Y. *Chem.—Eur. J.* **2004**, *10*, 1868.

(226) Nutiu, R.; Li, Y. *Methods* **2005**, *37*, 16.

(227) Cao, Z.; Suljak, S. W.; Tan, W. *Curr. Proteomics* **2005**, *2*, 31.

(228) Santoro, S. W.; Joyce, G. F. *Biochemistry* **1998**, *37*, 13330.

(229) Tyagi, S.; Bratu, D. P.; Kramer, F. R. *Nat. Biotechnol.* **1998**, *16*, 49.

(230) Tyagi, S.; Kramer, F. R. *Nat. Biotechnol.* **1996**, *14*, 303.

(231) Tyagi, A.; Marras, S. A. E.; Kramer, F. R. *Nat. Biotechnol.* **2000**, *18*, 1191.

(232) Dubertret, B.; Calame, M.; Libchaber, A. J. *Nat. Biotechnol.* **2001**, *19*, 365.

(233) Zhang, P.; Beck, T.; Tan, W. *Angew. Chem., Int. Ed.* **2001**, *40*, 402.

(234) Nutiu, R.; Li, Y. *Nucleic Acids Res.* **2002**, *30*, e94/1.

(235) Stojanovic, M. N.; De Prada, P.; Landry, D. W. *ChemBioChem* **2001**, *2*, 411.

(236) Perkins, T. A.; Wolf, D. E.; Goodchild, J. *Biochemistry* **1996**, *35*, 16370.

(237) Walter, N. G.; Burke, J. M. *RNA* **1997**, *3*, 392.

(238) Hanne, A.; Ramanujam, M. V.; Rucker, T.; Krupp, G. *Nucleosides, Nucleotides* **1998**, *17*, 1835.

(239) Singh, K. K.; Parwaresch, R.; Krupp, G. *RNA* **1999**, *5*, 1348.

(240) Jenne, A.; Gmelin, W.; Raffler, N.; Famulok, M. *Angew. Chem., Int. Ed.* **1999**, *38*, 1300.

(241) Jenne, A.; Hartig, J. S.; Piganeau, N.; Tauer, A.; Samarsky, D. A.; Green, M. R.; Davies, J.; Famulok, M. *Nat. Biotechnol.* **2001**, *19*, 56.

(242) Vitiello, D.; Pecchia, D. B.; Burke, J. M. *RNA* **2000**, *6*, 628.

(243) Stojanovic, M. N.; De Prada, P.; Landry, D. W. *Nucleic Acids Res.* **2000**, *28*, 2915.

(244) Murray, J. B.; Terwey, D. P.; Maloney, L.; Karpeisky, A.; Usman, N.; Beigelman, L.; Scott, W. G. *Cell* **1998**, *92*, 665.

(245) Rupert, P. B.; Ferre-D'Amare, A. R. *Nature* **2001**, *410*, 780.

(246) Perkins, T. A.; Goodchild, J. *Methods Mol. Biol.* **1997**, *74*, 241.

(247) Ferguson, A.; Boomer, R. M.; Kurz, M.; Keene, S. C.; Diener, J. L.; Keefe, A. D.; Wilson, C.; Cload, S. T. *Nucleic Acids Res.* **2004**, *32*, 1756.

(248) Srinivasan, J.; Cload, S. T.; Hamaguchi, N.; Kurz, J.; Keene, S.; Kurz, M.; Boomer, R. M.; Blanchard, J.; Epstein, D.; Wilson, C.; Diener, J. L. *Chem. Biol.* **2004**, *11*, 499.

(249) Chiuman, W.; Li, Y. *Nucleic Acids Res.* **2007**, *35*, 401.

(250) Swearingen, C. B.; Wernette, D. P.; Cropek, D. M.; Lu, Y.; Sweedler, J. V.; Bohn, P. W. *Anal. Chem.* **2005**, *77*, 442.

(251) Wernette, D. P.; Swearingen, C. B.; Cropek, D. M.; Lu, Y.; Sweedler, J. V.; Bohn, P. W. *Analyst* **2006**, *131*, 41.

(252) Boomer, D. W.; Powell, M. *J. Anal. Chem.* **1987**, *59*, 2810.

(253) Shen, Y.; Brennan, J. D.; Li, Y. *Biochemistry* **2005**, *44*, 12066.

(254) Kandadai, S. A.; Li, Y. *Nucleic Acids Res.* **2005**, *33*, 7164.

(255) Shen, Y.; Chiuman, W.; Brennan, J. D.; Li, Y. *ChemBioChem* **2006**, *7*, 1343.

(256) Kandadai, S. A.; Chiuman, W.; Li, Y. *Chem. Commun.* **2006**, 2359.

(257) Ali, M. M.; Kandadai, S. A.; Li, Y. F. *Can. J. Chem.* **2007**, *85*, 261.

(258) Wernette, D. P.; Mead, C.; Bohn, P. W.; Lu, Y. *Langmuir* **2007**, *23*, 9513.

(259) Yim, T.-J.; Liu, J.; Lu, Y.; Kane, R. S.; Dordick, J. S. *J. Am. Chem. Soc.* **2005**, *127*, 12200.

(260) Shaikh, K. A.; Ryu, K. S.; Goluch, E. D.; Nam, J.-M.; Liu, J.; Thaxton, C. S.; Chiesl, T. N.; Barron, A. E.; Lu, Y.; Mirkin, C. A.; Liu, C. *Proc. Natl. Acad. Sci. U.S.A.* **2005**, *102*, 9745.

(261) Chang, I.-H.; Tulock, J. J.; Liu, J.; Kim, W.-S.; Cannon, D. M., Jr.; Lu, Y.; Bohn, P. W.; Sweedler, J. V.; Cropek, D. M. *Environ. Sci. Technol.* **2005**, *39*, 3756.

(262) Travascio, P.; Li, Y.; Sen, D. *Chem. Biol.* **1998**, *5*, 505.

(263) Travascio, P.; Sen, D.; Bennet, A. J. *Can. J. Chem.* **2006**, *84*, 613.

(264) Lee, H.-W.; Chinnapen, D. J.-F.; Sen, D. *Pure Appl. Chem.* **2004**, *76*, 1537.

(265) Willner, I.; Willner, B.; Katz, E. *Bioelectrochemistry* **2007**, *70*, 2.

(266) Willner, I.; Baron, R.; Willner, B. *Biosens. Bioelectron.* **2007**, *22*, 1841.

(267) Xiao, Y.; Pavlov, V.; Gill, R.; Bourenko, T.; Willner, I. *ChemBioChem* **2004**, *5*, 374.

(268) Xiao, Y.; Pavlov, V.; Niazov, T.; Dishon, A.; Kotler, M.; Willner, I. *J. Am. Chem. Soc.* **2004**, *126*, 7430.

(269) Pavlov, V.; Xiao, Y.; Gill, R.; Dishon, A.; Kotler, M.; Willner, I. *Anal. Chem.* **2004**, *76*, 2152.

(270) Niazov, T.; Pavlov, V.; Xiao, Y.; Gill, R.; Willner, I. *Nano Lett.* **2004**, *4*, 1683.

(271) Weizmann, Y.; Beissenhirtz, M. K.; Cheglakov, Z.; Nowarski, R.; Kotler, M.; Willner, I. *Angew. Chem., Int. Ed.* **2006**, *45*, 7384.

(272) Cheglakov, Z.; Weizmann, Y.; Beissenhirtz, M. K.; Willner, I. *Chem. Commun.* **2006**, 3205.

(273) Shlyahovsky, B.; Li, D.; Weizmann, Y.; Nowarski, R.; Kotler, M.; Willner, I. *J. Am. Chem. Soc.* **2007**, *129*, 3814.

(274) Cheglakov, Z.; Weizmann, Y.; Basnar, B.; Willner, I. *Org. Biomol. Chem.* **2007**, *5*, 223.

(275) Tian, Y.; He, Y.; Mao, C. *ChemBioChem* **2006**, *7*, 1862.

(276) Shlyahovsky, B.; Li, D.; Katz, E.; Willner, I. *Biosens. Bioelectron.* **2007**, *22*, 2570.

(277) Liu, J.; Lu, Y. In *Functional Nucleic Acids for Analytical Applications*; Li, Y., Lu, Y., Eds.; Springer: New York, NY, in press.

(278) Lee, J. H.; Wang, Z.; Liu, J.; Lu, Y. *J. Am. Chem. Soc.* **2008**, *130*, 14217.

(279) Wang, Z. D.; Lee, J. H.; Lu, Y. *Adv. Mater.* **2008**, *20*, 3263.

(280) Wei, H.; Li, B.; Li, J.; Dong, S.; Wang, E. *Nanotechnology* **2008**, *19*, 095501.

(281) Zhao, W. A.; Lam, J. C. F.; Chiuman, W.; Brook, M. A.; Li, Y. F. *Small* **2008**, *4*, 810.

(282) Liu, J.; Lu, Y. *Chem. Commun.* **2007**, 4872.

(283) Xiao, Y.; Rowe, A. A.; Plaxco, K. W. *J. Am. Chem. Soc.* **2007**, *129*, 262.

(284) Roth, A.; Breaker, R. R. *Proc. Natl. Acad. Sci. U.S.A.* **1998**, *95*, 6027.

(285) Jayasena, S. D. *Clin. Chem.* **1999**, *45*, 1628.

(286) Mann, D.; Reinemann, C.; Stoltenburg, R.; Strehlitz, B. *Biochem. Biophys. Res. Commun.* **2005**, *338*, 1928.

(287) Stoltenburg, R.; Reinemann, C.; Strehlitz, B. *Anal. Bioanal. Chem.* **2005**, *383*, 83.

(288) Mendonsa, S. D.; Bowser, M. T. *J. Am. Chem. Soc.* **2004**, *126*, 20.

(289) Berezovski, M.; Drabovich, A.; Krylova, S. M.; Musheev, M.; Okhonin, V.; Petrov, A.; Krylov, S. N. *J. Am. Chem. Soc.* **2005**, *127*, 3165.

(290) Musheev, M. U.; Krylov, S. N. *Anal. Chim. Acta* **2006**, *564*, 91.

(291) Drabovich, A. P.; Berezovski, M.; Okhonin, V.; Krylov, S. N. *Anal. Chem.* **2006**, *78*, 3171.

(292) Berezovski, M.; Musheev, M.; Drabovich, A.; Krylov, S. N. *J. Am. Chem. Soc.* **2006**, *128*, 1410.

(293) Drabovich, A.; Berezovski, M.; Krylov, S. N. *J. Am. Chem. Soc.* **2005**, *127*, 11224.

(294) Berezovski, M.; Krylov, S. N. *Anal. Chem.* **2005**, *77*, 1526.

(295) Misono, T. S.; Kumar, P. K. R. *Anal. Biochem.* **2005**, *342*, 312.

(296) Peng, L.; Stephens, B. J.; Bonin, K.; Cubicciotti, R.; Guthold, M. *Microsc. Res. Tech.* **2007**, *70*, 372.

(297) Cox, J. C.; Rudolph, P.; Ellington, A. D. *Biotechnol. Prog.* **1998**, *14*, 845.

(298) Cox, J. C.; Ellington, A. D. *Bioorg. Med. Chem.* **2001**, *9*, 2525.

(299) Cox, J. C.; Hayhurst, J.; Hesselberth, J.; Bayer, T. S.; Georgiou, G.; Ellington, A. D. *Nucleic Acids Res.* **2002**, *30*, e108/1.

(300) Cox, J. C.; Rajendran, M.; Riedel, T.; Davidson, E. A.; Sooter, L. J.; Bayer, T. S.; Schmitz-Brown, M.; Ellington, A. D. *Comb. Chem. High Throughput Screening* **2002**, *5*, 289.

(301) Hybarger, G.; Bynum, J.; Williams, R. F.; Valdes, J. J.; Chambers, J. P. *Anal. Bioanal. Chem.* **2006**, *384*, 191.

(302) Nutiu, R.; Li, Y. *Angew. Chem., Int. Ed.* **2005**, *44*, 1061.

(303) Stubbs, M. T.; Bode, W. *Trends Biochem. Sci.* **1995**, *20*, 23.

(304) Wang, K. Y.; Krawczyk, S. H.; Bischofberger, N.; Swaminathan, S.; Bolton, P. H. *Biochemistry* **1993**, *32*, 11285.

(305) Wang, K. Y.; McCurdy, S.; Shea, R. G.; Swaminathan, S.; Bolton, P. H. *Biochemistry* **1993**, *32*, 1899.

(306) Macaya, R. F.; Schultze, P.; Smith, F. W.; Roe, J. A.; Feigon, J. *Proc. Natl. Acad. Sci. U.S.A* **1993**, *90*, 3745.

(307) Padmanabhan, K.; Padmanabhan, K. P.; Ferrara, J. D.; Sadler, J. E.; Tulinsky, A. *J. Biol. Chem.* **1993**, *268*, 17651.

(308) Macaya, R. F.; Waldron, J. A.; Beutel, B. A.; Gao, H.; Joesten, M. E.; Yang, M.; Patel, R.; Bertelsen, A. H.; Cook, A. F. *Biochemistry* **1995**, *34*, 4478.

(309) Tsiang, M.; Gibbs, C. S.; Griffin, L. C.; Dunn, K. E.; Leung, L. L. K. *J. Biol. Chem.* **1995**, *270*, 19370.

(310) Tasset, D. M.; Kubik, M. F.; Steiner, W. *J. Mol. Biol.* **1997**, *272*, 688.

(311) Kubik, M. F.; Stephens, A. W.; Schneider, D.; Marlar, R. A.; Tasset, D. *Nucleic Acids Res.* **1994**, *22*, 2619.

(312) Lin, C. H.; Patel, D. J. *Chem. Biol.* **1997**, *4*, 817.

(313) Sassanfar, M.; Szostak, J. W. *Nature* **1993**, *364*, 550.

(314) Hermann, T.; Patel, D. J. *Science* **2000**, *287*, 820.

(315) Joseph, M. J.; Taylor, J. C.; McGown, L. B.; Pitner, B.; Linn, C. P. *Biospectroscopy* **1996**, *2*, 173.

(316) Zhou, C.; Jiang, Y.; Hou, S.; Ma, B.; Fang, X.; Li, M. *Anal. Bioanal. Chem.* **2006**, *384*, 1175.

(317) Wood, A. E.; Bishop, G. R. *Molecules* **2004**, *9*, 67.

(318) Bishop, G. R.; Ren, J.; Polander, B. C.; Jeanfreau, B. D.; Trent, J. O.; Chaires, J. B. *Biophys. Chem.* **2007**, *126*, 165.

(319) Huang, C. C.; Chang, H. T. *Chem. Commun.* **2008**, 1461.

(320) Wang, J.; Jiang, Y.; Zhou, C.; Fang, X. *Anal. Chem.* **2005**, *77*, 3542.

(321) Jiang, Y.; Fang, X.; Bai, C. *Anal. Chem.* **2004**, *76*, 5230.

(322) Li, B.; Wei, H.; Dong, S. *Chem. Commun.* **2007**, 73.

(323) Nutiu, R.; Li, Y. *J. Am. Chem. Soc.* **2003**, *125*, 4771.

(324) Huang, C.-C.; Chiu, S.-H.; Huang, Y.-F.; Chang, H.-T. *Anal. Chem.* **2007**, *79*, 4798.

(325) McQuade, D. T.; Pullen, A. E.; Swager, T. M. *Chem. Rev.* **2000**, *100*, 2537.

(326) Thomas, S. W., III; Joly, G. D.; Swager, T. M. *Chem. Rev.* **2007**, *107*, 1339.

(327) Ho, H. A.; Najari, A.; Leclerc, M. *Acc. Chem. Res.* **2008**, *41*, 168.

(328) Ho, H.-A.; Boissinot, M.; Bergeron, M. G.; Corbeil, G.; Dore, K.; Boudreau, D.; Leclerc, M. *Angew. Chem., Int. Ed.* **2002**, *41*, 1548.

(329) Dore, K.; Dubus, S.; Ho, H.-A.; Levesque, I.; Brunette, M.; Corbeil, G.; Boissinot, M.; Boivin, G.; Bergeron, M. G.; Boudreau, D.; Leclerc, M. *J. Am. Chem. Soc.* **2004**, *126*, 4240.

(330) Ho, H.-A.; Bera-Aberem, M.; Leclerc, M. *Chem.—Eur. J.* **2005**, *11*, 1718.

(331) Ho, H.-A.; Leclerc, M. *J. Am. Chem. Soc.* **2004**, *126*, 1384.

(332) Aberem, M. B.; Najari, A.; Ho, H.-A.; Gravel, J.-F.; Nobert, P.; Boudreau, D.; Leclerc, M. *Adv. Mater.* **2006**, *18*, 2703.

(333) Dore, K.; Leclerc, M.; Boudreau, D. *J. Fluoresc.* **2006**, *16*, 259.

(334) Dore, K.; Neagu-Plesu, R.; Leclerc, M.; Boudreau, D.; Ritcey, A. M. *Langmuir* **2007**, *23*, 258.

(335) Ho, H. A.; Dore, K.; Boissinot, M.; Bergeron, M. G.; Tanguay, R. M.; Boudreau, D.; Leclerc, M. *J. Am. Chem. Soc.* **2005**, *127*, 12673.

(336) Najari, A.; Ho, H. A.; Gravel, J.-F.; Nobert, P.; Boudreau, D.; Leclerc, M. *Anal. Chem.* **2006**, *78*, 7896.

(337) He, F.; Tang, Y.; Wang, S.; Li, Y.; Zhu, D. *J. Am. Chem. Soc.* **2005**, *127*, 12343.

(338) He, F.; Tang, Y.; Yu, M.; Feng, F.; An, L.; Sun, H.; Wang, S.; Li, Y.; Zhu, D.; Bazan, G. C. *J. Am. Chem. Soc.* **2006**, *128*, 6764.

(339) Tang, Y.; Feng, F.; He, F.; Wang, S.; Li, Y.; Zhu, D. *J. Am. Chem. Soc.* **2006**, *128*, 14972.

(340) Okazawa, A.; Maeda, H.; Fukusaki, E.; Katakura, Y.; Kobayashi, A. *Bioorg. Med. Chem. Lett.* **2000**, *10*, 2653.

(341) Holeman, L. A.; Robinson, S. L.; Szostak, J. W.; Wilson, C. *Folding Des.* **1998**, *3*, 423.

(342) Grate, D.; Wilson, C. *Proc. Natl. Acad. Sci. U.S.A.* **1999**, *96*, 6131.

(343) Babendure, J. R.; Adams, S. R.; Tsien, R. Y. *J. Am. Chem. Soc.* **2003**, *125*, 14716.

(344) Sando, S.; Narita, A.; Aoyama, Y. *ChemBioChem* **2007**, *8*, 1795.

(345) Sando, S.; Narita, A.; Hayami, M.; Aoyama, Y. *Chem. Commun.* **2008**, 3858.

(346) Hirabayashi, M.; Taira, S.; Kobayashi, S.; Konishi, K.; Katoh, K.; Hiratsuka, Y.; Kodaka, M.; Uyeda, T. Q. P.; Yumoto, N.; Kubo, T. *Biotechnol. Bioeng.* **2006**, *94*, 473.

(347) Stojanovic, M. N.; Kolpashchikov, D. M. *J. Am. Chem. Soc.* **2004**, *126*, 9266.

(348) Kolpashchikov, D. M. *J. Am. Chem. Soc.* **2005**, *127*, 12442.

(349) Famulok, M. *Nature* **2004**, *430*, 976.

(350) Wang, Y.; Rando, R. R. *Chem. Biol.* **1995**, *2*, 281.

(351) Gilbert, B. A.; Sha, M.; Wathen, S. T.; Rando, R. R. *Bioorg. Med. Chem.* **1997**, *5*, 1115.

(352) Huang, C. C.; Chiang, C. K.; Lin, Z. H.; Lee, K. H.; Chang, H. T. *Anal. Chem.* **2008**, *80*, 1497.

(353) Jhaveri, S. D.; Kirby, R.; Conrad, R.; Maglott, E. J.; Bowser, M.; Kennedy, R. T.; Glick, G.; Ellington, A. D. *J. Am. Chem. Soc.* **2000**, *122*, 2469.

(354) Yamana, K.; Ohtani, Y.; Nakano, H.; Saito, I. *Bioorg. Med. Chem. Lett.* **2003**, *13*, 3429.

(355) Kamekawa, N.; Shimomura, Y.; Nakamura, M.; Yamana, K. *Chem. Lett.* **2006**, *35*, 660.

(356) Merino, E. J.; Weeks, K. M. *J. Am. Chem. Soc.* **2005**, *127*, 12766.

(357) Katilius, E.; Katiliene, Z.; Woodbury, N. W. *Anal. Chem.* **2006**, *78*, 6484.

(358) Dwarakanath, S.; Bruno, J. G.; Shastry, A.; Phillips, T.; John, A. A.; Kumar, A.; Stephenson, L. D. *Biochem. Biophys. Res. Commun.* **2004**, *325*, 739.

(359) Choi, J. H.; Chen, K. H.; Strano, M. S. *J. Am. Chem. Soc.* **2006**, *128*, 15584.

(360) Merino, E. J.; Weeks, K. M. *J. Am. Chem. Soc.* **2003**, *125*, 12370.

(361) Jhaveri, S.; Rajendran, M.; Ellington, A. D. *Nat. Biotechnol.* **2000**, *18*, 1293.

(362) Unruh, J. R.; Gokulrangan, G.; Wilson, G. S.; Johnson, C. K. *Photochem. Photobiol.* **2005**, *81*, 682.

(363) Li, J. J.; Fang, X.; Schuster, S. M.; Tan, W. *Angew. Chem., Int. Ed.* **2000**, *39*, 1049.

(364) Hamaguchi, N.; Ellington, A.; Stanton, M. *Anal. Biochem.* **2001**, *294*, 126.

(365) Stratis-Cullum, D. N.; Johnson, E. M.; Pellegrino, P. M. *Proc. SPIE—Int. Soc. Opt. Eng.* **2005**, *6007*, 60070T/1.

(366) Morse, D. P. *Biochem. Biophys. Res. Commun.* **2007**, *359*, 94.

(367) Stojanovic, M. N.; de Prada, P.; Landry, D. W. *J. Am. Chem. Soc.* **2001**, *123*, 4928.

(368) Ozaki, H.; Nishihira, A.; Wakabayashi, M.; Kuwahara, M.; Sawai, H. *Bioorg. Med. Chem. Lett.* **2006**, *16*, 4381.

(369) Urata, H.; Nomura, K.; Wada, S.-i.; Akagi, M. *Biochem. Biophys. Res. Commun.* **2007**, *360*, 459.

(370) Yang, C. J.; Jockusch, S.; Vicens, M.; Turro, N. J.; Tan, W. *Proc. Natl. Acad. Sci. U.S.A.* **2005**, *102*, 17278.

(371) Nagatoishi, S.; Nojima, T.; Galezowska, E.; Juskowiak, B.; Takenaka, S. *ChemBioChem* **2006**, *7*, 1730.

(372) Nagatoishi, S.; Nojima, T.; Galezowska, E.; Gluszynska, A.; Juskowiak, B.; Takenaka, S. *Anal. Chim. Acta* **2007**, *581*, 125.

(373) Nagatoishi, S.; Nojima, T.; Juskowiak, B.; Takenaka, S. *Angew. Chem., Int. Ed.* **2005**, *44*, 5067.

(374) Li, J. J.; Fang, X.; Tan, W. *Biochem. Biophys. Res. Commun.* **2002**, *292*, 31.

(375) Ono, A.; Togashi, H. *Angew. Chem., Int. Ed.* **2004**, *43*, 4300.

(376) Tanaka, Y.; Oda, S.; Yamaguchi, H.; Kondo, Y.; Kojima, C.; Ono, A. *J. Am. Chem. Soc.* **2007**, *129*, 244.

(377) Wang, Z.; Lee, J. H.; Lu, Y. *Chem. Commun.* , . in press.

(378) Yamamoto, R.; Baba, T.; Kumar, P. K. *Genes Cells* **2000**, *5*, 389.

(379) Yamamoto-Fujita, R.; Kumar, P. K. R. *Anal. Chem.* **2005**, *77*, 5460.

(380) Nutiu, R.; Mei, S.; Liu, Z.; Li, Y. *Pure Appl. Chem.* **2004**, *76*, 1547.

(381) Hartig, J. S.; Najafi-Shoushtari, S. H.; Gruene, I.; Yan, A.; Ellington, A. D.; Famulok, M. *Nat. Biotechnol.* **2002**, *20*, 717.

(382) Nutiu, R.; Li, Y. *Angew. Chem., Int. Ed.* **2005**, *44*, 5464.

(383) Tang, Z. W.; Mallikaratchy, P.; Yang, R. H.; Kim, Y. M.; Zhu, Z.; Wang, H.; Tan, W. H. *J. Am. Chem. Soc.* **2008**, *130*, 11268.

(384) Rankin, C. J.; Fuller, E. N.; Hamor, K. H.; Gabarra, S. A.; Shields, T. P. *Nucleosides, Nucleotides Nucleic Acids* **2006**, *25*, 1407.

(385) Li, N.; Ho, C. M. *J. Am. Chem. Soc.* **2008**, *130*, 2380.

(386) Wang, W. J.; Chen, C. L.; Qian, M. X.; Zhao, X. S. *Anal. Biochem.* **2008**, *373*, 213.

(387) Rupcich, N.; Nutiu, R.; Li, Y.; Brennan, J. D. *Anal. Chem.* **2005**, *77*, 4300.

(388) Rupcich, N.; Nutiu, R.; Li, Y.; Brennan, J. D. *Angew. Chem., Int. Ed.* **2006**, *45*, 3295.

(389) Elowe, N. H.; Nutiu, R.; Allali-Hassani, A.; Cechetto, J. D.; Hughes, D. W.; Li, Y.; Brown, E. D. *Angew. Chem., Int. Ed.* **2006**, *45*, 5648.

(390) Wang, Y. Y.; Wang, Y. S.; Liu, B. *Nanotechnology* **2008**, 19.

(391) Rajendran, M.; Ellington, A. D. *Nucleic Acids Res.* **2003**, *31*, 5700.

(392) Levy, M.; Cater, S. F.; Ellington, A. D. *ChemBioChem* **2005**, *6*, 2163.

(393) Sparano, B. A.; Koide, K. *J. Am. Chem. Soc.* **2005**, *127*, 14954.

(394) Sparano, B. A.; Koide, K. *J. Am. Chem. Soc.* **2007**, *129*, 4785.

(395) Di Giusto, D. A.; Wlassoff, W. A.; Gooding, J. J.; Messerle, B. A.; King, G. C. *Nucleic Acids Res.* **2005**, *33*, e64/1.

(396) Di Giusto, D. A.; King, G. C. *J. Biol. Chem.* **2004**, *279*, 46483.

(397) Di Giusto, D. A.; Knox, S. M.; Lai, Y.; Tyrelle, G. D.; Aung, M. T.; King, G. C. *ChemBioChem* **2006**, *7*, 535.

(398) Fredriksson, S.; Gullberg, M.; Jarvius, J.; Olsson, C.; Pietras, K.; Gustafsdottir, S. M.; Oestman, A.; Landegren, U. *Nat. Biotechnol.* **2002**, *20*, 473.

(399) Heyduk, E.; Heyduk, T. *Anal. Chem.* **2005**, *77*, 1147.

(400) Heyduk, T.; Heyduk, E. *Nat. Biotechnol.* **2002**, *20*, 171.

(401) Wang, X.-L.; Li, F.; Su, Y.-H.; Sun, X.; Li, X.-B.; Schluesener, H. J.; Tang, F.; Xu, S.-Q. *Anal. Chem.* **2004**, *76*, 5605.

(402) Yang, L.; Fung, C. W.; Cho, E. J.; Ellington, A. D. *Anal. Chem.* **2007**, *79*, 3320.

(403) Lakowicz, J. R. *Principles of Fluorescence Spectroscopy*; Kluwer Academic/Plenum: New York, 1999.

(404) Kwon, M.; Chun, S.-M.; Jeong, S.; Yu, J. *Mol. Cells* **2001**, *11*, 303.

(405) Fang, X.; Cao, Z.; Beck, T.; Tan, W. *Anal. Chem.* **2001**, *73*, 5752.

(406) Gokulrangan, G.; Unruh, J. R.; Holub, D. F.; Ingram, B.; Johnson, C. K.; Wilson, G. S. *Anal. Chem.* **2005**, *77*, 1963.

(407) Cai, X.; Xu, S.; Zhang, Z.; Liu, Z.; Lu, W. *Proc. SPIE—Int. Soc. Opt. Eng.* **2001**, *4414*, 50.

(408) Takahashi, T.; Tada, K.; Mihara, H. *Pept. Sci.* **2006**, *42*, 483.

(409) Li, W.; Wang, K.; Tan, W.; Ma, C.; Yang, X. *Analyst* **2007**, *132*, 107.

(410) Ye, B.-C.; Ying, B.-C. *Angew. Chem., Int. Ed.* **2008**, *47*, 8386.

(411) Cao, Z.; Tan, W. *Chem.—Eur. J.* **2005**, *11*, 4502.

(412) Potyrailo, R. A.; Conrad, R. C.; Ellington, A. D.; Hieftje, G. M. *Anal. Chem.* **1998**, *70*, 3419.

(413) McCauley, T. G.; Hamaguchi, N.; Stanton, M. *Anal. Biochem.* **2003**, *319*, 244.

(414) Hafner, M.; Schmitz, A.; Grune, I.; Srivatsan, S. G.; Paul, B.; Kolanus, W.; Quast, T.; Kremmer, E.; Bauer, I.; Famulok, M. *Nature* **2006**, *444*, 941.

(415) Hafner, M.; Vianini, E.; Albertoni, B.; Marchetti, L.; Grune, I.; Gloeckner, C.; Famulok, M. *Nat. Protoc.* **2008**, *3*, 579.

(416) Li, Y.; Lee, H. J.; Corn, R. M. *Anal. Chem.* **2007**, *79*, 1082.

(417) Green, L. S.; Jellinek, D.; Bell, C.; Beebe, L. A.; Fesitner, B. D.; Gill, S. C.; Jucker, F. M.; Janjic, N. *Chem. Biol.* **1995**, *2*, 683.

(418) Zhou, L.; Ou, L.-J.; Chu, X.; Shen, G.-L.; Yu, R.-Q. *Anal. Chem.* **2007**, *79*, 7492.

(419) Feng, K.; Kang, Y.; Zhao, J. J.; Liu, Y. L.; Jiang, J. H.; Shen, G. L.; Yu, R. Q. *Anal. Biochem.* **2008**, *378*, 38.

(420) Rye, P. D.; Nustad, K. *BioTechniques* **2001**, *30*, 290.

(421) Yang, X.; Li, X.; Prow, T. W.; Reece, L. M.; Bassett, S. E.; Luxon, B. A.; Herzog, N. K.; Aronson, J.; Shope, R. E.; Leary, J. F.; Gorenstein, D. G. *Nucleic Acids Res.* **2003**, *31*, e54/1.

(422) Jensen, K. B.; Atkinson, B. L.; Willis, M. C.; Koch, T. H.; Gold, L. *Proc. Natl. Acad. Sci. U.S.A.* **1995**, *92*, 12220.

(423) Bock, C.; Coleman, M.; Collins, B.; Davis, J.; Foulds, G.; Gold, L.; Greef, C.; Heil, J.; Heilig, J. S.; Hicke, B.; Hurst, M. N.; Husar, G. M.; Miller, D.; Ostroff, R.; Petach, H.; Schneider, D.; Vant-Hull, B.; Waugh, S.; Weiss, A.; Wilcox, S. K.; Zichi, D. *Proteomics* **2004**, *4*, 609.

(424) Bruno, J. G.; Kiel, J. L. *BioTechniques* **2002**, *32*, 178.

(425) Higuchi, A.; Siao, Y. D.; Yang, S. T.; Hsieh, P. V.; Fukushima, H.; Chang, Y.; Ruaan, R. C.; Chen, W. Y. *Anal. Chem.* **2008**, *80*, 6580.

(426) Kirby, R.; Cho, E. J.; Gehrke, B.; Bayer, T.; Park, Y. S.; Neikirk, D. P.; McDevitt, J. T.; Ellington, A. D. *Anal. Chem.* **2004**, *76*, 4066.

(427) Collett, J. R.; Cho, E. J.; Lee, J. F.; Levy, M.; Hood, A. J.; Wan, C.; Ellington, A. D. *Anal. Biochem.* **2005**, *338*, 113.

(428) Cho, E. J.; Collett, J. R.; Szafranska, A. E.; Ellington, A. D. *Anal. Chim. Acta* **2006**, *564*, 82.

(429) Kato, T.; Yano, K.; Ikebukuro, K.; Karube, I. *Analyst* **2000**, *125*, 1371.

(430) Li, Y.-Y.; Zhang, C.; Li, B.-S.; Zhao, L.-F.; Li, X.-b.; Yang, W.-J.; Xu, S.-Q. *Clin. Chem. (Washington, DC, U. S.)* **2007**, *53*, 1061.

(431) Taton, T. A.; Mirkin, C. A.; Letsinger, R. L. *Science* **2000**, *289*, 1757.

(432) Lee, M.; Walt, D. R. *Anal. Biochem.* **2000**, *282*, 142.

(433) Baldrich, E.; Restrepo, A.; O'Sullivan, C. K. *Anal. Chem.* **2004**, *76*, 7053.

(434) Baldrich, E.; Acero, J. L.; Reekmans, G.; Laureyn, W.; O'Sullivan, C. K. *Anal. Chem.* **2005**, *77*, 4774.

(435) Stojanovic, M. N.; Landry, D. W. *J. Am. Chem. Soc.* **2002**, *124*, 9678.

(436) Yguerabide, J.; Yguerabide, E. E. *Anal. Biochem.* **1998**, *262*, 137.

(437) Bohren, C. F.; Huffman, D. R. *Absorption and Scattering of Light by Small Particles*; Wiley: New York, 1983.

(438) Jin, R.; Wu, G.; Li, Z.; Mirkin, C. A.; Schatz, G. C. *J. Am. Chem. Soc.* **2003**, *125*, 1643.

(439) Mirkin, C. A.; Letsinger, R. L.; Mucic, R. C.; Storhoff, J. J. *Nature* **1996**, *382*, 607.

(440) Elghanian, R.; Storhoff, J. J.; Mucic, R. C.; Letsinger, R. L.; Mirkin, C. A. *Science* **1997**, *277*, 1078.

(441) Mirkin, C. A. *Inorg. Chem.* **2000**, *39*, 2258.

(442) Rosi, N. L.; Mirkin, C. A. *Chem. Rev.* **2005**, *105*, 1547.

(443) Pavlov, V.; Xiao, Y.; Shlyahovsky, B.; Willner, I. *J. Am. Chem. Soc.* **2004**, *126*, 11768.

(444) Huang, C.-C.; Huang, Y.-F.; Cao, Z.; Tan, W.; Chang, H.-T. *Anal. Chem.* **2005**, *77*, 5735.

(445) Lee, J.-S.; Han, M. S.; Mirkin, C. A. *Angew. Chem., Int. Ed.* **2007**, *46*, 4093.

(446) Lee, J. S.; Mirkin, C. A. *Anal. Chem.* **2008**, *80*, 6805.

(447) Liu, J.; Lu, Y. *Angew. Chem., Int. Ed.* **2006**, *45*, 90.

(448) Liu, J.; Lu, Y. *Adv. Mater.* **2006**, *18*, 1667.

(449) Liu, J.; Lee, J. H.; Lu, Y. *Anal. Chem.* **2007**, *79*, 4120.

(450) Mitchell, G. P.; Mirkin, C. A.; Letsinger, R. L. *J. Am. Chem. Soc.* **1999**, *121*, 8122.

(451) Guerroui, Z.; Libchaber, A. *Phys. Rev. Lett.* **2004**, *93*, 166108/1.

(452) Wargnier, R.; Baranov, A. V.; Maslov, V. G.; Stsiapura, V.; Artemyev, M.; Pluot, M.; Sukhanova, A.; Nabiev, I. *Nano Lett.* **2004**, *4*, 451.

(453) Oh, E.; Hong, M.-Y.; Lee, D.; Nam, S.-H.; Yoon, H. C.; Kim, H.-S. *J. Am. Chem. Soc.* **2005**, *127*, 3270.

(454) Dyadyusha, L.; Yin, H.; Jaiswal, S.; Brown, T.; Baumberg, J. J.; Booy, F. P.; Melvin, T. *Chem. Commun.* **2005**, 3201.

(455) Sato, K.; Hosokawa, K.; Maeda, M. *J. Am. Chem. Soc.* **2003**, *125*, 8102.

(456) Zhao, W.; Chiuman, W.; Brook, M. A.; Li, Y. *ChemBioChem* **2007**, *8*, 727.

(457) Zhao, W. A.; Chiuman, W.; Lam, J. C. F.; McManus, S. A.; Chen, W.; Cui, Y. G.; Pelton, R.; Brook, M. A.; Li, Y. F. *J. Am. Chem. Soc*. **2008**, *130*, 3610.

(458) Chen, S. J.; Huang, Y. F.; Huang, C. C.; Lee, K. H.; Lin, Z. H.; Chang, H. T. *Biosens. Bioelectron*. **2008**, *23*, 1749.

(459) Li, H.; Rothberg, L. *Proc. Natl. Acad. Sci. U.S.A*. **2004**, *101*, 14036.

(460) Li, H.; Rothberg, L. J. *J. Am. Chem. Soc*. **2004**, *126*, 10958.

(461) Li, H.; Rothberg, L. *J. Anal. Chem*. **2004**, *76*, 5414.

(462) Wang, L.; Liu, X.; Hu, X.; Song, S.; Fan, C. *Chem. Commun*. **2006**, 3780.

(463) Wei, H.; Li, B.; Li, J.; Wang, E.; Dong, S. *Chem. Commun*. **2007**, 3735.

(464) Li, D.; Wieckowska, A.; Willner, I. *Angew. Chem., Int. Ed*. **2008**, *47*, 3927.

(465) Zhang, J.; Wang, L. H.; Pan, D.; Song, S. P.; Boey, F. Y. C.; Zhang, H.; Fan, C. H. *Small* **2008**, *4*, 1196.

(466) Wang, J.; Wang, L. H.; Liu, X. F.; Liang, Z. Q.; Song, S. P.; Li, W. X.; Li, G. X.; Fan, C. H. *Adv. Mater*. **2007**, *19*, 3943.

(467) Glynou, K.; Ioannou, P. C.; Christopoulos, T. K.; Syriopoulou, V. *Anal. Chem*. **2003**, *75*, 4155.

(468) Liu, J.; Mazumdar, D.; Lu, Y. *Angew. Chem., Int. Ed*. **2006**, *45*, 7955.

(469) Kinoshita, T.; Hayashi, S.; Yokogawa, Y. *J. Photochem. Photobiol., A* **2001**, *145*, 101.

(470) Sivakumar, M.; Tominaga, R.; Koga, T.; Kinoshita, T.; Sugiyama, M.; Yamaguchi, K. *Sci. Technol. Adv. Mater*. **2005**, *6*, 91.

(471) Willner, I.; Zayats, M. *Angew. Chem., Int. Ed*. **2007**, *46*, 6408.

(472) Xiao, Y.; Plaxco, K. W. In *Functional Nucleic Acids for Analytical Applications*; Lu, Y., Li, Y., Eds.; Springer: New York, NY, in press.

(473) Ikebukuro, K.; Kiyohara, C.; Sode, K. *Biosens. Bioelectron*. **2005**, *20*, 2168.

(474) Ikebukuro, K.; Kiyohara, C.; Sode, K. *Anal. Lett*. **2004**, *37*, 2901.

(475) Centi, S.; Tombelli, S.; Minunni, M.; Mascini, M. *Anal. Chem*. **2007**, *79*, 1466.

(476) Polsky, R.; Gill, R.; Kaganovsky, L.; Willner, I. *Anal. Chem*. **2006**, *78*, 2268.

(477) Mir, M.; Vreeke, M.; Katakis, I. *Electrochem. Commun*. **2006**, *8*, 505.

(478) Papamichael, K. I.; Kreuzer, M. P.; Guilbault, G. G. *Sens. Actuators B* **2007**, *B121*, 178.

(479) Hianik, T.; Ostatna, V.; Zajacova, Z.; Stoikova, E.; Evtugyn, G. *Bioorg. Med. Chem. Lett*. **2005**, *15*, 291.

(480) Cheng, A. K. H.; Ge, B.; Yu, H.-Z. *Anal. Chem*. **2007**, *79*, 5158.

(481) Wang, X.; Zhou, J.; Yun, W.; Xiao, S.; Chang, Z.; He, P.; Fang, Y. *Anal. Chim. Acta* **2007**, *598*, 242.

(482) Shen, L.; Chen, Z.; Li, Y.; Jing, P.; Xie, S.; He, S.; He, P.; Shao, Y. *Chem. Commun*. **2007**, 2169.

(483) Katz, E.; Willner, I. *Electroanalysis* **2003**, *15*, 913.

(484) Rodriguez, M. C.; Kawde, A.-N.; Wang, J. *Chem. Commun*. **2005**, 4267.

(485) Radi, A.-E.; Sanchez, J. L. A.; Baldrich, E.; O'Sullivan, C. K. *Anal. Chem*. **2005**, *77*, 6320.

(486) Cai, H.; Lee, T. M.-H.; Hsing, I. M. *Sens. Actuators B* **2006**, *B114*, 433.

(487) Xu, Y.; Yang, L.; Ye, X.; He, P.; Fang, Y. *Electroanalysis* **2006**, *18*, 1449.

(488) Liao, W.; Cui, X. T. *Biosens. Bioelectron*. **2007**, *23*, 218.

(489) Xu, D.; Xu, D.; Yu, X.; Liu, Z.; He, W.; Ma, Z. *Anal. Chem*. **2005**, *77*, 5107.

(490) Lohndorf, M.; Schlecht, U.; Gronewold, T. M. A.; Malave, A.; Tewes, M. *Appl. Phys. Lett*. **2005**, *87*, 243902/1.

(491) Schlecht, U.; Malave, A.; Gronewold, T.; Tewes, M.; Loehndorf, M. *Anal. Chim. Acta* **2006**, *573−574*, 65.

(492) Schlecht, U.; Malave, A.; Gronewold, T. M. A.; Tewes, M.; Loehndorf, M. *Biosens. Bioelectron*. **2007**, *22*, 2337.

(493) Radi, A.-E.; O'Sullivan, C. K. *Chem. Commun*. **2006**, 3432.

(494) Zayats, M.; Huang, Y.; Gill, R.; Ma, C.-a.; Willner, I. *J. Am. Chem. Soc*. **2006**, *128*, 13666.

(495) Elbaz, J.; Shlyahovsky, B.; Li, D.; Willner, I. *ChemBioChem* **2008**, *9*, 232.

(496) De-los-Santos-Alvarez, N.; Lobo-Castanon, M. J.; Miranda-Ordieres, A. J.; Tunon-Blanco, P. *J. Am. Chem. Soc*. **2007**, *129*, 3808.

(497) Bang, G. S.; Cho, S.; Kim, B.-G. *Biosens. Bioelectron*. **2005**, *21*, 863.

(498) Xiao, Y.; Lubin, A. A.; Heeger, A. J.; Plaxco, K. W. *Angew. Chem., Int. Ed*. **2005**, *44*, 5456.

(499) Radi, A.-E.; Acero Sanchez, J. L.; Baldrich, E.; O'Sullivan, C. K. *J. Am. Chem. Soc*. **2006**, *128*, 117.

(500) Sanchez, J. L. A.; Baldrich, E.; Radi, A.E.-G.; Dondapati, S.; Sanchez, P. L.; Katakis, I.; O'Sullivan, C. K. *Electroanalysis* **2006**, *18*, 1957.

(501) Baker, B. R.; Lai, R. Y.; Wood, M. S.; Doctor, E. H.; Heeger, A. J.; Plaxco, K. W. *J. Am. Chem. Soc*. **2006**, *128*, 3138.

(502) White, R. J.; Phares, N.; Lubin, A. A.; Xiao, Y.; Plaxco, K. W. *Langmuir* **2008**, *24*, 10513.

(503) Li, Y.; Qi, H.; Peng, Y.; Yang, J.; Zhang, C. *Electrochem. Commun*. **2007**, *9*, 2571.

(504) Lai, R. Y.; Plaxco, K. W.; Heeger, A. *J. Anal. Chem*. **2007**, *79*, 229.

(505) Ferapontova, E. E.; Olsen, E. M.; Gothelf, K. V. *J. Am. Chem. Soc*. **2008**, *130*, 4256.

(506) Xiao, Y.; Piorek, B. D.; Plaxco, K. W.; Heeger, A. J. *J. Am. Chem. Soc*. **2005**, *127*, 17990.

(507) Wu, Z.-S.; Guo, M.-M.; Zhang, S.-B.; Chen, C.-R.; Jiang, J.-H.; Shen, G.-L.; Yu, R.-Q. *Anal. Chem*. **2007**, *79*, 2933.

(508) Lu, Y.; Li, X. C.; Zhang, L. M.; Yu, P.; Su, L.; Mao, L. Q. *Anal. Chem*. **2008**, *80*, 1883.

(509) Yoshizumi, J.; Kumamoto, S.; Nakamura, M.; Yamana, K. *Analyst* **2008**, *133*, 323.

(510) Hansen, J. A.; Wang, J.; Kawde, A.-N.; Xiang, Y.; Gothelf, K. V.; Collins, G. *J. Am. Chem. Soc*. **2006**, *128*, 2228.

(511) Cai, X.; Rivas, G.; Farias, P. A. M.; Shiraishi, H.; Wang, J.; Palecek, E. *Anal. Chim. Acta* **1996**, *332*, 49.

(512) Kawde, A.-N.; Rodriguez, M. C.; Lee, T. M. H.; Wang, J. *Electrochem. Commun*. **2005**, *7*, 537.

(513) Cui, Y.; Wei, Q.; Park, H.; Lieber, C. M. *Science* **2001**, *293*, 1289.

(514) Hahm, J.-i.; Lieber, C. M. *Nano Lett*. **2004**, *4*, 51.

(515) Chen, R. J.; Bangsaruntip, S.; Drouvalakis, K. A.; Kam, N. W. S.; Shim, M.; Li, Y.; Kim, W.; Utz, P. J.; Dai, H. *Proc. Natl. Acad. Sci. U.S.A*. **2003**, *100*, 4984.

(516) So, H.-M.; Won, K.; Kim, Y. H.; Kim, B.-K.; Ryu, B. H.; Na, P. S.; Kim, H.; Lee, J.-O. *J. Am. Chem. Soc*. **2005**, *127*, 11906.

(517) Yoon, H.; Kim, J. H.; Lee, N.; Kim, B. G.; Jang, J. *ChemBioChem* **2008**, *9*, 634.

(518) Minunni, M.; Tombelli, S.; Gullotto, A.; Luzi, E.; Mascini, M. *Biosens. Bioelectron*. **2004**, *20*, 1149.

(519) Bini, A.; Minunni, M.; Tombelli, S.; Centi, S.; Mascini, M. *Anal. Chem*. **2007**, *79*, 3016.

(520) Hianik, T.; Ostatna, V.; Sonlajtnerova, M.; Grman, I. *Bioelectrochemistry* **2007**, *70*, 127.

(521) Freudenberg, J.; von Schickfus, M.; Hunklinger, S. *Sens. Actuators B* **2001**, *B76*, 147.

(522) Josse, F.; Bender, F.; Cernosek, R. W. *Anal. Chem*. **2001**, *73*, 5937.

(523) Furtado, L. M.; Su, H.; Thompson, M.; Mack, D. P.; Hayward, G. L. *Anal. Chem*. **1999**, *71*, 1167.

(524) Schlensog, M. D.; Gronewold, T. M. A.; Tewes, M.; Famulok, M.; Quandt, E. *Sens. Actuators B* **2004**, *B101*, 308.

(525) Gronewold, T. M. A.; Glass, S.; Quandt, E.; Famulok, M. *Biosens. Bioelectron*. **2005**, *20*, 2044.

(526) Jung, A.; Gronewold, T. M. A.; Tewes, M.; Quandt, E.; Berlin, P. *Sens. Actuators B* **2007**, *B124*, 46.

(527) Wu, G.; Datar, R. H.; Hansen, K. M.; Thundat, T.; Cote, R. J.; Majumdar, A. *Nat. Biotechnol*. **2001**, *19*, 856.

(528) Savran, C. A.; Knudsen, S. M.; Ellington, A. D.; Manalis, S. R. *Anal. Chem*. **2004**, *76*, 3194.

(529) Lin, Y.; Jayasena, S. D. *J. Mol. Biol*. **1997**, *271*, 100.

(530) Markey, F. *Real-Time Anal. Biomol. Interact*. **2000**, 13.

(531) Rich, R. L.; Myszka, D. G. *Curr. Opin. Biotechnol*. **2000**, *11*, 54.

(532) Tombelli, S.; Minunni, M.; Mascini, M. *Anal. Lett*. **2002**, *35*, 599.

(533) Tombelli, S.; Minunni, M.; Luzi, E.; Mascini, M. *Bioelectrochemistry* **2005**, *67*, 135.

(534) Verhelst, S. H. L.; Michiels, P. J. A.; Van Der Marel, G. A.; Van Boeckel, C. A. A.; Van Boom, J. H. *ChemBioChem* **2004**, *5*, 937.

(535) Gebhardt, K.; Shokraei, A.; Babaie, E.; Lindqvist, B. H. *Biochemistry* **2000**, *39*, 7255.

(536) Kawakami, J.; Imanaka, H.; Yokota, Y.; Sugimoto, N. *J. Inorg. Biochem*. **2000**, *82*, 197.

(537) Fukusaki, E.-i.; Hasunuma, T.; Kajiyama, S.-i.; Okazawa, A.; Itoh, T. J.; Kobayashi, A. *Bioorg. Med. Chem. Lett*. **2001**, *11*, 2927.

(538) Wang, J. L.; Zhou, H. S. *Anal. Chem*. **2008**, *80*, 7174.

(539) Murphy, M. B.; Fuller, S. T.; Richardson, P. M.; Doyle, S. A. *Nucleic Acids Res*. **2003**, *31*, e110/1.

(540) Kim, D. K.; Kerman, K.; Hiep, H. M.; Saito, M.; Yamamura, S.; Takamura, Y.; Kwon, Y. S.; Tamiya, E. *Anal. Biochem*. **2008**, *379*, 1.

(541) Romig, T. S.; Bell, C.; Drolet, D. W. *J. Chromatogr., B* **1999**, *731*, 275.

(542) Michaud, M.; Jourdan, E.; Villet, A.; Ravel, A.; Grosset, C.; Peyrin, E. *J. Am. Chem. Soc*. **2003**, *125*, 8672.

(543) Deng, Q.; Watson, C. J.; Kennedy, R. T. *J. Chromatogr., A* **2003**, *1005*, 123.

(544) German, I.; Buchanan, D. D.; Kennedy, R. T. *Anal. Chem*. **1998**, *70*, 4540.

(545) Buchanan, D. D.; Jameson, E. E.; Perlette, J.; Malik, A.; Kennedy, R. T. *Electrophoresis* **2003**, *24*, 1375.

(546) Pavski, V.; Le, X. C. *Anal. Chem*. **2001**, *73*, 6070.

(547) Wang, H.; Lu, M.; Le, X. C. *Anal. Chem*. **2005**, *77*, 4985.

(548) Fu, H.; Guthrie, J. W.; Le, X. C. *Electrophoresis* **2006**, *27*, 433.

(549) Huang, C.-C.; Cao, Z.; Chang, H.-T.; Tan, W. *Anal. Chem.* **2004**, *76*, 6973.
(550) Haes, A. J.; Giordano, B. C.; Collins, G. E. *Anal. Chem.* **2006**, *78*, 3758.
(551) Zhang, H.; Wang, Z.; Li, X.-F.; Le, X. C. *Angew. Chem., Int. Ed.* **2006**, *45*, 1576.
(552) Li, T.; Li, B.; Dong, S. *Chem.—Eur. J.* **2007**, *13*, 6718.
(553) Li, T.; Li, B.; Dong, S. *Anal. Bioanal. Chem.* **2007**, *389*, 887.
(554) Ruta, J.; Ravelet, C.; Baussanne, I.; Decout, J.-L.; Peyrin, E. *Anal. Chem.* **2007**, *79*, 4716.
(555) Berezovski, M.; Krylov, S. N. *J. Am. Chem. Soc.* **2002**, *124*, 13674.
(556) Berezovski, M.; Nutiu, R.; Li, Y.; Krylov, S. N. *Anal. Chem.* **2003**, *75*, 1382.
(557) Nishikawa, F.; Arakawa, H.; Nishikawa, S. *Nucleosides, Nucleotides Nucleic Acids* **2006**, *25*, 369.
(558) Dick, L. W., Jr.; McGown, L. B. *Anal. Chem.* **2004**, *76*, 3037.
(559) Connor, A. C.; Frederick, K. A.; Morgan, E. J.; McGown, L. B. *J. Am. Chem. Soc.* **2006**, *128*, 4986.
(560) Turney, K.; Drake, T. J.; Smith, J. E.; Tan, W.; Harrison, W. W. *Rapid Commun. Mass Spectrom.* **2004**, *18*, 2367.
(561) Cho, S.; Lee, S.-H.; Chung, W.-J.; Kim, Y.-K.; Lee, Y.-S.; Kim, B.-G. *Electrophoresis* **2004**, *25*, 3730.
(562) Huang, Y.-F.; Chang, H.-T. *Anal. Chem.* **2007**, *79*, 4852.
(563) Cassidy, L. A.; Lebruska, L. L.; Benson, L. M.; Naylor, S.; Owen, W. G.; Maher, L. J., III *Anal. Biochem.* **2002**, *306*, 290.
(564) Cavanagh, J.; Benson, L. M.; Thompson, R.; Naylor, S. *Anal. Chem.* **2003**, *75*, 3281.
(565) Keller, K. M.; Breeden, M. M.; Zhang, J.; Ellington, A. D.; Brodbelt, J. S. *J. Mass Spectrom.* **2005**, *40*, 1327.
(566) Conrad, R.; Ellington, A. D. *Anal. Biochem.* **1996**, *242*, 261.
(567) Wang, Y. L.; Li, D.; Ren, W.; Liu, Z. J.; Dong, S. J.; Wang, E. K. *Chem. Commun.* **2008**, 2520.
(568) Jana, N. R.; Ying, J. Y. *Adv. Mater.* **2008**, *20*, 430.
(569) Huang, Y. C.; Ge, B. X.; Sen, D.; Yu, H. Z. *J. Am. Chem. Soc.* **2008**, *130*, 8023.
(570) Hind, A. R.; Bhargava, S. K.; McKinnon, A. *Adv. Colloid Interface Sci.* **2001**, *93*, 91.
(571) Liao, W.; Wei, F.; Liu, D.; Qian, M. X.; Yuan, G.; Zhao, X. S. *Sens. Actuators B* **2006**, *B114*, 445.
(572) Josephson, L.; Lewis, J.; Jacobs, P.; Hahn, P. F.; Stark, D. D. *Magn. Reson. Imaging* **1988**, *6*, 647.
(573) Shen, T.; Weissleder, R.; Papisov, M.; Bogdanov, A. J.; Brady, T. J. *Magn. Reson. Med.* **1993**, *29*, 599.
(574) Josephson, L.; Perez, J. M.; Weissleder, R. *Angew. Chem., Int. Ed.* **2001**, *40*, 3204.
(575) Perez, J. M.; Josephson, L.; O'Loughlin, T.; Hoegemann, D.; Weissleder, R. *Nat. Biotechnol.* **2002**, *20*, 816.
(576) Perez, J. M.; Josephson, L.; Weissleder, R. *ChemBioChem* **2004**, *5*, 261.
(577) Yigit, M. V.; Mazumdar, D.; Kim, H.-K.; Lee, J. H.; Odintsov, B.; Lu, Y. *ChemBioChem* **2007**, *8*, 1675.
(578) Yigit, M. V.; Mazumdar, D.; Lu, Y. *Bioconjugate Chem.* **2008**, *19*, 412.
(579) Yoshida, W.; Yokobayashi, Y. *Chem. Commun.* **2007**, 195.
(580) Wu, L.; Curran, J. F. *Nucleic Acids Res.* **1999**, *27*, 1512.
(581) Vuyisich, M.; Beal, P. A. *Chem. Biol.* **2002**, *9*, 907.
(582) Cong, X.; Nilsen-Hamilton, M. *Biochemistry* **2005**, *44*, 7945.
(583) Yoshida, W.; Sode, K.; Ikebukuro, K. *Anal. Chem.* **2006**, *78*, 3296.
(584) Chelyapov, N. *Biochemistry* **2006**, *45*, 2461.
(585) Chinnapen, D. J. F.; Sen, D. *Biochemistry* **2002**, *41*, 5202.
(586) Stojanovic, M. N. *J. Serb. Chem. Soc.* **2004**, *69*, 871.
(587) Mandal, M.; Breaker, R. R. *Nat. Rev. Mol. Cell Biol* **2004**, *5*, 451.
(588) Werstuck, G.; Green, M. R. *Science* **1998**, *282*, 296.
(589) Desai, S. K.; Gallivan, J. P. *J. Am. Chem. Soc.* **2004**, *126*, 13247.
(590) Lynch, S. A.; Desai, S. K.; Sajja, H. K.; Gallivan, J. P. *Chem. Biol.* **2007**, *14*, 173.
(591) Topp, S.; Gallivan, J. P. *J. Am. Chem. Soc.* **2007**, *129*, 6807.
(592) Buskirk, A. R.; Liu, D. R. *Chem. Biol.* **2005**, *12*, 151.
(593) Buskirk, A. R.; Landrigan, A.; Liu, D. R. *Chem. Biol.* **2004**, *11*, 1157.
(594) Bayer, T. S.; Smolke, C. D. *Nat. Biotechnol.* **2005**, *23*, 337.
(595) Soukup, G. A.; Breaker, R. R. *Trends Biotechnol.* **1999**, *17*, 469.
(596) Soukup, G. A.; Breaker, R. R. *Curr. Opin. Struct. Biol.* **2000**, *10*, 318.
(597) Nahvi, A.; Sudarsan, N.; Ebert, M. S.; Zou, X.; Brown, K. L.; Breaker, R. R. *Chem. Biol.* **2002**, *9*, 1043.
(598) Silverman, S. K. *RNA* **2003**, *9*, 377.
(599) Tuschl, T.; Eckstein, F. *Proc. Natl. Acad. Sci. U.S.A.* **1993**, *90*, 6991.
(600) Long, D. M.; Uhlenbeck, O. C. *Proc. Natl. Acad. Sci. U.S.A.* **1994**, *91*, 6977.
(601) Robertson, M. P.; Ellington, A. D. *Nucleic Acids Res.* **2000**, *28*, 1751.
(602) Levy, M.; Ellington, A. D. *J. Mol. Evol.* **2002**, *54*, 180.

(603) Tang, J.; Breaker, R. R. *Chem. Biol.* **1997**, *4*, 453.
(604) Tang, J.; Breaker, R. R. *Nucleic Acids Res.* **1998**, *26*, 4214.
(605) Araki, M.; Okuno, Y.; Hara, Y.; Sugiura, Y. *Nucleic Acids Res.* **1998**, *26*, 3379.
(606) Araki, M.; Hashima, M.; Okuno, Y.; Sugiura, Y. *Bioorg. Med. Chem.* **2001**, *9*, 1155.
(607) Soukup, G. A.; Breaker, R. R. *Structure* **1999**, *7*, 783.
(608) Wang, D. Y.; Sen, D. *Comb. Chem. High Throughput Screening* **2002**, *5*, 301.
(609) Yamazaki, S.; Tan, L.; Mayer, G.; Hartig, J. S.; Song, J. N.; Reuter, S.; Restle, T.; Laufer, S. D.; Grohmann, D.; Krausslich, H. G.; Bajorath, J.; Famulok, M. *Chem. Biol.* **2007**, *14*, 804.
(610) Jose, A. M.; Soukup, G. A.; Breaker, R. R. *Nucleic Acids Res.* **2001**, *29*, 1631.
(611) Soukup, G. A.; Breaker, R. R. *Proc. Natl. Acad. Sci. U.S.A.* **1999**, *96*, 3584.
(612) Soukup, G. A.; Emilsson, G. A. M.; Breaker, R. R. *J. Mol. Biol.* **2000**, *298*, 623.
(613) Koizumi, M.; Soukup, G. A.; Kerr, J. N. Q.; Breaker, R. R. *Nat. Struct. Biol.* **1999**, *6*, 1062.
(614) Seetharaman, S.; Zivarts, M.; Sudarsan, N.; Breaker, R. R. *Nat. Biotechnol.* **2001**, *19*, 336.
(615) Zivarts, M.; Liu, Y.; Breaker, R. R. *Nucleic Acids Res.* **2005**, *33*, 622.
(616) Piganeau, N.; Jenne, A.; Thuillier, V.; Famulok, M. *Angew. Chem., Int. Ed.* **2000**, *39*, 4369.
(617) Piganeau, N.; Thuillier, V.; Famulok, M. *J. Mol. Biol.* **2001**, *312*, 1177.
(618) Robertson, M. P.; Knudsen, S. M.; Ellington, A. D. *RNA* **2004**, *10*, 114.
(619) Robertson, M. P.; Ellington, A. D. *Nat. Biotechnol.* **1999**, *17*, 62.
(620) Levy, M.; Ellington, A. D. *Chem. Biol.* **2002**, *9*, 417.
(621) Cho, E. J.; Yang, L.; Levy, M.; Ellington, A. D. *J. Am. Chem. Soc.* **2005**, *127*, 2022.
(622) Hall, B.; Hesselberth, J. R.; Ellington, A. D. *Biosens. Bioelectron.* **2007**, *22*, 1939.
(623) Liu, J.; Lu, Y. *Angew. Chem., Int. Ed.* **2007**, *46*, 7587.
(624) Achenbach, J. C.; Nutiu, R.; Li, Y. *Anal. Chim. Acta* **2005**, *534*, 41.
(625) Wang, D. Y.; Lai, B. H. Y.; Sen, D. *J. Mol. Biol.* **2002**, *318*, 33.
(626) Cho, S.; Kim, J.-E.; Lee, B.-R.; Kim, J.-H.; Kim, B.-G. *Nucleic Acids Res.* **2005**, *33*, e177/1.
(627) Najafi-Shoushtari, S. H.; Famulok, M. *RNA* **2005**, *11*, 1514.
(628) Amontov, S.; Jaschke, A. *Nucleic Acids Res.* **2006**, *34*, 5032.
(629) Porta, H.; Lizardi, P. M. *Bio/Technology* **1995**, *13*, 161.
(630) Kuwabara, T.; Warashina, M.; Tanabe, T.; Tani, K.; Asano, S.; Taira, K. *Mol. Cell* **1998**, *2*, 617.
(631) Komatsu, Y.; Yamashita, S.; Kazama, N.; Nobuoka, K.; Ohtsuka, E. *J. Mol. Biol.* **2000**, *299*, 1231.
(632) Wang, D. Y.; Sen, D. *J. Mol. Biol.* **2001**, *310*, 723.
(633) Wang, D. Y.; Lai, B. H. Y.; Feldman, A. R.; Sen, D. *Nucleic Acids Res.* **2002**, *30*, 1735.
(634) Sando, S.; Sasaki, T.; Kanatani, K.; Aoyama, Y. *J. Am. Chem. Soc.* **2003**, *125*, 15720.
(635) Hartig, J. S.; Gruene, I.; Najafi-Shoushtari, S. H.; Famulok, M. *J. Am. Chem. Soc.* **2004**, *126*, 722.
(636) Burke, D. H.; Ozerova, N. D. S.; Nilsen-Hamilton, M. *Biochemistry* **2002**, *41*, 6588.
(637) Kossen, K.; Vaish, N. K.; Jadhav, V. R.; Pasko, C.; Wang, H.; Jenison, R.; McSwiggen, J. A.; Polisky, B.; Seiwert, S. D. *Chem. Biol.* **2004**, *11*, 807.
(638) Penchovsky, R.; Breaker, R. R. *Nat. Biotechnol.* **2005**, *23*, 1424.
(639) Sekella, P. T.; Rueda, D.; Walter, N. G. *RNA* **2002**, *8*, 1242.
(640) Li, D.; Shlyahovsky, B.; Elbaz, J.; Willner, I. *J. Am. Chem. Soc.* **2007**, *129*, 5804.
(641) Knudsen, S. M.; Lee, J.; Ellington, A. D.; Savran, C. A. *J. Am. Chem. Soc.* **2006**, *128*, 15936.
(642) Ogawa, A.; Maeda, M. *Bioorg. Med. Chem. Lett.* **2007**, *17*, 3156.
(643) Hollenstein, M.; Hipolito, C.; Lam, C.; Dietrich, D.; Perrin, D. M. *Angew. Chem., Int. Ed.* **2008**, *47*, 4346.
(644) Li, M. Y.; Lin, N.; Huang, Z.; Du, L. P.; Altier, C.; Fang, H.; Wang, B. H. *J. Am. Chem. Soc.* **2008**, *130*, 12636.
(645) Lin, N.; Yan, J.; Huang, Z.; Altier, C.; Li, M. Y.; Carrasco, N.; Suyemoto, M.; Johnston, L.; Wang, S. M.; Wang, Q.; Fang, H.; Caton-Williams, J.; Wang, B. H. *Nucleic Acids Res.* **2007**, *35*, 1222.
(646) Hesselberth, J. R.; Robertson, M. P.; Knudsen, S. M.; Ellington, A. D. *Anal. Biochem.* **2003**, *312*, 106.
(647) Collett, J. R.; Cho, E. J.; Ellington, A. D. *Methods* **2005**, *37*, 4.
(648) Xue, X.; Wang, F.; Liu, X. *J. Am. Chem. Soc.* **2008**, *130*, 3244.

CR030183I